Catarina Gonçalves Pimpão
Licenciada em Bioquímica

Screening and Validation of Aquaporin Inhibitors for Cancer Therapeutics

Dissertação para obtenção do Grau de Mestre em
Bioquímica para a Saúde

Orientadora: Prof. Drª Graça Soveral, Professora Associada com Agregação, Faculdade de Farmácia, Universidade de Lisboa

Setembro 2019

Catarina Gonçalves Pimpão
Licenciada em Bioquímica

Screening and Validation of Aquaporin Inhibitors for Cancer Therapeutics

Dissertação para obtenção do Grau de Mestre em
Bioquímica para a Saúde

Orientadora: Prof. Drª Graça Soveral, Professora Associada com Agregação, Faculdade de Farmácia, Universidade de Lisboa

Júri:

Presidente: Prof. Drª Maria Teresa Nunes Mangas Catarino
Arguente: Prof. Drª Maria Alice Santos Pereira
Vogal: Prof. Drª Graça Soveral

Faculdade de Ciências e Tecnologia da Universidade Nova de Lisboa

Setembro 2019

Screening and Validation of Aquaporin Inhibitors for Cancer Therapeutics

Part of the results obtained during this work were included in three conference abstracts and in a published scientific article:

C. Pimpão, A.S. Coxixo, M. Aureliano, A. Rompel, G. Soveral, "Screening Polyoxometalates as Aquaporin Inhibitors for Cancer Therapeutics" in *FEBS Congress 2019: From Molecules To Living Systems, 6-11 July 2019, Krakow, Poland.*

C. Pimpão, A.S. Coxixo, M. Aureliano, A. Rompel, G. Soveral, "Polyoxometalates as Aquaporin Inhibitors with Potential Anticancer Properties" in *11th iMed.ULisboa Postgraduate Students Meeting & 4rd i3DU Meeting, 15 July 2019, Lisbon, Portugal.*

A. Serrano, **C. Pimpão,** A.S. Coxixo, G. Fraqueza, A. Rompel, G. Soveral, M. Aureliano, "Polyoxotungstates with anticancer activity: Are membrane proteins attractive targets?" in *SINAL 2019: 10th Meeting in Signal Transduction, 18-19 October 2019, Olhão, Algarve, Portugal.*

C. Rodrigues**, C. Pimpão** *et al.*, "Human Aquaporin-5 Facilitates Hydrogen Peroxide Permeation and Cancer Cell Migration," *Cancers (Basel).*, vol. 11, 2019.

This article was adapted for Chapter 4.2. in Results and Discussion section.

Acknowledgments

Chegou ao fim mais uma etapa da minha vida. Esta fase que tanto esforço e dedicação pediu e que é mais uma prova da determinação e persistência que me caracteriza, além de uma enorme superação pessoal. Foi um ano de muitas aprendizagens, cheio de boas experiências a fazer aquilo que mais gosto. Claro que este caminho não teria sido feito sem o apoio e suporte das pessoas certas que contribuíram para o meu sucesso e bem-estar a quem quero expressar o meu agradecimento.

Quero primeiro agradecer à Professora Graça Soveral por me ter acolhido no seu laboratório, por estar sempre lá quando alguma coisa corria menos bem e por me ter dado esta oportunidade de fazer aquilo que gosto. Além disso, agradeço imenso ter tido a oportunidade de ir ao Congresso da FEBS em Cracóvia para apresentar os meus resultados, foi com certeza muito enriquecedor tal como ter trabalhado com Brech Aikman e Simon Krabbe em que me pôs em contacto com outras formas de trabalhar.

À Andreia, Claúdia e Inês tenho muito a agradecer. Obrigado pela paciência, pelo apoio e ajuda no que precisasse. Em especial à Claúdia, um obrigado pela música de fundo no laboratório e em geral, pela animação diária naquele laboratório. Muito orgulhosa da tua conquista, Doutora! Também um obrigado especial à Inês pela companhia nos congressos e pelos cappuccinos do Sr. Joaquim.

À Ana Coxixo, que no início era a minha colega de tese e que rapidamente se revelou num apoio e companhia diária naquele laboratório. A ti, um obrigado pela amizade, pelas conversas, por me fazeres rir mesmo quando estávamos em desespero, pela companhia nos dias compridos, por teres estado ao meu lado no Hospital Santa Maria durante aquelas longas oito horas e claro, a surpresa no dia da minha partida. Apesar de muitas dúvidas pelo meio, conseguimos amiga, tese feita!

Às minhas amigas Andreia, Sara, Inês, Kiki, Teresa, Painho e Carina, um especial obrigado pelo apoio neste último ano, foram cruciais para o meu sucesso no mestrado! Em especial, Andreia, Sara e Kiki, obrigada pelos lanchinhos, jantares e afins que me faziam descontrair do dia-a-dia. Andreia e Sara, obrigada por alinharem comigo em escrever a tese no caleidoscópio, que foi sempre uma boa desculpa para nos encontrarmos e apoiarmos mutuamente nesta fase.

Ao João, que chegou mais tarde, mas que sem dúvida foi das pessoas que esteve presente em todos os meus sucessos e nos momentos menos bons. Obrigada por nunca vacilares, pelos jantares e fins de semana que me aliviam do stress e por seres o companheiro de todas as horas, sempre a dar-me força e confiança para atingir os meus objectivos. À família do João, a minha segunda família que sempre me acolheu e compreendeu.

Quero também agradecer à Professora Teresa Catarino, sempre disponível para ajudar e esclarecer dúvidas e tão bem acolheu a nossa turma de mestrado. Também um obrigado aos meus colegas de mestrado e à FCT/UNL, ITQB e NMS por me terem acolhido e por todas as vivências.

Um obrigado também aos escuteiros, que preencheram e animaram os meus fins-de-semana. É e sempre será uma parte essencial na minha vida e que moldou os meus princípios e valores, permitindo-me chegar onde cheguei. Aos caminheiros, à Rute e a todos os meus chefes e principalmente aos meus miúdos, o meu grande obrigado.

Por último, agradecer à minha família que teve sempre uma palavra de força, principalmente durante todo aquele mês de Agosto. Um grande obrigado por me apoiarem incondicionalmente e confiarem em mim e nas minhas capacidades.

Resumo

As aquaporinas (AQPs) são proteínas transmembranares que facilitam a difusão da água e glicerol através das membranas celulares, cruciais para a homeostase da água e metabolismo. As AQPs encontram-se sobre-expressas em diversas células e tecidos cancerígenos, estando envolvidas na proliferação, migração celular e tumorigénese, revelando o seu potencial como alvos terapêuticos. A identificação de novos inibidores de aquaporinas é essencial. Neste trabalho, foram avaliados compostos metálicos (polioxometalatos, compostos de vanádio, cobre, zinco e ouro) como inibidores de aquaporinas, utilizando como modelos celulares eritrócitos humanos (RBCs) e leveduras transformadas com aquaporinas humanas. O efeito inibidor das AQPs foi avaliado pela determinação da permeabilidade membranar à água e ao glicerol, utilizando a técnica de *stopped-flow*. O polioxotungstato-A (POT-A) revelou ser um inibidor da AQP3, com um IC_{50} de (0.71 ± 0.04) µM em RBCs. Em leveduras, POT-A inibiu AQP3 a 100%, confirmando os resultados obtidos para os RBCs. O composto de vanádio P103 inibiu AQP1 com um IC_{50} de (9.11 ± 0.03) µM em RBCs. O composto de ouro RBA29, mostrou inibir a AQP3 em RBCs com um IC_{50} de (2.29 ± 0.03) µM. Ainda, os compostos RBA29, RBA31 e STAM013 mostraram inibir a AQP9 em leveduras, com um IC_{50} de (6.64 ± 0.09) µM para RBA29. Neste trabalho, foi também avaliado o efeito de mutações na permeabilidade da AQP5 através da técnica de *stopped-flow*. Deste modo, foi descrito um novo mecanismo de regulação em que His73 localizada no filtro de seletividade interage com Ser183 fosforilada, levando à constrição do poro. Foi também avaliada a função de aquaporinas de diversos organismos, em que a aquaporina de tardígrado revelou maior permeabilidade e seletividade para a água do que as outras aquaporinas testadas. Os resultados obtidos contribuem para a descoberta e desenho de inibidores seletivos com aplicação terapêutica.

Termos chave: aquaporinas; permeabilidade; inibidores; cancro.

Abstract

Aquaporins (AQPs) are transmembrane proteins that facilitate the diffusion of water and glycerol across cell membranes, crucial for water and energy homeostasis. These proteins were found overexpressed in different cancer cells and tissues, being involved in tumor formation, cell proliferation and migration, suggesting their great potential as drug targets for cancer treatment. Identification of novel aquaporin modulators to be used in cancer therapeutics is of utmost importance. In this study, the inhibitory effect of polyoxometalates, vanadium, copper, zinc and gold-based compounds was screened by the stopped-flow technique in human red blood cells (RBCs) and then validated in aquaporin-expressing yeast cells. From the set of polyoxometalates, polyoxotungstate-A (POT-A) revealed as the most promising AQP3 inhibitor with an IC_{50} of (0.71 ± 0.04) μM. Using yeast cells individually expressing human aquaporins, POT-A showed to selectively inhibit AQP3 with 100% inhibition, corroborating the results of RBCs assays. The vanadium compound P103, showed highly inhibition of AQP1 with an IC_{50} of (9.11 ± 0.03) μM in RBCs. The gold-based compound RBA29 revealed as a promising AQP3 inhibitor with an IC_{50} of (2.29 ± 0.03) μM in RBCs. Moreover, compounds RBA29, RBA31 and STAM013 showed an inhibitory effect in AQP9-tranformed yeasts, with an IC_{50} of (6.64 ± 0.09) μM for RBA29. In addition, investigation of the channel residues important for AQP5 permeability revealed a new gating mechanism where His73 located in the selectivity filter interacts with phosphorylated Ser183, conducting to the pore constriction. Furthermore, the activity of aquaporins from diverse organisms was evaluated, wherein aquaporin from tardigrade revealed to be water selective and exhibited higher water permeability than the other aquaporins tested. Overall, these data contribute to the discovery and design of selective inhibitors with potential therapeutic application.

Keywords: aquaporins; permeability; inhibitors; cancer.

Table of Contents

Index of Figures

Index of Tables

List of Abbreviations

AQP(s) – Aquaporin(s)

AQP1 – Aquaporin-1

AQP2 – Aquaporin-2

AQP3 – Aquaporin-3

AQP4 – Aquaporin-4

AQP5 – Aquaporin-5

AQP7 – Aquaporin-7

AQP9 – Aquaporin-9

Arg197 – Arginine 197

Asn76 – Asparagine 76

Asn192 – Asparagine 192

[Au(phen)Cl_2]Cl - Auphen

cAMP – Cyclic adenosine monophosphate

CFDA - 5(6)-carboxyfluorescein diacetate

CNS – Central nervous system

CPE – Choroid plexus epithelium

CSF – Cerebrospinal fluid

Cys40 – Cysteine 40

Cys189 – Cysteine 189

Cys191 – Cysteine 191

E_a – Activation energy ($J.mol^{-1}$)

FO – Forward osmosis

GFP – Green fluorescent protein

GlpF – Glycerol facilitator from *Escherichia coli*

hAQP(s) – Human aquaporin(s)

H173A – Histidine replaced by alanine

H173W – Histidine replaced by tryptophan

His67 – Histidine 67

His173 – Histidine 173

His182 – Histidine 182

Met47 – Methionine 47

NDI - Nephrogenic diabetes insipidus

NMO - Neuromyelities optica

NPA – Asparagine-proline-alanine

OD – Optical density

PBS - Phosphate buffered saline

P_f - Water permeability coefficient

P_{gly} - Glycerol permeability coefficient

Phe58 – Phenylalanine 58

Phen - 1,10 – phenanthroline

PIP(s) - Plasma membrane intrinsic protein(s)

PKA – Protein kinase A

POMs – Polyxoxometalates

POTs – Polyoxotungstates

POVs – Polyoxovanadates

RBCs – Red blood cells

RO – Reverse osmosis

ROS – Reactive oxygen species

RT – Room temperature

S156A – Serine replaced by alanine

S156E – Serine replaced by glutamic acid

S183A – Serine replaced by alanine

S183E – Serine replaced by glutamic acid

SEM – Standard error of the mean

Ser156 – Serine 156

Ser183 – Serine 183

V_{rel} – Relative cell volume

1. Introduction

1.1. Importance of water in living cells and discovery of aquaporins

Water is an important and abundant component for all living cells, where the maintenance of water homeostasis is essential to the organisms' physiological processes [1]–[3]. Over the last decades, water exchanges between the inside and outside of the cells have been investigated and major advances have been achieved. At first, when lipid bilayer was discovered, investigators proposed that water permeability would occur only by simple diffusion through the lipid plasma membrane. However, studies in various cell models, as red blood cells (RBCs) [4] suggested that water permeability by simple diffusion through the hydrophobic bilayer could not explain the high water permeability observed. Therefore, it was proposed the existence of specialized water-selective channels in the cells' plasma membranes [3]. Currently, it is well known that water crosses the cell membranes by two distinct pathways: partition/diffusion of water molecules across the hydrophobic bilayer and single water diffusion through specialized protein channels known as aquaporins [5]. Considering that the activation energy (E_a) measures the energy barrier to water movement across a membrane, water transport mediated by aquaporins present lower values of E_a compared with diffusion through lipid bilayer [5], [6].

The first water channel was discovered in erythrocytes' membrane and was named CHIP28; when cloned in oocytes from *Xenopus laevis*, it induced increased osmotic water permeability. When RBCs were incubated with $HgCl_2$, a known potent inhibitor of water channels, water permeability decreased and could be restored by incubation with reducing agents [7]. Prior to these experiments with CHIP28, the discovery of the effect of these two reagents in RBCs' water permeability was reported by Robert Macey and colleagues that concluded that the water channel protein should contain a free sulfhydryl in the pore [3]. Moreover, considering that both reagents did not affect water transport across the lipid bilayer, Agre and co-workers concluded that CHIP28 protein, presently called as aquaporin-1 (AQP1), was a functional unit of membrane water channels [7]. Later, the developed work by Peter Agre and colleagues in this field, was recognized with the Chemistry Nobel Prize in 2003.

1.2. Aquaporins

Aquaporins (AQPs) belong to a highly conserved and diversified group of membrane proteins called membrane intrinsic proteins (MIPs) that facilitate the transport of water, glycerol and other small solutes as urea, ammonia, hydrogen peroxide and carbon dioxide across cell

membranes. This family of ubiquitous channel proteins comprise more than 1700 integral membrane proteins found in all-living organisms [8]. Therefore, aquaporins have representatives in all kingdoms: archaea, eubacteria, fungi, plants and animals [9]. In archaea, it was identified an aquaporin-like sequence – AqpM - that showed to be a moderate water channel and a very poor glycerol transporter with high thermostability [10]. Various eubacteria possess only one orthodox aquaporin and one aquaglyceroporin. For example, *Escherichia coli* has AQPZ as an aquaporin strictly selective for water and one AQP-like sequence, the glycerol facilitator (GlpF) [11], [12]. In the case of yeast *Saccharomyces cerevisiae*, it was identified two orthodox aquaporins (ScAqy1 and ScAqy2) and two aquaglyceroporins (YFL054Cp and ScFps1) [13]. Also, plant aquaporins show a high multiplicity of isoforms and are divided into four subgroups: plasma membrane intrinsic proteins (PIPs), tonoplast intrinsic proteins (TIPs), nodulin-26-like intrinsic membrane proteins (NIPs) and small basic intrinsic proteins (SIPs) [14]. Finally, in mammalian cells, in particular in human cells, there are 13 aquaporin isoforms (AQP0-12) found differentially expressed in organs and tissues that can be divided into three subfamilies:

(1) classical or orthodox aquaporins (AQP0, AQP1, AQP2, AQP4, AQP5, AQP6, AQP8), considered strictly selective to water. However, AQP6 also transports anions as nitrate and AQP8 transports free radicals as hydrogen peroxide (H_2O_2);

(2) aquaglyceroporins (AQP3, AQP7, AQP9, AQP10) that besides water, are also permeable to small uncharged molecules, in particular glycerol, and other small solutes;

(3) S-aquaporins (AQP11, AQP12), also called subcellular aquaporins, that show deviations from AQP signature sequence (asparagine-proline-alanine (NPA) boxes that will be described below) [15], [16]. AQP11 was recently reported to transport both water and glycerol [17] however, AQP12 function is still not clear.

1.2.1. Aquaporins structure and function

In 2001, the first AQP1 structure from bovine RBCs was determined by X-ray crystallography at a 2.2 Å resolution [18] (**Figure 1.1**).

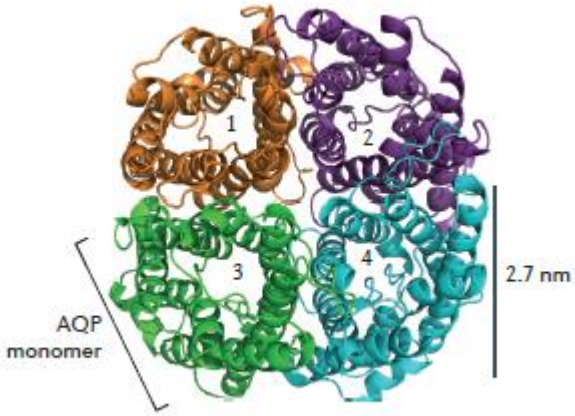

Figure 1.1: Top view of the extracellular face of an aquaporin-1 (APQ1) homotetramer, with monomers labelled from 1 to 4, based on the X-ray structure of bovine AQP1. (Adapted from [19]).

As shown in **Figure 1.1**, AQP1 is organized as tetramers in membranes where each monomer functions as an independent water pore, granting higher selectivity and higher water permeation [20]. The arrangement of the 4 monomers creates a central pore that may act as a gas (CO_2, NO) or a cation channel [21]. Nowadays, more high-resolution structures of AQPs are available, allowing to understand the atomic-level mechanisms and enabling their application for molecular dynamics simulations and virtual screening [18], [20].

Earlier to the identification of AQP1 structure by X-ray crystallography, the studies on AQP structure began with electron crystallographic analyses of 2D crystals purified from red blood cells [22], with low-resolution, that allowed the comprehension of the general topology of AQPs [19]. In 2000, these analyses reached a final density map with a resolution of 3.8 Å that was sufficient to build an atomic model for AQP1, revealing for the first time the architecture of an AQP water pore [23] (**Figure 1.2**).

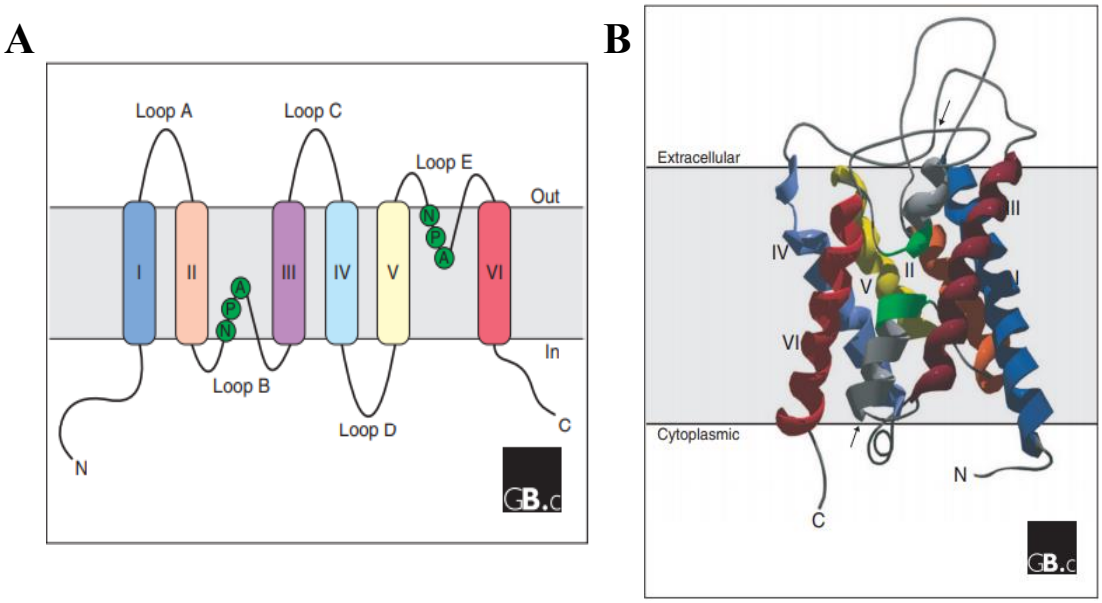

Figure 1.2: Topology and three-dimensional structure of an aquaporin protein within the membrane. **A** – Topology structure of an aquaporin within the membrane, representing the six transmembrane helices from I to VI and the five loops from A to E. Loops B and E contains the conserved NPA motifs. C represents the carboxyl terminus and N represents the amino terminus. **B** – "Hourglass" three-dimensional structure of an aquaporin monomer (a ribbon model of NtAQP1, a PIP1 protein from tobacco) within the membrane. The arrows represent short α-helices, that were formed by loop B and E, entering the membrane from the extracellular and intracellular surfaces; the two NPA boxes are indicated in green; the six transmembrane helices from I to VI are also shown. (Adapted from [9]).

AQPS monomeric units are ≈ 30 kDa [19] and consist of six transmembrane helices (from I to VI) and five connecting loops (from A to E), with N- and C-terminal domains located in the cytoplasm. Loops A, C and E are extracellular and loops B and D are intracellular. The protein is composed of two internal tandem repeats, comprising the amino- and carboxy terminal halves of the protein. Each one of the repeats includes three transmembrane helices and a highly conserved loop following the second transmembrane helix – loop B and loop E – that include NPA sequences, a conserved signature motif. Loops B and E form short α-helices (HB and HE) that folds back into the membrane, with loop B entering the membrane from the cytoplasmic side and loop E from the extracellular side. The NPA boxes are orientated in 180 degrees to each other, creating an aqueous pathway through the aquaporin pore as proposed in the hourglass model [9] (**Figure 1.2B**).

This hourglass-shaped structure of AQPs has an extracellular and a cytoplasmic vestibule where water molecules are presented to be permeated through a central amphipathic pore region of 20-25 Å, that connects the two vestibules. In AQPs amphipathic pore, two-stage filters responsible for high selectivity to water and glycerol permeation are found: one corresponding to the NPA motifs interaction at the membrane centre, that generates an electrostatic barrier for proton exclusion, and a selectivity filter located approximately 10 Å away from these motifs [24]. This selectivity filter is also known as the aromatic/arginine (ar/R) constriction, because it is composed by conserved aromatic and arginine residues [18]. It is located at the narrowest point

of the channels, being formed by three (in aquaglyceroporins) or four (in orthodox aquaporins) residues that determine the size of molecules allowed to be permeated, distinguishing features that identify the aquaporins subfamilies [23], [25], [26].

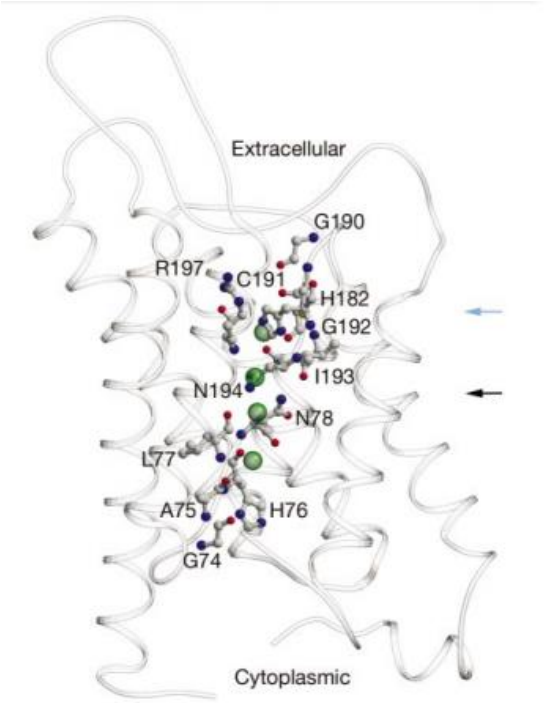

Figure 1.3 – AQP1 selectivity filter, important amino acid residues and water molecules forming the hydrophilic face of the channel pore. Cut-away side view of the channel with secondary structure shown in ribbon format. Side chains critical to establishing the hydrophilic path across the length of the selectivity filter are shown. The four water molecules located within the selectivity filter are represented as green spheres. Of these four water molecules only the middle two are close enough to form a hydrogen bond between water molecules. The constriction region and NPA motifs are indicated by light blue and black arrows, respectively. (Adapted from [18]).

AQPs strictly prevent the conduction of protons through the pore, being highly selective to water or glycerol transport. The mechanism for proton exclusion was proposed by Murata and co-workers from the AQP1 structure obtained by electron crystallography [23]. Loops B and E are held together by Van der Waals interactions between the proline residues of the NPA motifs, close to the centre of the pore. On the other hand, the two asparagine residues of the NPA motifs (Asn76 and Asn192) are held tightly in position and extend their polar side chain residues into the pore. Due to the positive electrostatic field generated by the dipole moments of the pore helices, a water molecule approaches the pore centre and orients itself to the side of NPA motifs to allow the oxygen atom form hydrogen bonds with the amine groups of the two asparagine residues [22], [23] (**Figure 1.4A e 1.4B**). Consequently, the two hydrogen atoms from the water molecule are oriented perpendicular to the pore axis, preventing the formation of hydrogen bonds with the adjacent water molecules (**Figure 1.4C**). Therefore, the water molecule can only form hydrogen bonds to the NPA motifs by the oxygen atom while the hydrogen atoms can only establish hydrogen bonds outwards the centre of the pore and towards the extracellular and

cytoplasmic pore entrance. Thus, NPA motifs are essential to compensate the energy cost of dehydration by replacing the interactions from the solvent, and to establish a pathway for coordinating water transport (or glycerol in aquaglyceroporins), guaranteeing the blockage of the protons permeation [18], [19], [23], [24].

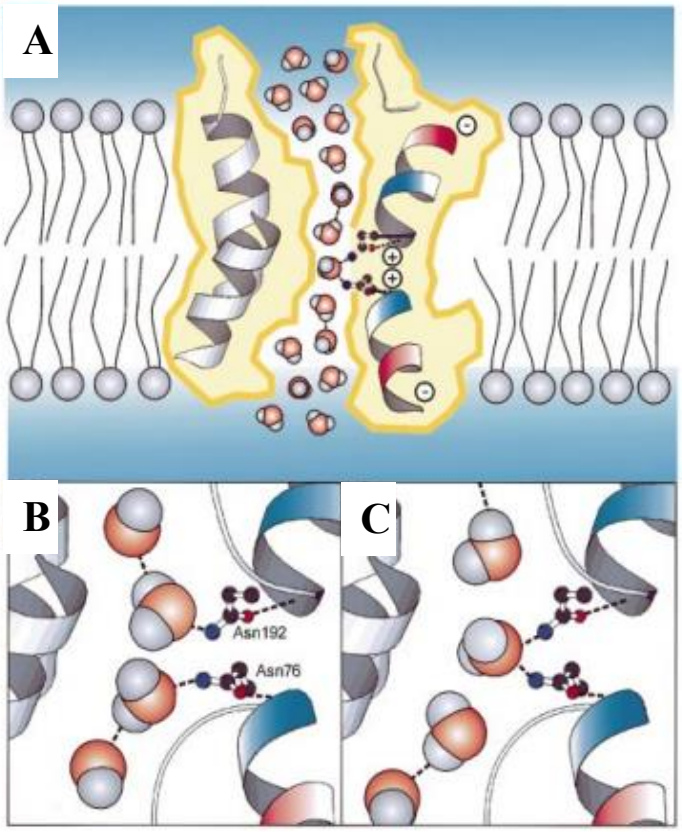

Figure 1.4: Representation of the mechanism for water permeation and blockage of proton transport of AQP1. **A** – Representation of how the partial charges from the short helices' dipoles reorient the water molecules passing through the constriction of the pore. **B** and **C** – Representation of the hydrogen bonding of the oxygen atom of the water molecule to the amide groups of Asn76 and Asn192. (Adapted from [23]).

The ar/R constriction region in AQP1 is located at the beginning of 20 Å long selectivity filter. At the constriction region, residues His182 and Arg197, along with the accessible carbonyl oxygen of residue Cys189, compose the hydrophilic face of the pore. The imidazole ring of His182 is extended into the pore while Arg197 is pointed upwards, parallel to the pore axis [18]. Concerning Cys189, it is the site for blockage of AQP1 by $HgCl_2$. Its side chain extends to the pore from the extracellular side of the constriction region, suggesting that inhibition by this mercury compound results in physical blockage of the water transport. Opposite to the hydrophilic face, there is the hydrophobic face where Phe58 is located. Therefore, ar/R constriction region in AQP1 is formed by Arg197, His182, Phe58 and Cys189 being the first three residues highly conserved across water-specific aquaporins. This region corresponds to the narrowest point of the pore with a 3 Å diameter that limits the size of substrates allowed to permeate the pore, which is

only slightly larger than the 2.8 Å diameter of a water molecule [22]. Therefore, the pore constriction prevents permeation of all molecules bigger than water, including hydrated ions. For aquaglyceroporins, in the case of GlpF, His182 is replaced by glycine that provides additional room to Cys191 be replaced by phenylalanine. These two substitutions increase the size and hydrophobicity of the GlpF constriction region, allowing simultaneously the transport of glycerol and the low permeability to water [24].

1.2.2. Localization, biological functions of aquaporins and associated pathologies

AQPs are widely expressed in the body, especially in tissues that involve fluid transport since their function is to facilitate the water and glycerol transport through the plasma membrane. Therefore, these channels are involved in many physiological processes in epithelia, central nervous system, epidermis, adipocytes, collecting duct of kidney, among others [9], [19], [27]. Studies of phenotypes of AQP-knockout mice have provided information about the AQP physiology and, consequently, of the pathologies associated, being also relevant for the discovery of potential AQP modulators. Below, data from AQP-knockout mice studies are discussed for the main aquaporins' physiological functions, especially detailed for the aquaporins under study in this work: AQP1, AQP3, AQP5, AQP7 and AQP9.

1.2.2.1. Transepithelial water transport

AQPs facilitate transepithelial water transport in the kidneys, in response to osmotic gradients created by transport of active ions and neutral solutes. AQP1 is expressed in the apical and basolateral membrane of the renal proximal tubule and the thin descending limb of Henle, as well as in the endothelial cells of descending vasa recta. Studies with mice deficient in AQP1 revealed the reduced water permeability leading to the impairment of the water reabsorption in the renal proximal tubule and of the renal count-current multiplication in descending limb of Henle and vasa recta. Therefore, AQP1-knockout mice are unable to concentrate urine leading to water diuresis, enhancing the important role of this aquaporin in the renal urinary concentrating mechanism [19], [28]. Moreover, this defects in urine concentration when AQP1 is not being expressed are unlikely to affect NaCl and urea permeabilities since AQP1 does not permeate these solutes, suggesting that the water diuresis is just a result of water permeability depletion [29].

Aquaporin-2 (AQP2), aquaporin-3 (AQP3) and aquaporin-4 (AQP4) are located in the kidney collecting duct epithelial cells: AQP2 is expressed in the apical membrane and intracellular vesicles and AQP3 and AQP4 are expressed in the basolateral membrane [30]. For an effective water reabsorption, kidney cells from the collecting duct require a high transepithelial permeability to water that is attained by the constitutively active AQP3 and AQP4 in basolateral cell membrane and also by the vasopressin-induced trafficking of AQP2 from intracellular

vesicles to the apical cell membrane [19]. In mice deficient of AQP2, AQP3 and AQP4, the urine concentration is impaired in the collecting duct, being expected that potential modulators of these AQPs would present a similar effect, such as the vasopressin V_2 receptor antagonists that can regulate AQP2 expression [31]. Mutations in AQP2 that interfere with its folding and cellular processing and/or its intrinsic water function, are often associated with nephrogenic diabetes insipidus (NDI), one of the known aquaporinopathies, which demonstrates the essential role of this aquaporin in the urine concentrating mechanism [32]. NDI, a hereditary disease, is characterized by polydipsia and polyuria, being the latter the main cause for the death of mutant neonatal mice since it induces renal failure [33].

Aquaporin-5 (AQP5) is expressed at the luminal membrane of serous epithelial cells in submucosal glands in nasopharynx and upper airways. Data from knockout-mice lacking AQP5 studies suggest that this aquaporin facilitates fluid secretion in submucosal glands meaning that its modulation could alter the gland secretions in cystic fibrosis or in other airway diseases [34].

Moreover, AQP1 is expressed in the apical membrane of the choroid plexus epithelium (CPE), being important to facilitate the water transport across the CPE membrane during the secretion of cerebrospinal fluid (CSF). Mice lacking AQP1 present a lower osmotic permeability that produce a significant reduction in CPE permeability and in CSF production. Consequently, the intercranial pressure decreases, suggesting that discovery of novel AQP1 inhibitors would be important to treat elevated intercranial pressure [35]. Furthermore, this aquaporin is also expressed in ciliary epithelium in the eye and data from AQP1-knockout mice revealed the decrease in aqueous fluid production and in intraocular pressure, suggesting that AQP1 inhibitors would be important to treat elevated intraocular pressure in diseases as glaucoma [36].

1.2.2.2. Central nervous systems – brain swelling, epilepsy and NMO

Aquaporin-4 (AQP4) is most abundant in astrocytes and ependymal-cerebrospinal fluid barrier, with its highest expression on the astrocytes end-feet that surround blood vessels in the central nervous system (CNS), being responsible for the control of the bidirectional fluid exchange [37], [38]. Studies with AQP4-null mice revealed the role of AQP4 in regulation of the water flux across the blood-brain barrier being involved in: water uptake into brain tissue in cytotoxic edema [39], [40] (water moves into the brain through an intact blood–brain barrier); water clearance after vasogenic edema [41] (water moves into the brain by bulk fluid flow through a leaky blood-brain barrier [27]); absorption of cerebrospinal fluid in hydrocephalus [42] and a novel therapeutic target for control of seizures, in particular, for epilepsy, since AQP4 knockout mice increase the seizure duration with increment in extracellular space volume [43]. Besides the pathophysiological functions already mentioned, this orthodox aquaporin is also implicated in neuroinflammation. Neuromyelities optica (NMO) is an autoimmune inflammatory demyelinating disease of CNS that affects optic nerves and spinal cord, associated with

autoantibodies against AQP4, the target antigen [27], [37], [44]. Also, about 50% of patients lose vision in at least one eye or are unable to walk independently [45]. The binding of AQP4-IgG to AQP4 in astrocyte end-feet activates the complement, leading to the primary astrocyte injury. After this lesion, inflammatory cells are recruited which further cause the blood-brain barrier disruption. The astrocyte loss and inflammation lead to demyelination of oligodendrocytes and neuron loss. Current NMO treatments include general immunosuppression, immunomodulation and plasma exchange [46].

1.2.2.3. Tumor – cell migration, proliferation and angiogenesis

Considering that the aim of this work is focused on the role of AQPs overexpression in cancer, their implication in this disease will be described in more detail in this chapter and especially focused for the aquaporins under study: AQP1, AQP3, AQP5, AQP7 and AQP9.

Cancer is known to be the second leading cause of mortality and is estimated to account for 9.6 million death in 2018. It is characterized by the growth of abnormal cells that have the ability to invade surrounding tissue and spread throughout the body [47]. As a result of the major progress for the comprehension of this disease, treatment has evolved for the past decades, improving cancer survival. Still, much more advances are needed in this field in terms of efficacy and improving life quality, since the therapies available are very toxic and lack effectiveness [48]. Therefore, it is essential to find new possible therapeutic targets. Considering that aquaporins are overexpressed in several types of cancer tissues, they could be potential drug targets to discover new cancer therapies.

AQP1 is highly expressed in vascular endothelial cells [49] in several different tumor cell types (as brain, breast colorectal, lung, ovarian, among others) [50] where it increases the membrane water permeability. Saadoun *et al.* reported that mice lacking AQP1 have reduced angiogenesis *in vivo*, leading to reduced tumor growth and extensive tumor necrosis [51]. Additionally, it was found evidences that AQP1 is involved in cell migration, revealing that AQP1-expressing tumors increase their invasiveness and their ability to metastasize by crossing microvascular endothelial barriers [51], [52]. It has been proposed a mechanism for AQPs in cell migration that involves a series of cellular events: first, AQPs are polarized on the front edge of cell protrusions (lamellipodium) in migrating cells, that combined with actin cleavage and the ion uptake at the tip of lamellipodium, creates osmotic gradients leading to the influx of water across the cell membrane. This causes the increase of the local hydrostatic pressure, inducing the expansion of the lamellipodium, which can create space for actin polymerization and aquaporin-dependent cell migration (**Figure 1.5**). Therefore, this suggests that AQPs mediate the rapid changes in cell shape when migrating cells squeeze through the extracellular matrix, since these cell changes demand rapid water fluxes that can only be performed in the presence of aquaporins. This explains the need of overexpression of AQPs in tumor cells, increasing the invasion and

metastasis to local tissue. Accordingly, several *in vitro* and *in vivo* assays have confirmed a decreased ability of cells to migrate when AQP1 is not being expressed [50]–[53].

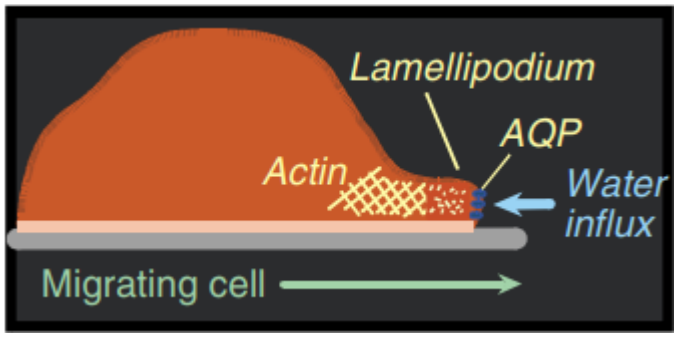

Figure 1.5 - Proposed mechanism of AQP-dependent cell migration, showing water influx through AQP at the tip of a lamellipodium. (Adapted from [30]).

AQP5 is expressed in the epithelial cells of secretory tissues [54], being upregulated in various tumors such as lung, colon and breast tumors, among others [50]. In the case of lung adenocarcinomas, AQP5 is highly expressed at the apical membrane of the alveolar type I cells, strongly increasing water permeability, with potential for local invasiveness and metastasis (normally at lymph nodes) [55], [56]. When AQP5 gene is silenced, migration and invasion are decreased, indicating that AQP5 plays an important role in the development of lung adenocarcinoma. AQP5 is also overexpressed in the ductal epithelial cells of human breast cancer tissues, normally associated with invasive carcinoma with lymph node metastasis. The highly expression of AQP5 in these cells, propose its essential role in the tumorigenesis, cancer proliferation and migration. These processes are strongly reduced when the AQP5 expression is decreased. Furthermore, Jung *et al.* suggested that the alterations in osmolarity conditions of the tumor microenvironment could be related to the progression of breast cancer through cell proliferation and migration [57]. Additionally, AQP5 is upregulated in the membrane of gastric carcinoma cells, being also overexpressed in lymph node metastasis. This upregulation leads to an increased water permeability that conducts to enhanced metastatic potential and increment of cell proliferation and migration, as in the other tumors mentioned [54].

Aquaporin-3 (AQP3) is an aquaglyceroporin expressed at the basolateral membrane of epithelial cells in kidney collecting duct, airways, intestine, urinary bladder, conjunctiva, cornea, among others. AQP3, in mammalian skin, is expressed in keratinocytes residing in the plasma membranes of the basal epidermal cell layer, being overexpressed in skin tumors [50], [58]. Hara-Chikuma and Verkman reported that AQP3-null mice are resistant to the formation of skin tumors, probably as a result of the impairment of glycerol uptake by tumor cells, with absence of papillomas. Furthermore, this deletion and reduced glycerol content leads to the decrease of intracellular ATP, suggesting that glycerol is the key regulator of ATP. For this reason, AQP3-

facilitated glycerol transport is essential for the growth and survival of tumor cells, being glycerol the main energy source for its deregulated metabolism [50], [58], [59].

Aquaporin-7 (AQP7) is expressed in the plasma membranes of normal ovarian epithelium and of benign tumor cells and nuclear membrane of borderline and malignant tumor cells whereas AQP9 is expressed in the basolateral membranes of ovarian benign and borderline tumor cells and throughout the plasma membranes of malignant cells. Yang and co-workers showed that both AQP7 and AQP9 expression is higher in malignant tumors, indicating their role in energy metabolism in ovarian epithelial tumors and in ovarian carcinogenesis [60].

Aquaporin-9 (AQP9) is uniformly distributed in the surface of the astrocytes, being localized at the border of the cerebrospinal fluid spaces and responsible for brain water homeostasis. During ischemia and in malignant gliomas, the lactate permeability of AQP9 increases as a response to lactate acidosis, resulting in glycerol and lactate clearance from the extracellular space [61]. Moreover, unlike the other cases described, AQP9 was reported to be down regulated in hepatocellular carcinoma, being localized in the basolateral membrane of hepatocytes in the liver. This aquaglyceroporin when overexpressed in these tissues, conducts to the decrease in invasion and migration of the tumor cells, preventing the tumor growth and metastasis [62].

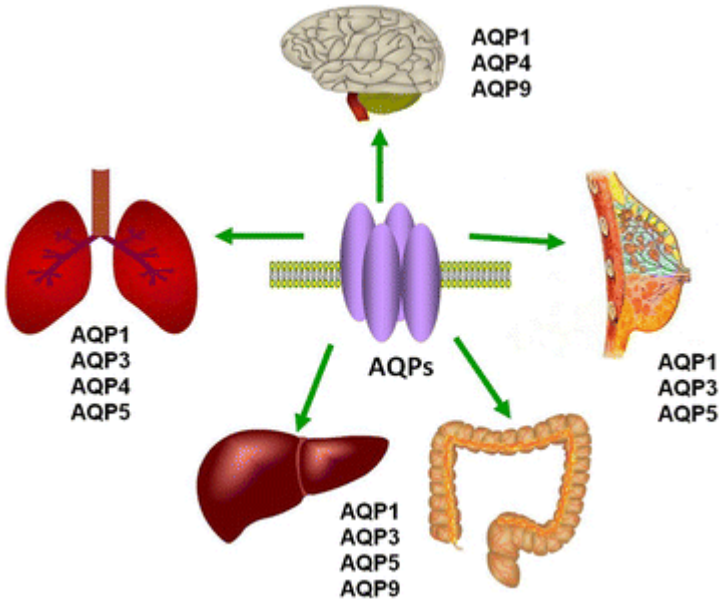

Figure 1.6 – Overexpression of aquaporins in various types of cancer: brain, lung, liver, colorectal and breast. (Adapted from [63]).

1.2.2.4. Aquaglyceroporins functions

Besides their role in the energy metabolism and progression of the tumor, there are other functions associated to aquaglyceroporins. Due to their broad pathophysiological functions already reported, the aquaglyceroporins under study (AQP3, AQP7 and AQP9) will be specifically discussed in this chapter.

As already mentioned, AQP3 is expressed in keratinocytes localized in the basolateral layer of the epidermis. By acting as a water-retaining "humectant", glycerol is essential to preserve the skin moisture. Studies with mice lacking AQP3 showed reduction of the glycerol content, leading to a decrease in stratum corneum (SC) hydration and, consequently, a decrease in skin elasticity. With glycerol replacement, the skin hydration and elasticity were restored, as well as barrier properties, evidencing the involvement of AQP3 in skin physiology [64], [65]. Moreover, AQP3-null mice have shown defective wound healing, that involves the impairment of cell proliferation and migration. As a result of AQP3-facilitated water transport, cell migration is accelerated while glycerol transport via AQP3 is required in cell proliferation [66].

Moreover, AQP3 is strongly expressed at the basolateral membrane of colonic epithelial cells. When mice have colitis and are not expressing AQP3, the colonic epithelial cells proliferation is impaired and is restored after glycerol supplementation, improving the survival and reducing the severity of colitis [67]. AQP3 is also localized in peritoneal macrophages being involved in the water and glycerol transport through the membrane in macrophage phagocytosis and migration [68].

AQP7 is expressed in adipocytes and AQP9 is expressed in hepatocytes, being both involved in the adipose metabolism. Hara-Chikuma and co-workers reported that AQP7-null mice had reduced adipocyte glycerol permeability, resulting in the intracellularly increase of glycerol and consequently, triglycerides accumulation and adipocyte hypertrophy [69]. Thus, it is proposed that AQP7 is responsible for the secretion and uptake of glycerol from the adipocyte. When AQP7 is downregulated, triglycerides start to accumulate, resulting in the development of obesity and could also result in higher concentrations of insulin due to the increase of intracellular glycerol [70]. About AQP9, it is responsible for hepatic uptake of glycerol and may be associated with the development of diabetes in terms of glycerol and glucose metabolism. In AQP9-defficient mice, levels of glycerol and triglycerides are increased and since AQP9 is not being expressed, glycerol cannot enter the cell and consequently, hepatic gluconeogenesis is impaired. This implies that glucose is not being produced and so, with glycerol oral administration, the levels of glycerol and triglycerides return to normal, enabling the production of glucose [71].

1.2.2.5. Peroxiporins and their role in cancer

Recent evidences showed that some AQPs can transport H_2O_2, called peroxiporins. H_2O_2 is a major redox metabolite, present in all aerobic organism, that intervenes in redox sensing, signalling and redox regulation [72]. It belongs to the reactive oxygen species (ROS) and when their production is imbalanced, it results in oxidative stress in the cells, causing cell damage, namely in lipids, proteins DNA, and even cell death, playing a key role in cancer development [73]–[75]. In particular, the permanent modification of DNA by oxidative damage is a critical step in mutagenesis and consequently, leads to carcinogenesis. On the other hand, H_2O_2 is an

important intracellular signalling molecule. Recent studies have reported that redox-dependent signalling is also essential to multiple cell processes such as differentiation and growth and can act as second messengers in immune cells, being involved in autophagy and mitophagy [75] and in cancer cells apoptosis. In addition to the participation in many cell processes, ROS are responsible for triggering cellular defense mechanisms that end up as a long-term protective shield [76]. Therefore, H_2O_2 has a dual effect wherein at intracellular concentrations below toxic levels, it functions as a second messenger in homeostatic redox signalling, designated as oxidative eustress. At higher concentrations, hydrogen peroxide leads to adaptive stress responses being involved in biomolecules' damage and designated as oxidative distress [72]. The regulation of these processes is maintained by multiple intracellular redox-regulating molecules such as thioredoxins that have cysteine residues for which H_2O_2 is highly reactive [73], [74]. For this redox regulation, aquaporins also play an important role since they control the passage of H_2O_2 through the membrane and thus, control H_2O_2 intracellular concentration. Currently, the aquaporins that are known to permeate hydrogen peroxide are: AQP3, AQP5, AQP8, AQP9 and probably also AQP11. Recent studies suggested that some aquaporins are able to transport NOX-derived H_2O_2, affecting redox signalling pathways mediated by hydrogen peroxide, being associated with leukaemia cell proliferation [77].

In our lab, it was recently studied the transport of hydrogen peroxide for AQP5 that plays a crucial role in cancer. Accordingly, AQP5 has been reported to be overexpressed in cancer cells and tumor tissues, suggesting its implication in tumor formation, cell migration, proliferation and adhesion to human cancer [78]. Likewise, it is hypothesized that this upregulation is due to the ability of AQP5 to permeate H_2O_2 besides water, that are essential for the cancer progression [73], [79]. In addition, AQP5 is found preferentially phosphorylated in tumor cells by cAMP-dependent phosphorylation through PKA, that regulate the expression and trafficking of this aquaporin. When there is a short exposure to cAMP, it results in AQP5 internalization from the plasma membrane while in a long exposure to this molecule, AQP5 is translocated to the plasma membrane, being abundantly expressed [78], [80]. Furthermore, Woo et. al showed that phosphorylation of the PKA consensus site – Ser156 – on AQP5, activates the Ras signalling pathway increasing cell proliferation [81], [82]. Moreover, AQP5 can change between open and closed state by a tap-like mechanism caused by the translation of His67 in the cytoplasmic end. Also, when in the open state, the selectivity filter regulates the passage of water molecules by two conformations: wide and narrow. When His173 is close to Ser183, the channel is in the narrow conformation, restricting the water passage. In the wide state, the two residues are far from each other, allowing the passage of water molecules. Moreover, by rAQP5 studies in our lab, it was showed that AQP5 phosphorylation along with deprotonation of His183 residue at pH 7.4, leads to the widening of the pore. Therefore, AQP5 might be regulated by pH dependent on phosphorylation and might also be involved in cell oxidative stress response [79]. In this work,

considering what is already known about AQP5 trafficking and expression regulation, human AQP5 regulation by phosphorylation and pH was assessed, unveiling the important residues for water permeation.

1.2.3. Aquaporin inhibitors

Considering the numerous physiological functions of aquaporins and the pathologies associated, AQPs have shown their great potential as drug targets for various diseases, including cancer. However, the identification of AQP modulators for therapeutic and diagnosis purposes has revealed to be challenging. Until now, four classes of AQP-targeted small molecules have been reported: (1) heavy metal-based inhibitors; (2) small molecules that are reported to inhibit water conductance; (3) small-molecules targeting the interaction between AQP4 and NMO autoantibody; and (4) agents that act as chemical chaperones to facilitate the cellular processing of NDI-causing AQP2 mutants [25], [50]. However, most of them show severe side effects due to the lack of selectivity, low efficiency and bioavailability. Therefore, there is an emergent need to find potent and selective aquaporin inhibitors with minimum toxicity, that could be applied to cancer therapeutics. This chapter will be focused on the most promising inhibitors identified until now for the aquaporins of interest (AQP1, AQP3, AQP5, AQP7 and AQP9), consisting in heavy-metal and small molecule inhibitors. It will be given special emphasis to polyoxometalates, compounds of vanadium, copper, zinc and gold, that were tested in this work as potential AQP inhibitors.

1.2.3.1. Heavy metal inhibitors

It is known that AQPs can be regulated by various factors, including protein phosphorylation, pH and metal ions, such as divalent transition metal cations [50]. This group of metals has been studied to assess their possible effects on aquaporins permeability. Ni^{2+} ($NiCl_2$) was reported to inhibit water permeability in AQP3 in lung epithelial cells. Later, it was found that both Ni^{2+} and Cu^{2+} ($CuSO_4$) inhibited glycerol and water permeability of AQP3 and Pb^{2+}($Pb(CH_3COO)$) and Zn^{2+} ($ZnCl_2$) had no effect on AQP3 permeability [83]. Ni^{2+} and Cu^{2+} bind to extracellular amino acid residues of AQP3 as Ser152, responsible for their effect in the aquaporin.

Mercurial compounds as $HgCl_2$ have been widely applied in aquaporin assays to assess their function, since mercury strongly inhibits these channels. The mechanism of inhibition consists of Hg^{2+} ions binding to AQPs cysteine residues. For AQP1, mercury binds to Cys189, located in the ar/R constriction region, preventing the passage of water molecules. These mercurial compounds are known to be very toxic due to their non-specificity and thus, are not suitable for therapeutic applications [50].

Furthermore, silver compounds have been tested as possible aquaporin inhibitors. In fact, silver nitrate and silver sulfadiazine were tested in RBCs and led to a rapid and irreversible inhibition of AQP1. These silver compounds showed to be more potent inhibitors than mercury compounds [84], [85].

The compounds tested throughout this work were all composed by heavy metals. The screened polyoxometalates, vanadium, copper, zinc and gold-based compounds will be addressed below.

1.2.3.1.1. Polyoxometalates

Polyoxometalates (POMs) are clusters of transition metal (W, Mo, V, Nb) and oxygen atoms. These compounds exhibit diverse sizes and structures with multiple properties and functions that are applied in catalysis, nanoscience, macromolecular crystallography and medicine. POMs have been reported as promising anticancer drug candidates however, they exhibit high toxicity and low selectivity. In this work, it was tested polyoxotungstates (POTs) and polyoxovanadates (POVs), where the latter ones have been described as more active than POTs in terms of antitumoral activity [86]. Their inhibitory effect was evaluated in aquaporins in order to predict their role in cancer and because they were reported as inhibitors of ATPases activity, that are membrane proteins just as aquaporins. The interest in POMs has been increasing due to their capacity in interacting with important enzymes including alkaline phosphatases, ecto-nucleotidases and ATPases and also due to their potential to interfere with cellular processes such as mitochondria respiration. Gumerova and colleagues identified POTs as potential inhibitors of P-type ATPases, namely Ca^{2+}-ATPase and Na^{+}/K^{+} ATPase [87], where P_2W_{18} presented the highest inhibitory activity for Na^{+}/K^{+} ATPase with 100% inhibition at 10 µM and the second highest for Ca^{2+}-ATPase with an IC_{50} value of 0.6 µM. Moreover, some polyoxovanadates have exhibited high inhibitory effect on Na^{+}/K^{+} ATPase and Ca^{2+}-ATPase [88], [89] . In addition, Bijelic *et al.* highlighted the importance of the functionalization of POMs with organic groups or the use of nanoparticles for delivery to try to mitigate the toxic effects and the lack of cell penetration, obtaining compounds with anticancer properties, suitable for therapeutic application.

1.2.3.1.2. Vanadium, copper and zinc compounds

Vanadium is a metal of high physiological, environmental and industrial importance and for the last years, vanadium compounds have been investigated for their potential as therapeutic agents for the treatment of malignancies. It appears that this metal reduces growth and spread of tumors through inhibition of tumor cell proliferation and metastasis and by inducing apoptosis and autophagy [90]. Therefore, vanadium shows potential to be an anticancer metallodrug and consequently, arouses the interest of evaluating its inhibitory effect on aquaporins permeability.

Copper is found in all living organisms and is important for the function of various enzymes and proteins in energy metabolism, respiration and DNA synthesis, which includes cytochrome oxidase, superoxide dismutase, ascorbate oxidase and tyrosinase. The main function of this metal involves redox reactions where it reacts directly with oxygen to produce free radicals and for that reason, it is tightly regulated, preventing possible toxic effect. Until now, various copper complexes have been studied for their potential antitumor activity [91]. As already mentioned above, copper has been reported as an aquaporin inhibitor, specifically for AQP3 [84]. Moreover, Ana Paula Martins and colleagues reported Cuphen inhibition of AQP3 with an IC_{50} value of (81.9 ± 4.1) μM that is particularly high, suggesting an inhibitory effect with low efficacy [92]. Also, Yukutake and co-workers described Cu^{2+} as an AQP4 inhibitor via Cys178 with an IC_{50} value of (7.7 ± 2.5) μM [93].

Zinc is an important cytotoxic/tumor suppressor agent in various types of cancer. When zinc is present in malignant cells, it has a cytotoxic effect leading to altered metabolic effects or inhibition of growth/proliferation and of invasion/migration. Therefore, this metal displays great antitumor activity [94]. As previously mentioned, studies with Zn^{2+} showed its lack of potency for AQP3 inhibition, however Yukutake and co-workers found that zinc can inhibit AQP4 expressed in proteoliposomes in a rapid and reversible way by bonding with low efficacy to Cys178 (IC_{50} value of (287 ± 58.5) μM) [93].

1.2.3.1.3. Gold-based compounds

Recently, coordination gold(III) compounds have been identified as selective and effective aquaglyceroporin inhibitors. Our lab reported a potent and selective inhibitor of AQP3 by a water-soluble gold(III) coordination compound – $[Au(phen)Cl_2]Cl$ (phen = 1,10 – phenanthroline, Auphen) (**Figure 1.7**) [95], [96] . Auphen inhibited AQP3 glycerol permeability in erythrocytes with an IC_{50} value of (0.8 ± 0.08) μM, while having a modest inhibitory effect on AQP1 water permeability [96]. Moreover, Auphen's capacity in inhibiting cell proliferation in multiple cell lines with different levels of AQP3 expression was reported [97], corroborating the results for AQP3 inhibition in RBCs. To understand the binding sites of Au(III) to AQP3, a homology model of human AQP3 was built and compared to the structure of human AQP1, enabling the identification and characterization of protein binding pockets. It is known that Au(III) ions interact with sulphur-donor groups of proteins such as the thiolate of cysteine or the thioether of methionine residues. In the case of AQP1, there is no cysteine, methionine or histidine residue accessible for gold binding, whereas thiol group of Cys40 of AQP3 is projected towards the extracellular space, approaching the channel pore. Therefore, it appears that this residue is the binding site for Auphen and other Au(III) compounds, being able to block the channel, preventing the passage of glycerol via AQP3 [96]. Moreover, after incubation with Auphen, the AQP3

activity can be recovered by addition of a reducing agent, 2-mercaptoethanol. Other Au(III) compounds were also tested for their glycerol transport inhibition in human RBCs being the most promising ones Aubipy and Auterpy [92] (**Figure 1.7**).

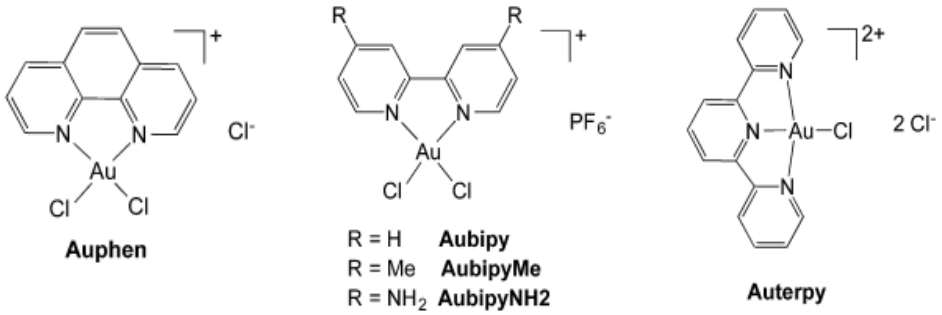

Figure 1.7: Gold(III) coordination compounds as inhibitors of aquaglyceroporins. (Adapted from [25]).

Both Aubipy and Auterpy were very effective in inhibiting the glycerol transport of AQP3 with IC_{50} values of (2.3 ± 0.7) µM and (1.0 ± 0.2) µM, respectively, being similar to Auphen in terms of potency and also in terms of reversible binding to Cys40 [92]. Due to these promising results, Auphen has revealed to be the most potent gold(III) compound in inhibiting AQP3 and for that reason, it was tested in another aquaglyceroporin, AQP7, expressed in adipocytes to assess the selectivity of this compound. Adipocytes treated with 15 µM Auphen showed a decrease on water and glycerol permeability of 63% and 79%, respectively. Through docking studies, it was found that Auphen binds close to the constriction pore and interacts with the sulphur atom of Met47 through its gold(III) centre [25], [98]. Therefore, Auphen is able to inhibit both AQP3 and AQP7 with great potency by binding to sulphur groups of certain residues, with the advantage of being non-toxic for the cells [96].

1.2.3.2. Small molecules inhibitors

Tetraethylammonium (TEA) was identified as an inhibitor of human AQP1 expressed in *Xenopus* oocytes, and acetazolamide, a carbonic anhydrase inhibitor, induced a reduction of water permeability in rat AQP1. However, it was discovered later that they did not inhibit AQP1 water permeability in RBCs [99]. In fact, Esteva-Font and co-workers tested the proposed 12 potential AQP1 inhibitors (at 50 µM) and did not find any significant water transport inhibition. Therefore, they suggested that no small molecules inhibitors actually have the capacity of affecting AQP, meaning that , until now, the heavy metal-based compounds are the only ones reported as good AQP1 inhibitors [100] .

Phloretin is a non-specific aquaglyceroporin inhibitor, being capable of inhibiting AQP3, AQP9 and the urea transporter (UT-A1). Treatment with 100 µM of phloretin leads to an AQP9

inhibition of 86% when expressed in *Xenopus* oocytes and treatment with 500 μM phloretin produces an AQP3 inhibition of 83% in proteoliposomes [84].

A new set of aquaglyceroporin inhibitors has been identified with special highlight for DFP00173 and Z433927330. The first one selectively inhibited AQP3 with slight inhibition of AQP7 and AQP9 and Z433927330 strongly inhibited AQP7 with low AQP3 and AQP9 inhibition. In terms of inhibition of AQP3 permeability in erythrocytes, DFP00173 and Z433927330 exhibited an IC_{50} value of 0.2 μM and 0.6 μM, respectively. In Chinese hamster ovary (CHO) cells expressing these three aquaglyceroporins, DFP00173 selectively inhibited AQP3 with an IC_{50} value of 0.1 μM while Z433927330 selectively inhibited AQP7 ($IC_{50} \approx 0.2$ μM) with lower inhibition of AQP3 ($IC_{50} \approx 0.7$ μM) and AQP9 ($IC_{50} \approx 1.1$ μM) [84], [101].

Overall, few drug structures were identified so far as selective AQPs inhibitors. New molecules with potency and selectivity to modulate individual AQPs are urgently needed, to foster research and development of new cancer therapeutics.

2.Thesis aims

In this project, the first aim is the screening of compounds as aquaporin modulators using as experimental models' human RBCs and yeast cells transformed with plasmid encoding human aquaporins.

The compounds will be first tested in RBCs that endogenously express AQP1 and AQP3 that are water and glycerol channels, respectively. Interestingly, AQP1, AQP3 and AQP5 are the AQPs isoforms most overexpressed in cancer tissues.

The inhibitory effect of these compounds in RBCs will be assessed by performing membrane water and glycerol permeability assays using the light scattering stopped-flow technique, already optimized and currently in use in our lab. Using this screening cell system, the inhibitory potency (IC_{50}), reversibility and selectivity will be evaluated for the compounds of interest. Their inhibitory potency and selectivity will then be validated in yeast cells devoid of endogenous aquaporins (aqy-null) and transformed with plasmid encoding individual human AQP isoforms, being an excellent tool to validate inhibitors selectivity. In this case, membrane permeability will be assayed in transformed yeasts loaded with a volume sensitive fluorophore, by a fluorescence stopped-flow technique. Overall, the data from these studies will contribute for the discovery of potent and selective AQP inhibitors with potential application for cancer therapeutics.

Moreover, knowing that AQP5 is overexpressed in cancer and so far with no inhibitors identified, mechanism of AQP5 permeation will be investigated by mutagenesis studies and permeability assays, to identify the residues responsible for permeability further contributing to the design of new drugs.

Using the optimized stopped-flow technique, the functional characterization of aquaporins from various organisms with unknown activity (eucalyptus, rice, potato, tardigrade, *Methanocella conradii*, K*yrpidia tusciae*, *Methanothermobacter thermautotrophicus* and *Novibacillus thermophilus*) will also be performed to ascertain their activity.

3. Materials and Methods

3.1 Compounds preparation

3.1.1. Polyoxometalates

The polyoxometalates (POMs) of vanadium and tungstate were sent by a collaborator from Faculty of Sciences and Technology of the University of Algarve, already in solution. Their molecular and anion formulas are summarized in the following table (**Table 3.1**).

Table 3.1: Compounds and respective anions formula and the location where the polyoxometalates were synthetized.

Compound	Molecular formula	Anion
1	$K_{12}[\alpha\text{-}H_2P_2W_{12}O_{48}].24H_2O$	$P_2W_{12}O_{48}$
3	$Na_6[TeW_6O_{24}].22H_2O$	TeW_6O_{24}
4	NH_4VO_3 pH 4.0	$V_{10}O_{28}$
5	NH_4VO_3 pH 8.48	VO_4
6	$K_3MnV_{11}O_{30}$	$MnV_{11}O_{30}^{3-}$
7	$K_7MnV_{13}O_{33}$	$MnV_{13}O_{33}^{7-}$
A	$K_6[\alpha\text{-}P_2W_{18}O_{62}].14H_2O$	P_2W_{18}
B	$K_{10}[\alpha\text{-}P_2W_{17}O_{61}].20H_2O$	P_2W_{17}
C	$Na_{12}[\alpha\text{-}P_2W_{15}O_{56}].24H_2O$	P_2W_{15}
E	$K_{28}Li_5H_7[P_8W_{48}O_{184}].16H_2O$	P_8W_{48}
F	$(NH4)_{14}[NaP_5W_{30}O_{110}].31H_2O$	P_5W_{30}

The POMs marked as 1, 3, 4, 5, 6 and 7 were sent at a concentration of 1 mM which was the concentration used in the performed experiments. The ones marked as A, B, C, E and F were sent at a concentration of 5 mM that were then diluted to 1 mM in Milli Q water to be used in the stopped-flow experiments. Since compound B, E and F were not totally soluble, they were sonicated (1 cycle for 15 minutes except for E that was sonicated and heated by bath at 30ºC multiple times).

3.1.2. Vanadium, copper and zinc compounds

12 compounds from Instituto Superior Técnico were screened by stopped-flow in this work: 3 of vanadium (P90, P91 and P103), 3 of copper (P93, P94 and P98), 3 of zinc (P96, P99 and P102) and the 3 scaffolds (Phen, Amphen and Me_2phen). The structures of these 12 metallodrugs are compiled in the next image (**Figure 3.1**).

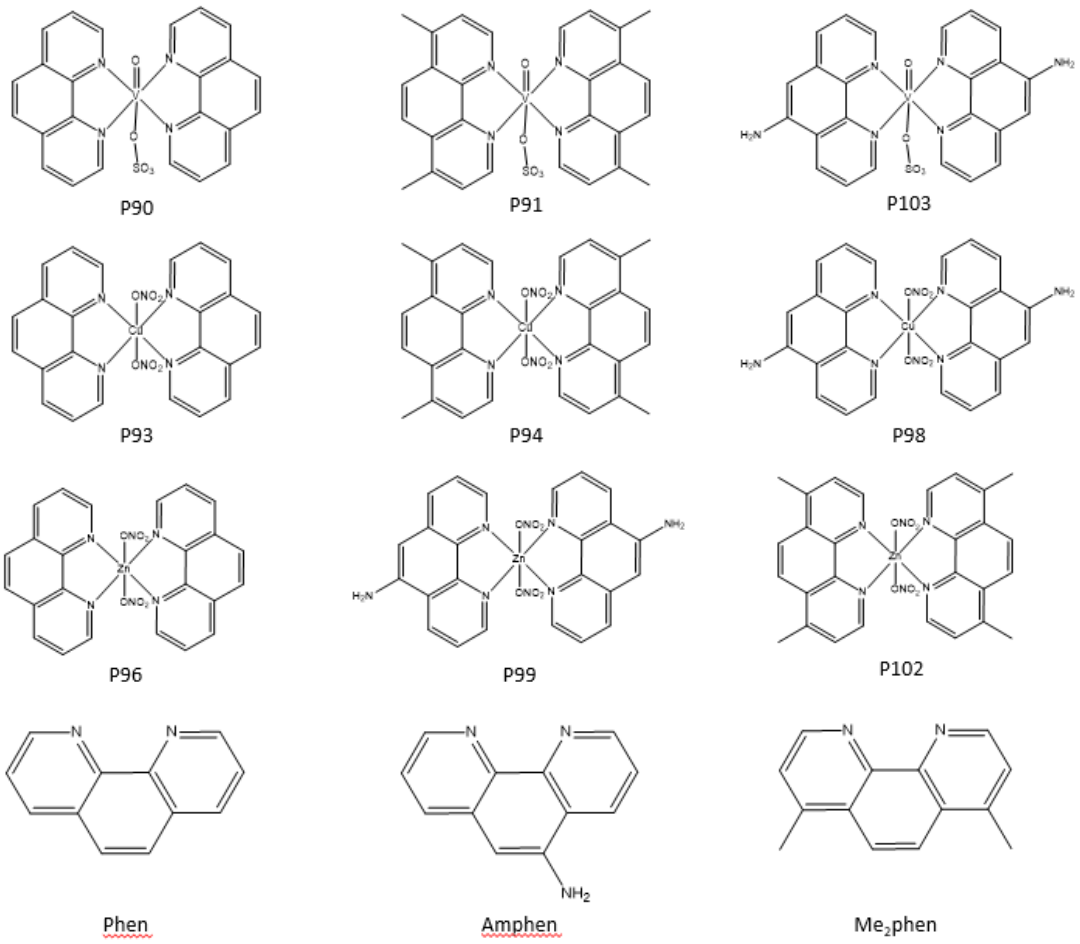

Figure 3.1: Structures of the metallodrugs provided by the Instituto Superior Técnico.

The metallodrugs arrived in powder to be prepared as a stock solution with DMSO. Most of them were prepared for a final concentration of 10 mM except for P103 and P102 which final concentration was 2.1 mM and 8.12 mM, respectively. $NaVO_3$ and NH_4VO_3 were also prepared for a final concentration of 10 mM adjusting the pH solution at 10. Subsequently, all the compounds were diluted to 1 mM with phosphate buffer saline (PBS) solution to perform the permeability assays.

3.1.3. Gold compounds

The gold compounds: RBA31, STAM013 and RBA29 from Cardiff University were screened in this work by stopped-flow. Their structures are summarized in the following image (**Figure 3.2**).

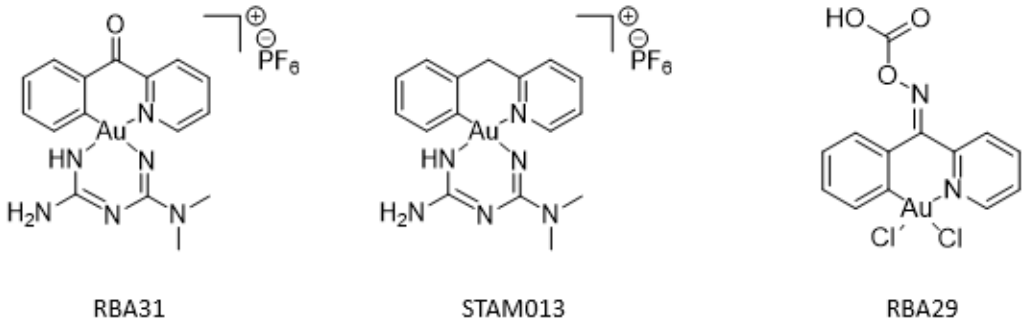

Figure 3.2: Structures of the gold compounds provided by Cardiff University.

These gold compounds arrived in powder to be prepared at a final concentration of 10 mM. First, according to the instructions from Cardiff University, the compounds RBA31 and STAM013 were solubilized in water and RBA29 was solubilized in 50:50 (DMSO/water). After following this protocol, the compounds solubilization was not achieved even after cycles of sonication and heating. In a second try, RBA31 and STAM013 were solubilized in 50:50 (DMSO/water) for a final concentration of 5 mM and then sonicated (two cycles of 15 minutes for RBA31 and one cycle of 15 minutes for STAM013). Then, they were diluted to a concentration of 1 mM to perform the experiments. RBA29 was dissolved to a final concentration of 5 mM in DMSO, being the working solution for the stopped-flow assays.

3.2. RBCs assays

The effect of the compounds on AQPs activity was first assessed in RBCs since these cells endogenously express a large amount of two aquaporin isoforms: AQP1, an orthodox aquaporin strictly selective to water and AQP3, an aquaglyceroporin that transports glycerol besides water [96]. These two isoforms are representative of the two major classes of aquaporins, rendering RBCs an excellent screening model to evaluate the inhibitory effect of compounds.

3.2.1.Ethics statement

Venous blood samples were obtained from healthy human volunteers following a protocol approved by the Ethics Committee of the Faculty of Pharmacy of the University of Lisbon. Informed written consent was obtained from all participants [92], [96].

3.2.2. Buffers and solutions preparation

The composition of the buffer used in RBCs assays is summarized in the following table.

Table 3.2: Composition of the phosphate buffered saline solution.

PBS buffer solution 300 mM pH 7.4	
Component	**Final concentration (mM)**
NaCl	137
KCl	2.7
Na_2HPO_4	10
KH_2PO_4	1.8
Adjust pH at 7.4 with HCl if necessary	

The hyperosmotic solutions used to impose osmotic shocks and cell volume changes during the permeability assays, were based in PBS buffer solution adding sucrose (impermeant solute, inducing water movements) or glycerol (permeated through aquaglyceroporins, if these are functional). Osmotic solutions were prepared to a final concentration of 200 mM.

3.2.3. Erythrocyte sampling, preparation and compound incubation

First, venous blood samples were collected from an anonymous human donor in citrate anticoagulant (2.7% citric acid, 4.5% trisodium citrate and 2% glucose) to prevent coagulation. The blood was centrifuged at 750 × *g* for less than 10 minutes at room temperature (RT) to isolate the erythrocytes discarding the plasma (yellowish supernatant) and the white blood cells (white buffy coat). The RBCs isolated were washed with PBS, capped and inverted a few times to gently mix, being then centrifuged in the same conditions as previously mentioned. This wash was repeated two more times. Subsequently, the erythrocytes were diluted to a 0.5% suspension in which 250 µL of RBCs were added to 50 mL of PBS and kept on ice to be immediately used in the experiments. Each one of the compounds were incubated in 2 mL of 0.5% suspension for 30 minutes at RT to assess their effect on RBCs permeability by stopped-flow experiments [96].

3.2.4. Reversibility assay

To assess the reversibility of the inhibition on erythrocytes permeability by the most promising compounds tested, it was selected a fixed concentration higher than the IC_{50} value of the compound to be then incubated for 30 minutes at RT in 2 mL of RBCs suspension. Subsequently, they were washed with PBS or with the reducing agent 2-mercaptoethanol (*Sigma-Aldrich*) prepared in 300 mM PBS.

In the first case, the erythrocytes with the compound were centrifuged at 750 × *g* for less than 10 minutes at RT and the supernatant was discarded. They were then washed with PBS, capped and inverted a few times to gently mix and the cells were centrifuged again. This wash was repeated one more time and with the final supernatant discarded, the RBCs were immediately tested by the stopped-flow technique.

In the second case, 2 µL of 1 mM of 2-mercaptoethanol prepared in PBS was incubated in RBCs in the presence of the compound for 30 minutes at RT and were subsequently tested in the stopped-flow equipment. A sample of erythrocytes without compound was also incubated with this reducing agent to be used as a control of its effect. This assay allows to understand if the compound of interest binds to aquaporins' cysteine residues since this reducing agent can compete for the same binding site [92].

3.3. Yeast assays

3.3.1. Strains

For the yeast assays, *Saccharomyces cerevisiae* strain -YSH 1770 – transformed with a recombinant plasmid – pUG35 - that grants the advantage of expressing only one aquaporin at a time, is available in our lab. YSH 1770 was silenced for endogenous aquaporins and subsequently transformed with recombinant plasmids constructed from amplified gene sequences that express the human aquaporins. Throughout this work, yeast cells were transformed with the empty vector and with plasmid encoding the following human aquaporins:

- YSH 1770/pUG35 (empty vector);
- YSH 1770/hAQP3;
- YSH 1770/hAQP5 and mutants (H173A, H173W, S156A, S156E, S183A, S183E) with or without GFP;
- YSH 1770/hAQP7;
- YSH 1770/hAQP9;

The plasmid pUG35 (from U. Güldener and J. H. Hegemann) was chosen since it allows the cloning of any gene of interest in line with yeast-enhanced green fluorescent protein (yEGFP3) gene, used as a reporter of *Saccharomyces cerevisiae* gene expression. Thus, when the expressed aquaporin is fused with GFP, it enables the detection of its localization in the cell. pUG35 has one selectable marker for *Saccharomyces cerevisiae* – URA3 – allowing the transformation of YSH 1770 (auxotrophic for uracil) with this plasmid. Moreover, this gene region is under the regulation of MET25 promoter and when in presence of methionine, the aquaporins expression levels are significantly decreased.

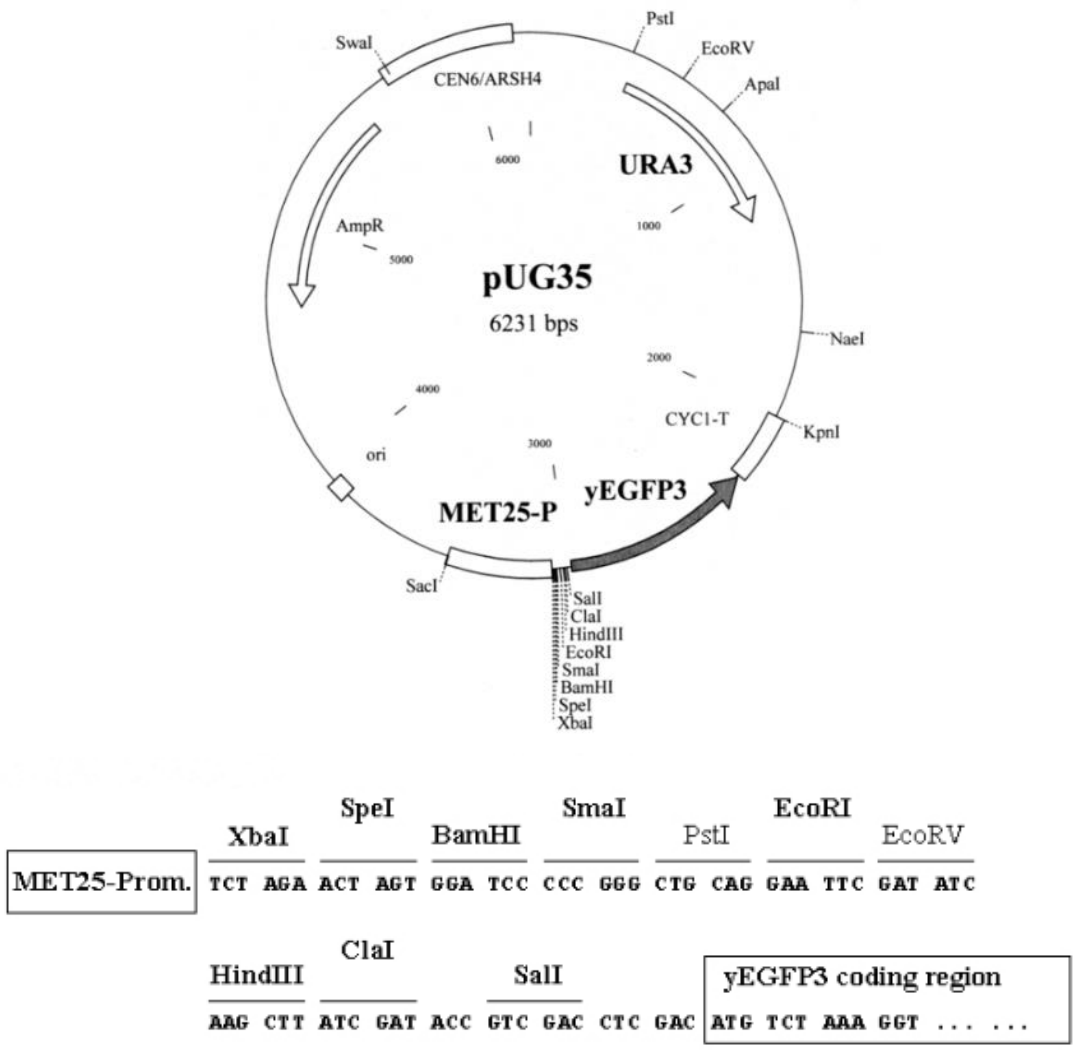

Figure 3.3: Circular map of pUG35 vector with restriction site to insert the aquaporin gene, regulated by MET25 promoter and in line with yEGFP3, the GFP gene.

Since these strains can express one aquaporin at a time allowing the validation of the potency and selectivity of the most promising aquaporin inhibitors, this model was used to validate the results obtained by RBCs assays.

3.3.2. Buffers, culture media and amino acids preparation

The composition of the buffer used to prepare the hyperosmotic and isotonic solutions for yeast assays is summarized in the following table.

Table 3.3: Composition of the potassium-citrate buffer.

Potassium-citrate buffer (50 mM) pH 5.0 and pH 7.4	
Component	**Final concentration (mM)**
Potassium Citrate	50
Phosphoric Acid	50
This buffer is at pH 5.0. To have this buffer at pH 7.4, adjust the pH with KOH	

The hyperosmotic solutions used to impose osmotic shocks and cell volume changes during the permeability assays, were based in potassium-citrate buffer solution adding sorbitol (impermeant solute, inducing water movements) or glycerol (permeated through aquaglyceroporins, if these are functional). Osmotic solutions were prepared to a final concentration of 2.1 M. The isotonic solution sorbitol at 1.4 M was also prepared in this buffer.

The composition of the culture media used to yeast growth is described in the following table.

Table 3.4: Composition of the yeast nitrogen base (YNB) culture media for *Saccharomyces cerevisiae*.

Component	Final concentration
Yeast Nitrogen Base without amino acids [10x]	67 mg/mL
Glucose [10x]	2% (w/v)
Histidine	20 mg/mL
Leucine	40 mg/mL
Tryptophan	15 mg/mL
Methionine	20 mg/mL
Agar	2% (w/v)

For the preparation of this culture media, YNB without amino acids was supplemented with the amino acids' solutions prepared: histidine, leucine, tryptophan and methionine. After the culture media and amino acids solutions preparation, both must be sterilized via sterile vacuum filtration before usage.

3.3.3. Growth and maintenance conditions

For the growth and maintenance of *Saccharomyces cerevisiae* -YSH 1770, the yeast cells were kept in test tubes in which the YNB culture media (supplemented with 2% (w/v) glucose,

2% (w/v) agar, 20 mg/mL histidine, 40 mg/mL leucine, 15 mg/mL tryptophan and 20 mg/mL methionine), was set at a slope and then grown at 27ºC for 48 hours.

To perform the stopped-flow experiments, it was essential to do a pre-inoculum and an inoculum of the yeast cells and follow the culture growth by measuring the optical density (OD) at 600 nm in a spectrophotometer (Thermo Scientific Genesys 20). The pre-inoculum was done by cell growth at 27ºC overnight with constant stirring in YNB media supplemented with 2% (w/v) glucose, 20 mg/mL histidine, 40 mg/mL leucine, 15 mg/mL tryptophan and 20mg/mL methionine, being the latter the vector repressor, allowing the yeast growth without aquaporin expression. In the day after, methionine was removed from the culture by centrifugation at 5000 × *g* for 10 minutes at RT, enabling the aquaporin expression and then yeast cells were inoculated in YNB media and grown at 27ºC overnight with constant stirring. In the next day, the cells were washed following a specific protocol and were ready to be used in the stopped-flow experiments.

3.3.4. Storage of the yeast cells

For the long-time storage of the yeast cells, they were kept in glycerol stocks at -80ºC. For this purpose, yeast cell cultures were inoculated in YNB media (2% (w/v) glucose, 20 mg/mL histidine, 40 mg/mL leucine, 15 mg/mL tryptophan and 20 mg/mL methionine) and they were grown overnight at 27ºC with constant stirring. In the following day, it was added 500 µL of pre-sterilized 30% glycerol solution to 500 µL of cell culture for 5 replicates in microtubes, that were inverted before being stored at -80ºC. When needed, the strain was revived by scraping some cells off the cell stock partially thaw and then inoculated in YNB media solid plates (2% (w/v) agar, 2% (w/v) glucose, 20 mg/mL histidine, 40 mg/mL leucine, 15 mg/mL tryptophan and 20 mg/mL methionine).

3.3.5. Yeast cells preparation and compound incubation

After the pre-inoculation, yeast cells were inoculated in YNB media (2% (w/v) glucose, 20 mg/mL histidine, 40 mg/mL leucine and 15 mg/mL tryptophan) overnight at 27ºC in the absence of methionine. In the next day, the cells were harvested in the exponential phase (OD_{600nm} ≈ 1) by centrifugation at 5000 × *g* for 10 minutes at 4ºC. Then, the cell pellet was washed three times with sorbitol 1.4 M at pH 5.0 or pH 7.4 that is an isotonic solution prepared in 50 mM citrate-phosphate buffer to maintain cell balance and avoid pH interference throughout the experiments. After this set of centrifugations, the cell pellet was resuspended in 3 mL of the same isotonic solution per gram of pellet, to normalize the number of cells. To perform the stopped-flow experiments, the yeast cells were preloaded for 20 minutes at 30ºC with the membrane-permeable non-fluorescent precursor 5(6)-carboxyfluorescein diacetate (CFDA, *Sigma-Aldrich*) with a 1 mM concentration, that is cleaved intracellularly by nonspecific esterases, producing the impermeable fluorescent form, carboxyfluorescein. Since it is a volume sensitive fluorescent dye,

allows the observation of cell volume alterations inside the cell even though yeast cells possess a rigid cell wall. After the incubation with CFDA, the cells were diluted in sorbitol 1.4 M (1:10) to be immediately used in the experiments. Each one of the compounds were incubated in 2 mL of the cell suspension for 30 minutes at RT to assess their effect on yeast permeability by stopped-flow experiments [102], [103].

3.3.6. Detection of aquaporin localization through fluorescence microscopy

For subcellular localization of GFP-tagged hAQP5 in *Saccharomyces cerevisiae*, yeast cells were first inoculated in YNB media (2% (w/v) glucose, 20 mg/mL histidine, 40 mg/mL leucine and 15 mg/mL tryptophan) overnight at 27ºC. When the cells were in the exponential phase, an aliquot of cell suspension was placed on a coverslip and were observed using a fluorescence microscope (Zeiss AAxiovert 200) at 495 nm excitation and 535 nm emission wavelengths. The images from the microscope were captured with a digital camera (CoolSNAP EZ, Photometrics, Tucson, AZ) using Metafluor software (Molecular Devices, Sunyvale, CA) [103].

3.4. Aquaporins functional assays using the stopped-flow spectroscopy

The stopped-flow technique is the main method used to determine the permeability of cell suspensions as RBCs and yeast cells [96] by following the fast-kinetics of cell volume changes over time in a millisecond-to-second scale after a rapidly imposed osmotic or solute gradient. These cell volume changes produce an analytical signal that is perceived by a suitable detection system with the ability of measuring scattering light intensity or fluorescence of a cell suspension [104]–[106]. An illustrative scheme of the apparatus operation is shown in **Figure 3.4**.

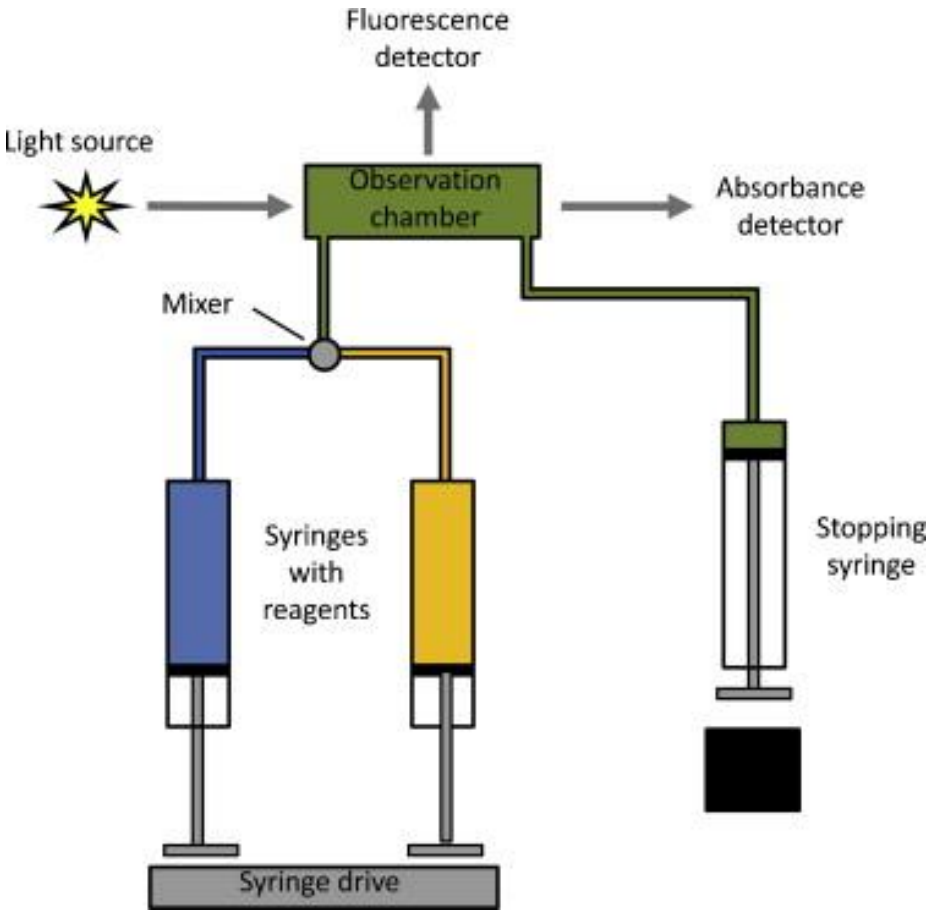

Figure 3.4: Scheme of the stopped-flow technique . (Adapted from [104]).

This approach uses two propelling syringes: one with cell suspensions balanced in an isotonic buffer and one with a solution with different osmolarity (hypo- or hyperosmotic solution) that, by a pneumatic device, inject equal volumes of the two solutions to a chamber where they are rapidly mixed, exposing the cells to an osmotic or solute gradient [106]. These solute or water fluxes from the inside and outside of the cell produce changes in the cell volume that leads to alterations in scattering light intensity in the case of RBCs or in fluorescence in the case of yeast cells [2]. The latter ones must be loaded with a volume sensitive fluorescent dye (such as CFDA). The data acquisition of the alterations in scattered light intensity or fluorescence starts when the flow suddenly stops by using a third stopping syringe, right after the mix of the two solutions where the cell suspension is subjugated to an osmotic shock [106]. Considering that there is a linear relation between the scattering light intensity or fluorescence measured and the cell volume, the water movements could be followed until osmotic equilibrium was reached. Then, by analysing the relative volume changes, it is possible to determine the osmotic (P_f) and solute permeability coefficients (P_s) [2].

Throughout this work, the stopped-flow experiments were performed on a HI-TECH Scientific PQ/SF-53 apparatus, which has a 2 ms dead time (interval between the start of the mixing and the earliest possible observation time), temperature controlled and interfaced with a computer [105]. For both cell models, the experiments were performed at 23ºC for glycerol permeability (P_{gly}) and water permeability (P_f) and for each compound concentration, 4-10 replicates were analysed. For the yeast cells, the E_a measurements were done in a temperature range between 9ºC and 34ºC.

3.4.1. Functional assays for RBCs

The RBCs functional assays were performed to assess the water and glycerol transport through AQP1 and AQP3 respectively, in control RBCs (absence of compound) and in the presence of an aquaporin inhibitor, at pH 7.4 (human physiological pH). To evaluate the water transport, 100 µL of a fresh erythrocytes' suspension (0.5% suspension prepared in 300 mM PBS) was mixed with 100 µL of 200 mM hyperosmotic sucrose solution (500 mOsM) which is a non-permeable solute that causes an osmotic gradient, leading to fast water efflux and consequently, to a rapid cell shrinkage [107] (**Figure 3.5**).

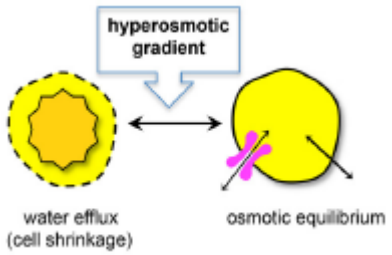

Figure 3.5: Cell shrinkage due to water efflux after an imposed hyperosmotic gradient with a non-permeable solute. (Adapted from [2]).

To assess the effect of the compounds of interest, 2 mL of RBCs were incubated with different concentrations of compounds for 30 minutes at RT before the stopped-flow experiments. The time course of cell volume changes (5 seconds to observe water transport and 40 seconds to observe glycerol transport) was followed through alterations in scattered light intensity at 90º at the wavelength of 400 nm until a stable scatter signal was reached. When cells shrink, the scatter light increases and when they reswell, the scatter light decreases, demonstrating the linear relation between these two variables [108]. Then, P_f in control and treated RBCs was calculated by the following equation:

$$P_f = k\,(V_0/A)(1/V_w(osm_{out})_\infty) \quad (cm/s)$$

where V_w is the molar volume of water, V_0/A is the initial cell volume to area ratio, $(osm_{out})_\infty$ is the final medium osmolarity after the applied osmotic gradient and k is the single exponential time constant fitted to the light scattering signal of water efflux. The k (s^{-1}) was determined by an

exponential fit to the acquired signal and was used to calculate the water permeability. Regarding the evaluation of the glycerol transport by AQP3, 100 µL of a fresh erythrocytes' suspension (0.5% suspension prepared in 300 mM PBS) was mixed with 100 µL of 200 mM hyperosmotic glycerol solution (500 mOsM) which is a permeable solute that creates a glycerol gradient directed into the cell. The cells start to shrink due to water efflux while glycerol enters the cell as a result of its chemical gradient, leading also to water influx, and consequently, to cell reswelling. Since this solute is not diffused through the lipid bilayer, cell reswelling indicates glycerol influx via functional aquaporins (**Figure 3.6**).

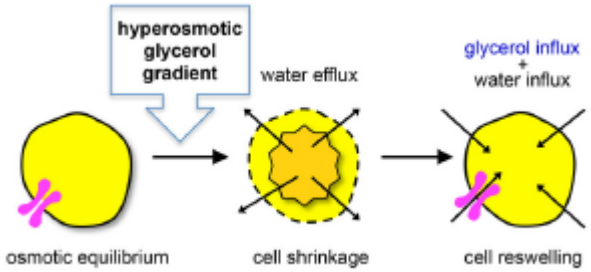

Figure 3.6: Cell volume change after imposing a hyperosmotic glycerol solution. First, the cells shrink rapidly due to water efflux while glycerol enters the cell followed by water influx, causing the reswelling of the cell. (Adapted from [2]).

To assess the effect of the compounds in glycerol permeability, cells were treated with compounds at the same conditions previously described for water permeability. The P_{gly} in control and treated RBCs was determined by the following equation:

$$P_{gly} = k\,(V_0/A) \quad (cm/s)$$

where k is the single exponential time constant fitted to the light scattering signal of glycerol influx. Just as performed for water permeability, k was determined by an exponential fit to the acquired signal for glycerol transport and was used to calculate the glycerol permeability.

For the analysis of the compounds' effect on AQP1 and AQP3 activity, the inhibitor concentration that corresponds to 50% inhibition – IC_{50} – was calculated by nonlinear regression of dose-response curves (GraphPad Prism software) using the following equation:

$$y = 100/(1+10\text{^}((\text{Log}IC_{50}\text{-}X) \times \text{HillSlope}))$$

where HillSlope describes the steepness of the family of curves.

3.4.2. Functional assays for yeast cells

Yeast cells were used to perform functional assays and assess the water transport through orthodox aquaporins (hAQP5 and respective mutants) and the glycerol transport through

aquaglyceroporins (hAQP3, hAQP7 and hAQP9) at pH 5.0 or pH 7.4, considering that pH 5.0 is the physiological pH for yeast cells growth and pH 7.4 is the physiological pH for human cells. Yeasts transformed with the empty vector were used as a control. To monitor the cell volume changes, the cells were loaded with CFDA, that is a concentration-dependent self-quenching fluorophore. CFDA is cleaved intracellularly by non- specific esterases yielding the impermeable fluorescent form that gets trapped inside the cells. When the cells shrink, the fluorophore concentration increases [109]. Therefore, when the cells are mixed with a hyperosmotic solution that causes water efflux, cells shrinkage can be followed by an increase in fluorescence. To evaluate water transport, 100 µL of cell suspension (1:10 dilution) in 1.4 M sorbitol was mixed with 100 µL of 2.1 M sorbitol, which is a hyperosmotic solution with a non-permeable solute that causes an osmotic gradient leading to fast water efflux and consequently, to cell shrinkage. The two solutions of sorbitol (1.4 M and 2.1 M) were prepared in potassium-citrate buffer at pH 7.4 or pH 5.0. To assess the effect of the compounds of interest, 2 mL of yeast cells suspension were incubated with different concentrations of compound for 30 minutes at RT before the stopped-flow experiments. The fluorophore was excited using the light source with a 470 nm interference filter and detected using a 530 nm cut-off filter. The time course of cell volume change (5 - 10 seconds for water transport and 50 seconds for glycerol transport) was followed by fluorescence quenching of the intracellular fluorophore [110]. To evaluate the glycerol transport, 100 µL of cell suspension (1:10 dilution) in 1.4 M sorbitol was mixed with 100 µL of 2.1 M glycerol, which is a hyperosmotic solution (2.1 OsM) with a permeable solute that causes a glycerol gradient driven into the cell [103]. The cells start to shrink due to water efflux while glycerol enters the cell as a result of its chemical gradient, leading also to water influx, and consequently, to cell reswelling. Since this solute is not diffused through the lipid bilayer, cell reswelling indicates glycerol influx via functional aquaporins. The solutions of 1.4 M of sorbitol and 2.1 M of glycerol were prepared in potassium-citrate buffer at pH 7.4. To assess the effect of the compounds of interest, cells were incubated with compounds at the same conditions described above for water permeability. In a first stage, P_{gly} and P_f were determined by the same equations used to calculate the water and glycerol permeabilities for RBCs assays. The analysis of the compound's effect in the aquaporins was evaluated by IC_{50} values determined by nonlinear regression of dose-response curves using GraphPad Prism, as performed for RBCs assays.

To obtain accurate permeability values in yeast cells experiments, in situations where the fluorescent signal produced by yeast cell volume change turned out difficult to analyse, the software Berkeley Madonna was used to obtain P_f and P_{gly} using customized mathematical models previously published by our group [103], [111]. To use this tool, the output fluorescence signal was converted into relative cell volume (V_{rel}) for both water and glycerol transport. The converted traces obtained enable to directly relate the cell volume change along the time, allowing to directly visualize the cell behaviour in response to an osmotic shock. This transformation was achieved

by: $(V/V_0) = V_{rel} = a\ F + b$ where V is the cell volume attained after an osmotic shock, V_0 is the initial cell volume being the ratio of V/ V_0 the relative change in cell volume, F is the ratio F/F_0 that represents the variation of the fluorescence signals and a (slope) and b (y-intercept) are constants that were estimated for each osmotic perturbation using the Berkeley Madonna software. This software uses mathematical models that allow the simulation of the cell volume behaviour when subjugated to osmotic or solute gradients and enable the estimation of permeability parameters by fitting theoretical curves to the experimental data of cell volume changes [103], [111]. To obtain these permeability values, it was first necessary to provide to the model some data such as the universal gas constant (R), the absolute temperature (T), the molar volume of water (V_w), the initial fluorescence value (F_0), the start and stop time, the initial cell radius (r), the tonicity (Λ), the initial external osmolarity ($(osm_{out})_0$), the added osmolarity and also the initial values estimated for P_f and P_{gly}. Therefore, by running the model with all the equations needed, it was possible to determine and optimize the values of water and glycerol permeability.

Furthermore, the activation energies (E_a) for water transport were assessed by performing the permeability assays at a range of temperatures from 9ºC to 34ºC, and were determined from the slope of the Arrhenius plot that relates the ln of the permeabilities with the inverse of the temperature (1/T): $\ln(P) = \ln(A) - \frac{-Ea}{R}\frac{1}{T}$ where P is the water or glycerol permeability (cm/s), A is the pre-exponential factor, E_a is the activation energy ($kcal.mol^{-1}$), R is the universal gas constant ($J.K^{-1}.mol^{-1}$) and T is the absolute temperature (K) [6]. To calculate E_a, P_f was determined at various temperatures since at high temperatures, diffusion through the lipid membrane dominates and at low temperatures, where lipids are more rigid, water transport through aquaporin channels is dominant [5]. Considering these two pathways for water permeability, lower activation energies indicate that water is being transported through aquaporin channels and higher E_a indicates that water crosses the membrane via the hydrophobic bilayer.

3.5. Statistical analysis

Data are presented as mean ± standard error of the mean (SEM). Data were first analysed with Shapiro-Wilk normality test to understand if the data followed a Gaussian distribution and then analysed using the student's t-test. For the first test, a value of $P \leq 0.05$ meant that the assumption of a normal distribution had to be rejected and for the second test, a value of $P < 0.05$ meant that the data were statistically significant.

4. Results and Discussion

4.1. Screening of metallodrugs as aquaporin inhibitors

It is known that RBCs largely express AQP1, that is strictly selective to water and AQP3, that transports glycerol and other small solutes besides water. This indicates that RBCs are a good screening model to unveil new potent and selective aquaporin inhibitors since they can be tested in AQP1, an orthodox aquaporin and in AQP3, an aquaglyceroporin, enabling the direct evaluation of their effect in water and glycerol permeability, respectively, by the stopped-flow technique. To assess the effect of the compounds in water and glycerol permeability, 2 mL of RBCs were incubated with different metallodrugs at different concentrations for 30 minutes at RT. Afterwards, using the stopped-flow technique, RBCs were rapidly mixed with 200 mM hyperosmotic sucrose solution to evaluate the water permeability or with 200 mM hyperosmotic glycerol solution to evaluate the glycerol permeability. These two hyperosmotic solutions impose osmotic shocks, changing the cell volume and consequently, altering the scattered light intensity. The representative stopped-flow traces of water and glycerol transport in control RBCs and in the presence of aquaporin inhibitors are shown in the following figure. (**Figure 4.1**).

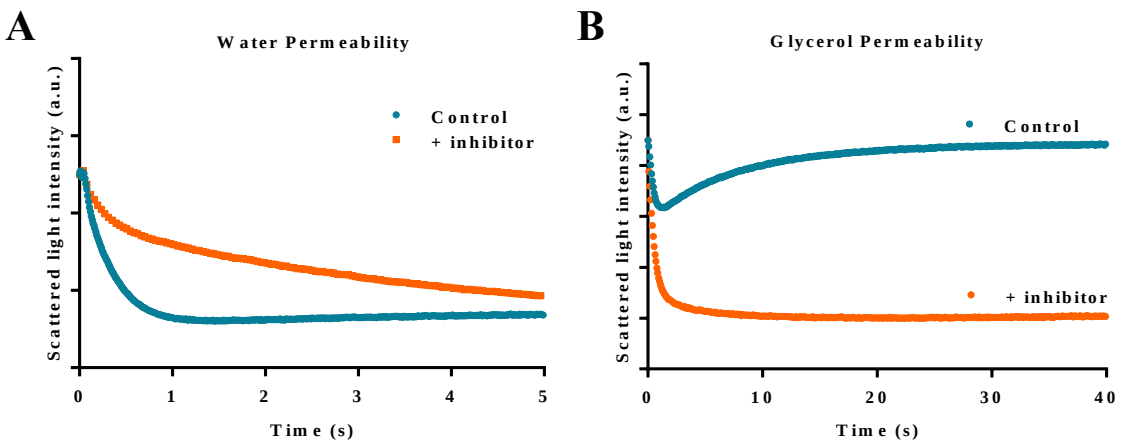

Figure 4.1: Traces of water and glycerol transport through cell membrane. **A** – Stopped-flow representative signal for water transport after imposing a hyperosmotic sucrose solution to the cells, in control RBCs and in the presence of inhibitor. **B** – Stopped-flow representative signal for glycerol transport after imposing a hyperosmotic glycerol solution to the cells, in control RBCs and in the presence of an inhibitor.

By **Figure 4.1A**, it is observed that after an imposed hyperosmotic sucrose solution, the volume of the control cells starts to decrease showing that the sucrose solution, as a non-permeable solute, creates an osmotic gradient that leads to the fast water efflux and consequently, to a rapid cell shrinkage. In the presence of an inhibitor, the water takes longer to exit the cell

considering that the aquaporin is blocked and cannot facilitate the water transport, thus the water only passes through the membrane lipids. Under the conditions of a hyperosmotic glycerol solution, which is a permeable solute, the control erythrocytes start to shrink due to the water outflow while glycerol starts to enter the cell as a response to its chemical gradient, leading also to water influx and consequently, to cell reswelling. In the presence of an inhibitor, there is no glycerol uptake since the glycerol transport is blocked. Thus, the cells shrink and are not capable to reswell. The stopped-flow experiments were performed at 23ºC for pH 7.4 (human physiological pH) and for each tested concentration, 4 signals were acquired. From doing an exponential fit to these signals, it was possible to determine the k (s^{-1}) and consequently, to calculate the P_f and P_{gly} for the control cells and the for the presence of the metallodrugs.

In order to validate the results obtained by the RBCs assays, the most promising metallodrugs were tested in yeast cells. In *Saccharomyces cerevisiae* -YSH 1770, the genes expressing endogenous aquaporins were silenced (aqy-null cells) being then transformed with pUG35 plasmid to grant the advantage of expressing only one human aquaporin at a time.

For this purpose, cells incubated with the volume sensitive dye CFDA, balanced in an isotonic solution, were treated with the metallodrugs at different concentrations for 30 minutes at RT and were then mixed with a 2.1 M hyperosmotic glycerol solution to evaluate glycerol permeability, using the stopped-flow fluorescence. All the experiments were performed at 23ºC for pH 7.4, since mammalian aquaporins are being expressed, and 5 signals were acquired for each concentration. It was possible to calculate P_{gly} by determining the k through an exponential fit of the acquired signals in the absence and in the presence of compound. To obtain accurate permeability values in yeast cells experiments, in situations where the fluorescent signal produced by yeast cell volume change turned out difficult to analyse, the software Berkeley Madonna was used to obtain P_f and P_{gly} using customized mathematical models previously published by our group [103], [111]. Through this software, the fluorescence signals were converted to relative cell volume to obtain traces that enable the direct visualization of the cell behaviour in response to an osmotic shock, as for the signals in RBCs assays.

For both RBCs and yeast assays, for the study of the metallodrugs' inhibitory effect on glycerol transport, it was necessary to calculate the IC_{50} (mean ± SEM) by doing a nonlinear regression of the dose-response curves for each of them, using GraphPad Prism.

4.1.1. Inhibition studies of water and glycerol permeability in aquaporins by polyoxometalates

4.1.1.1. Inhibitory effect of polyoxometalates in RBCs permeability

The 11 polyoxometalates compounds were grouped in three sets and labelled: 1 and 3 are polyoxotungstates, 4 to 7 are polyoxovanadates, and A, B, C, E and F are polyoxotungstates. They were first screened in RBCs in the conditions mentioned above and in the following figure, it is possible to observe the effect induced by polyoxometalates on AQP1 (water permeability) and on AQP3 (glycerol permeability), expressed as the percent of permeability relative to the control (%) (**Figure 4.2**).

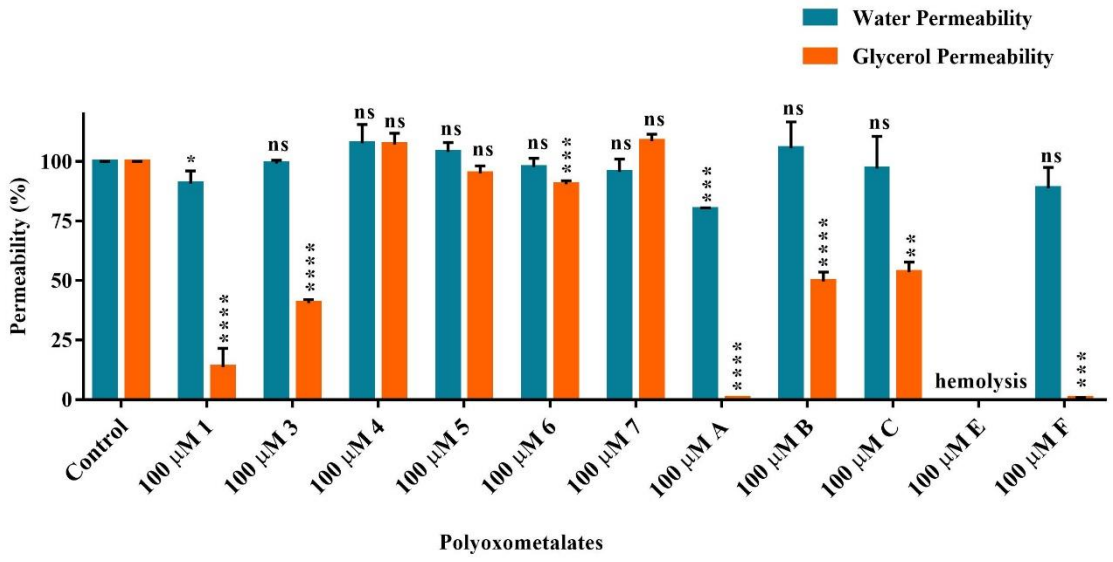

Figure 4.2: Inhibition of water and glycerol transport in RBCs by eleven polyxoxometalates at a concentration of 100 µM after 30 minutes incubation at RT. Data are shown as media ± SEM for one or two experiments. Significance levels: **** P < 0.0001, *** P < 0.001, ** P < 0.01, * P < 0.05, ns – nonsignificant, compared to the control by student t-test.

By **Figure 4.2**, it was possible to observe that most of the compounds exhibited glycerol permeability inhibition except for compounds 4, 5, 6 and 7. Considering that these four compounds are the only ones that contain vanadium as a bonding metal to AQP3, this suggests that polyoxovanadates (POVs) have no effect on glycerol permeability and therefore, they are not AQP3 inhibitors. Even though the values of glycerol permeability for POV-6 showed to be statistically significant relative to the control probably due to its low SEM, POV-6 inhibition has a weak inhibition potency on AQP3 which is confirmed by the very close values of P_{gly} for control cells and for the presence of POV-6: $(1.30 \pm 0.02) \times 10^{-5}$ (cm/s) and $(1.17 \pm 0.02) \times 10^{-5}$ (cm/s),

respectively. In addition, their lack of effect on water permeability also indicated that they did not show potential to be AQP1 inhibitors.

The polyoxotungstates (POTs), in general, showed inhibition of glycerol permeability, revealing their potential as AQP3 inhibitors. Moreover, they presented a slight effect on water permeability except for POT-A that showed the higher inhibition of water transport of all these compounds. A plausible explanation is that AQP3 transports both water and glycerol and since POT-A inhibited drastically the glycerol transport of AQP3, suggested that the percent of inhibition of water permeability corresponded to the inhibition of AQP3 water transport. Furthermore, it was not possible to analyse the water and glycerol transport in the presence of POT-E as it did not solubilize, causing the erythrocytes' hemolysis. Overall, polyoxotungstates did not exhibit potential to be AQP1 inhibitors, however their potential to be AQP3 inhibitors is a valuable starting point to discover a potent and selective inhibitor that could later be used for cancer therapeutics, which is the aim of this work.

The following graphs display the results obtained for the inhibition of glycerol permeability by polyoxotungstates and IC_{50} values (**Figure 4.3 to Figure 4.8**).

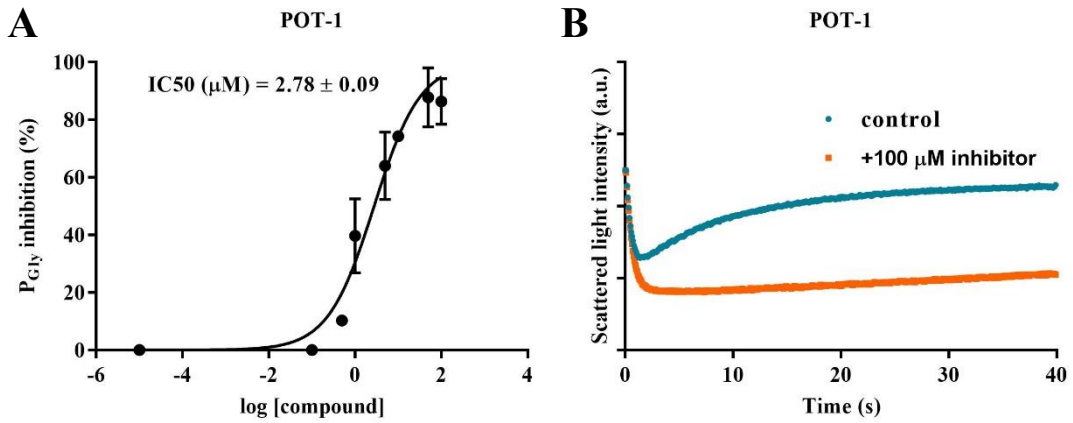

Figure 4.3: Inhibitory effect of POT-1 on RBCs glycerol permeability. **A** - Concentration dependent inhibition of glycerol permeability in RBCs by POT-1 for concentrations between 0.1-100 μM (incubated for 30 minutes at RT) with an IC_{50} value of (2.78 ± 0.09) μM (n=2) **B** – Stopped-flow signal for glycerol transport after imposing a hyperosmotic glycerol solution on the cells, for control RBCs and in the presence of 100 μM of POT-1.

The value determined for the IC_{50} of POT-1 was (2.78 ± 0.09) μM and by being a low concentration value (micromolar range), it demonstrated that this compound strongly inhibited the glycerol permeability. This inhibition can be observed in **Figure 4.3B**, where after the osmotic shock, the RBCs in the presence of this POT were not capable of reswelling since AQP3 was inhibited and could not facilitate the glycerol transport into the cell. Consequently, there was no water influx through this aquaporin, leading to cell shrinkage. Considering that Auphen is a

known AQP3 potent inhibitor with an IC50 of (0.8 ± 0.08) µM, it suggested that POT-1 was not as potent as Auphen since the IC_{50} value for POT-1 was higher.

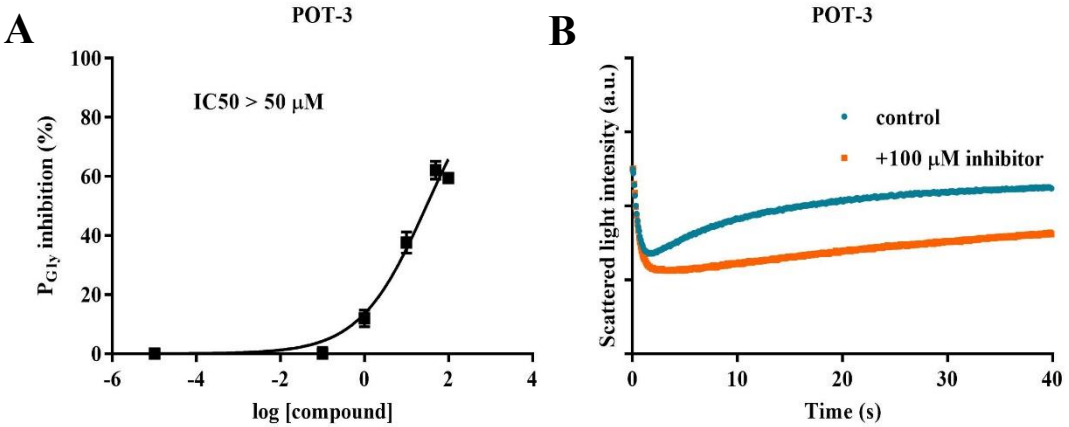

Figure 4.4: Inhibitory effect of POT-3 on RBCs glycerol permeability. **A** - Concentration dependent inhibition of glycerol permeability in RBCs by POT-3 for concentrations between 0.1-100 µM (incubated for 30 minutes at RT) with an IC_{50} > 50 µM (n=1) **B** – Stopped-flow signal for glycerol transport after imposing a hyperosmotic glycerol solution on the cells, for control RBCs and in the presence of 100 µM of POT-3.

By **Figure 4.4A**, it was interpreted that POT-3 slightly inhibited the glycerol permeability with an IC_{50} higher than 50 µM. Accordingly, as observed in **Figure 4.4B**, the cells could still reswell in its presence which confirmed that this compound is not a potent AQP3 inhibitor.

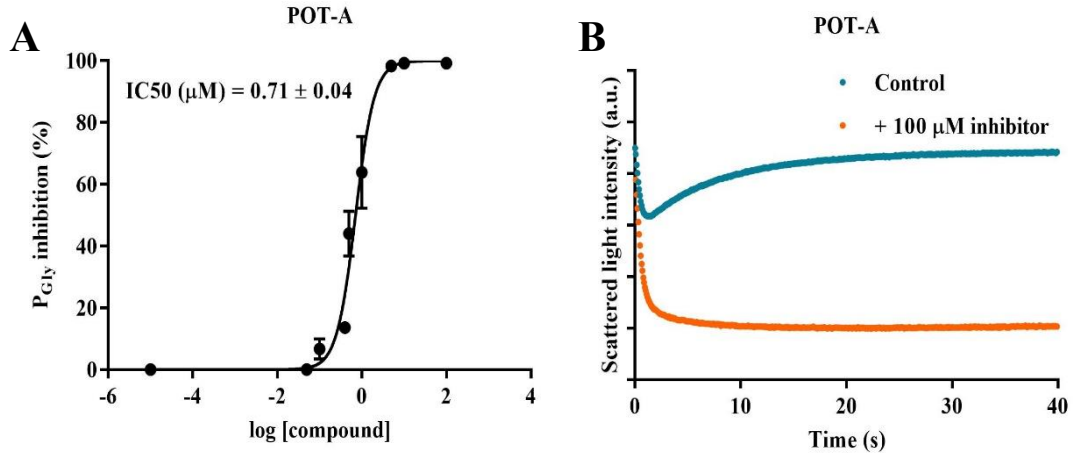

Figure 4.5: Inhibitory effect of POT-A on RBCs glycerol permeability. **A** - Concentration dependent inhibition of glycerol permeability in RBCs by POT-A for concentrations between 0.1-100 µM (incubated for 30 minutes at RT) with an IC_{50} value of (0.71 ± 0.04) µM (n=2) **B** – Stopped-flow signal for glycerol transport after imposing a hyperosmotic glycerol solution on the cells, for control RBCs and in the presence of 100 µM of POT-A.

POT-A exhibited a very low IC_{50} value of (0.71 ± 0.04) µM showing that this compound drastically inhibited the glycerol transport of AQP3. This evidence was supported by the cell behaviour showed in **Figure 4.5B** where the RBCs treated with this compound, after being exposed to a hyperosmotic glycerol solution, did not reswell as AQP3 was blocked and could not facilitate the glycerol transport into the cell. Therefore, the cells shrink due to the water efflux caused by the osmotic shock. Comparing to the potent inhibitor of AQP3 – Auphen – POT-A displayed a very similar IC_{50} value: 0.8 µM for Auphen and 0.71 µM for POT-A. This revealed that POT-A was as potent as Auphen in inhibiting AQP3 being this polyoxotungstate the most promising inhibitor of AQP3 glycerol permeability of all the POTs that were tested. Moreover, in the literature, this compound has exhibited high inhibitory activity for Na^+/K^+ ATPase (100% inhibition at 10 µM) and for Ca^{2+}-ATPase (IC_{50} = 0.6 µM), showing a similar inhibitory effect both on P-type ATPases and on AQP3 [87].

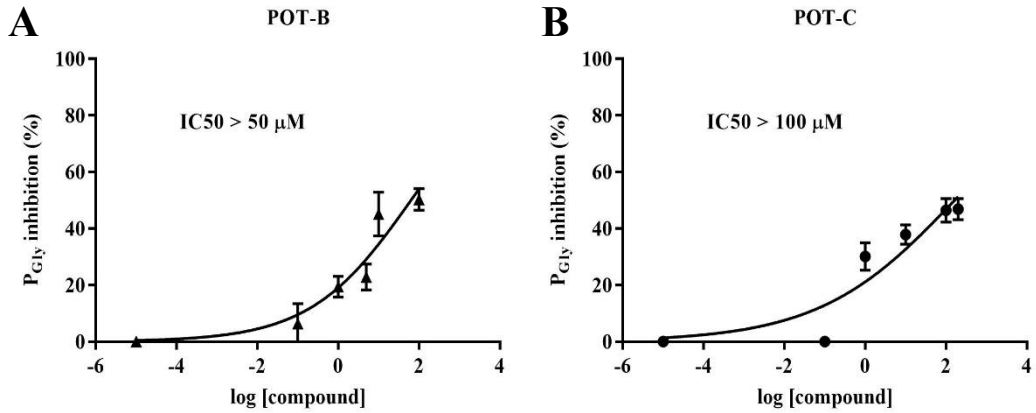

Figure 4.6: Inhibitory effect of POT-B and POT-C on RBCs glycerol permeability. **A** - Concentration dependent inhibition of glycerol permeability in RBCs by POT-B for concentrations between 0.1-100 µM (incubated for 30 minutes at RT) with an IC_{50} > 50 µM (n=1) **B** – Concentration dependent inhibition of glycerol permeability in RBCs by POT-C for concentrations between 0.1-100 µM (incubated for 30 minutes at RT) with an IC_{50} > 100 µM (n=1).

By **Figure 4.6**, it was observed that both POT-B and POT-C slightly inhibited the glycerol permeability since they presented high values of IC_{50}. Therefore, these two POTs did not affect the AQP3 activity and had no potential to be AQP3 inhibitors.

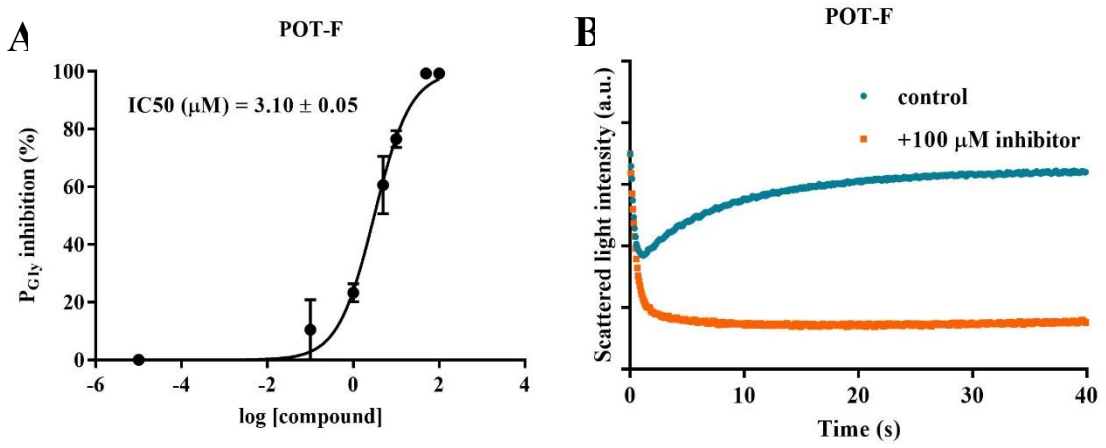

Figure 4.7: Inhibitory effect of POT-F on RBCs glycerol permeability. **A** - Concentration dependent inhibition of glycerol permeability in RBCs by POT-F for concentrations between 0.1-100 μM (incubated for 30 minutes at RT) with an IC_{50} value of (3.10 ± 0.05) μM (n=2) **B** – Stopped-flow signal for glycerol transport after imposing a hyperosmotic glycerol solution on the cells, for control RBCs and in the presence of 100 μM of POT-F.

By **Figure 4.7A**, it was noticeable that POT-F exhibited a low IC_{50} value of about (3.10 ± 0.05) μM, demonstrating its potency in decreasing the glycerol transport via inhibition of AQP3. In **Figure 4.7B**, it was shown that in the presence of this compound, the cells subjugated to an osmotic shock could not reswell since AQP3 is blocked. This cell behaviour suggested that AQP3 was strongly inhibited and could not facilitate the glycerol transport into the cell. Comparing this POT to Auphen, that has an IC_{50} of 0.8 μM, it was possible to affirm that POT-F was not as potent in inhibiting the glycerol permeability via AQP3 as Auphen. The same could be concluded by comparing the IC_{50} from POT-F with the ones for POT-1 and POT-A, since both exhibited lower IC_{50} values than 3.10 μM.

Overall, POT-A revealed to be the most promising AQP3 inhibitor of this set of compounds with a very low IC_{50} value (0.71 ± 0.04) μM. Hence, this compound exhibited great potency and efficacy in inhibiting glycerol transport in RBCs.

In order to assess the reversibility of AQP3 inhibition by POT-A and understand the possible binding sites of this compound, it was selected a fixed concentration of 5 μM, higher than the IC_{50} value (0.71 μM), to be incubated in 2 mL of RBCs suspension for 30 minutes at RT. After the incubation period, cells were washed with PBS or with 1 mM of the reducing agent, 2-mercaptoethanol prepared in 300 mM PBS. The results from this assay are shown in the next bar graph (**Figure 4.8**).

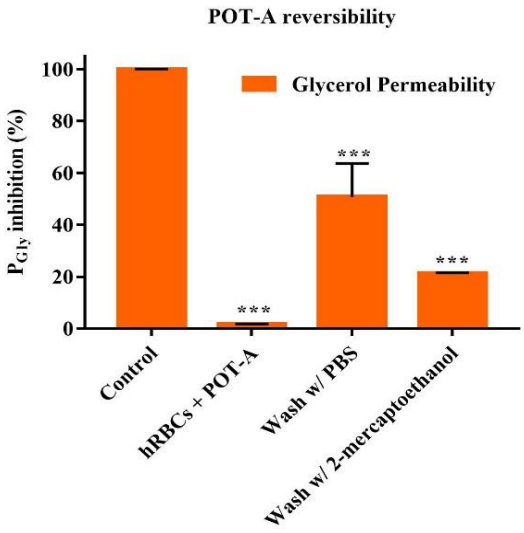

Figure 4.8: Inhibition of glycerol permeability of RBCs after treatment with 5 µM of POT-A (incubated for 30 minutes at RT) and assessment of reversibility by washing with PBS or by incubation with 1 mM of 2-mercaptoethanol (for 30 minutes at RT). Data are shown as media ± SEM for one experiment. Significance levels: *** $P < 0.001$, compared to the control by student t-test.

As observed in **Figure 4.8**, washing the cells with PBS led to a partial recovery of glycerol permeability of about 50%, indicating that the bonding of POT-A to the aquaporin is partially reversible. Thus, AQP3 activity can still be partially recovered by washing with PBS, even after being incubated with the compound. Concerning the incubation with 1 mM of 2-mercaptoethanol, this assay is usually performed to understand if the compound binds AQP3 cysteine residues since this reducing agent can compete for the same binding site. This was investigated for Auphen that showed that its gold ions had affinity to bind to sulfhydryl groups, suggesting that 2-mercaptoethanol competed with this compound, leading to an almost complete recovery of glycerol permeability via AQP3. By **Figure 4.8**, it is noticed that in the presence of this reducing agent, the glycerol permeability recovered poorly so it is very likely that POT-A has no binding affinity for AQP3's cysteine residues. Accordingly, there was no competition with 2-mercaptoethanol for sulfhydryl groups hence, further studies are needed to identify the binding sites to which tungstate shows affinity.

4.1.1.2. Inhibitory effect of POT-A in aquaporin-expressing yeast cells permeability

POT-A was tested in yeast transformed with either the empty plasmid pUG35 and in yeast transformed with plasmid encoding human AQP3 (hAQP3), hAQP7 or hAQP9, which were the aquaglyceroporin-expressing strains available in the lab at the time. The results obtained for the

effect induced by POT-A on glycerol permeability for the three aquaglyceroporins: hAQP3, hAQP7 and hAQP9 are shown in the next graphs (**Figure 4.9**).

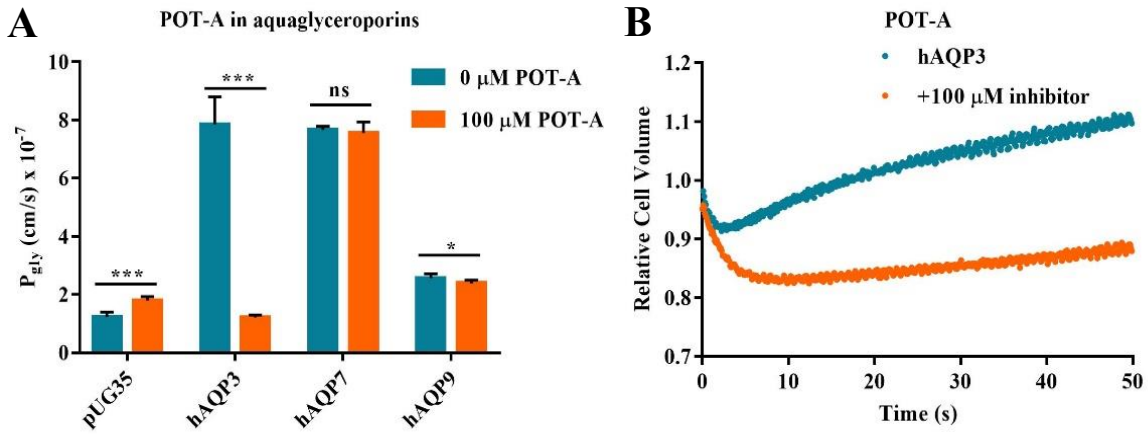

Figure 4.9: Inhibitory effect of POT-A in pUG35, hAQP3, hAQP7 and hAQP9. **A** - Effect of POT-A in pUG35, hAQP3, hAQP7 and hAQP9 (incubation for 30 minutes at RT at a concentration of 100 µM and 50 µM for pUG35 cells). Data are shown as media ± SEM for one experiment. **B** – Time course of the relative cell volume changes after a hyperosmotic glycerol solution, for yeast cells transformed with plasmid encoding hAQP3 in the absence of compound and in the presence of 100 µM of POT-A. Significance levels: *** $P < 0.001$, * $P < 0.05$, ns – nonsignificant, compared to the control by student t-test.

From **Figure 4.9A**, it was observed that POT-A drastically inhibited glycerol permeability via AQP3 with a percent of inhibition near 100 %. This can also be confirmed considering that the values of glycerol permeability for hAQP3 in presence of POT-A and for empty vector control are very similar: $(1.42 \pm 0.20) \times 10^{-7}$ (cm/s) and $(1.21 \pm 0.09) \times 10^{-7}$ (cm/s), respectively, demonstrating that AQP3 is fully blocked by POT-A action. This AQP3 blockage is corroborated by **Figure 4.9B**, where the yeast cells expressing hAQP3 treated with POT-A, did not reswell after being subjugated to a hyperosmotic glycerol solution since AQP3 was drastically inhibited and could not facilitate the glycerol transport into the cell.

For both hAQP7 and hAQP9, the glycerol permeability was not affected by this compound, thus POT-A does not show potential to be an AQP7 or AQP9 inhibitor. Overall, the stopped-flow experiments with aquaporin-expressing yeast cells validated the results from RBCs assays, since it was confirmed that POT-A is the most promising compound in inhibiting AQP3 glycerol permeability of this set of polyoxometalates. Besides confirming that this compound is a potent inhibitor of AQP3, the data about the inhibitory effect of POT-A in three aquaglyceroporins allowed to conclude that POT-A is selective to AQP3, considering that it drastically inhibits AQP3 and has no effect on AQP7 and AQP9. Comparing with Auphen that inhibits both AQP3 and AQP7, POT-A exhibits great advantage in being potent and selective to AQP3. Further studies with POT-A are needed to establish structure/activity relationships and to confirm its potential as a suitable drug candidate by testing it in cancer cell lines (on-going studies

in our lab), in order to investigate its anticancer properties and possible applications in cancer therapy.

4.1.2. Inhibition studies of water and glycerol permeability in aquaporins by vanadium, copper and zinc compounds

4.1.2.1. Inhibitory effect of vanadium, copper and zinc compounds in RBCs permeability

12 metallodrugs were screened in RBCs: 3 of vanadium (P90, P91 and P103), 3 of copper (P93, P94 and P98), 3 of zinc (P96, P94 and P98) and the 3 scaffolds (Phen, Amphen and Me_2phen) which structures are represented in **Figure 3.1** in Materials and Methods section. Moreover, $NaVO_3$ and NH_4VO_3 were also tested to assess the effect of vanadium without the presence of scaffolds. The inhibitory effect of these metallodrugs on water permeability mediated by AQP1 and on glycerol permeability mediated by AQP3 is showed in the next bar graph, expressed as the percent of permeability relative to the control (%) (**Figure 4.10**).

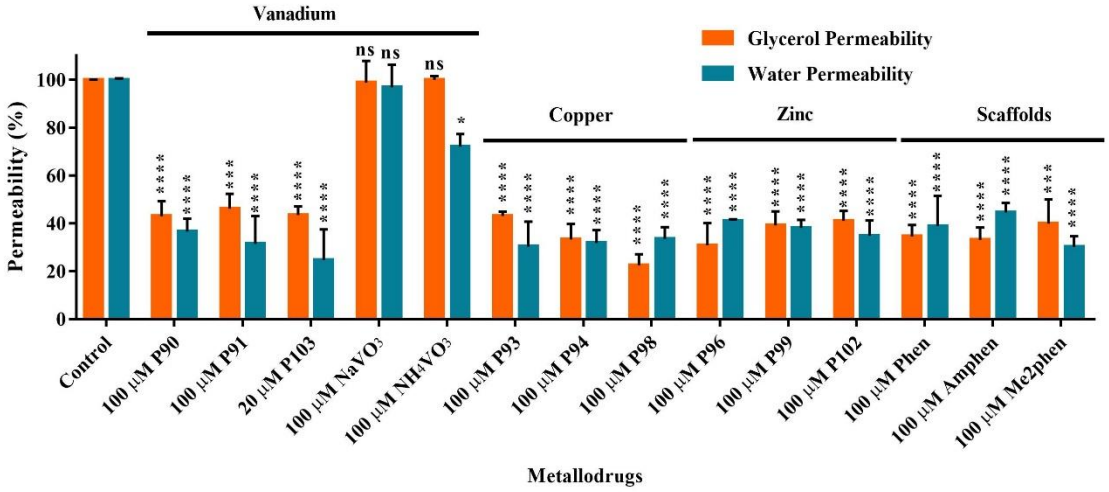

Figure 4.10: Inhibition of water and glycerol transport in RBCs by metallodrugs at a concentration of 100 µM after 30 minutes incubation at RT. For P103, the maximum concentration tested was 20 µM considering that above this concentration, the cells decrease their volume due to the effect of the compound. Data are shown as media ± SEM from one to three experiments. Significance levels: **** $P < 0.0001$, *** $P < 0.001$, * $P < 0.05$, ns – nonsignificant, compared to the control by student t-test.

Most of the compounds inhibited the glycerol and water permeability, except for compounds $NaVO_3$ and NH_4VO_3 that showed permeability's inhibitions with very low or none significance. This can be explained by the fact that these two compounds were composed of free vanadium and by neither of the three scaffolds that inhibited RBCs permeability, suggesting that vanadium in the absence of one of these scaffolds, was not capable of affecting neither glycerol nor water permeability. Therefore, $NaVO_3$ and NH_4VO_3 do not have potential to be AQP1 or AQP3 inhibitors.

In general, the majority of the set of metallodrugs and their scaffolds showed similar values of percent of inhibition for water and glycerol permeability, suggesting that their inhibitory effect is probably due to the presence of the scaffolds. To understand if these compounds had the potential to be AQP1 and AQP3 inhibitors, the IC_{50} value was calculated for each one.

The following graphs display the results obtained for the inhibition of glycerol and water permeability by metallodrugs of vanadium, copper and zinc and their IC_{50} values (**Figure 4.11 to Figure 4.14**).

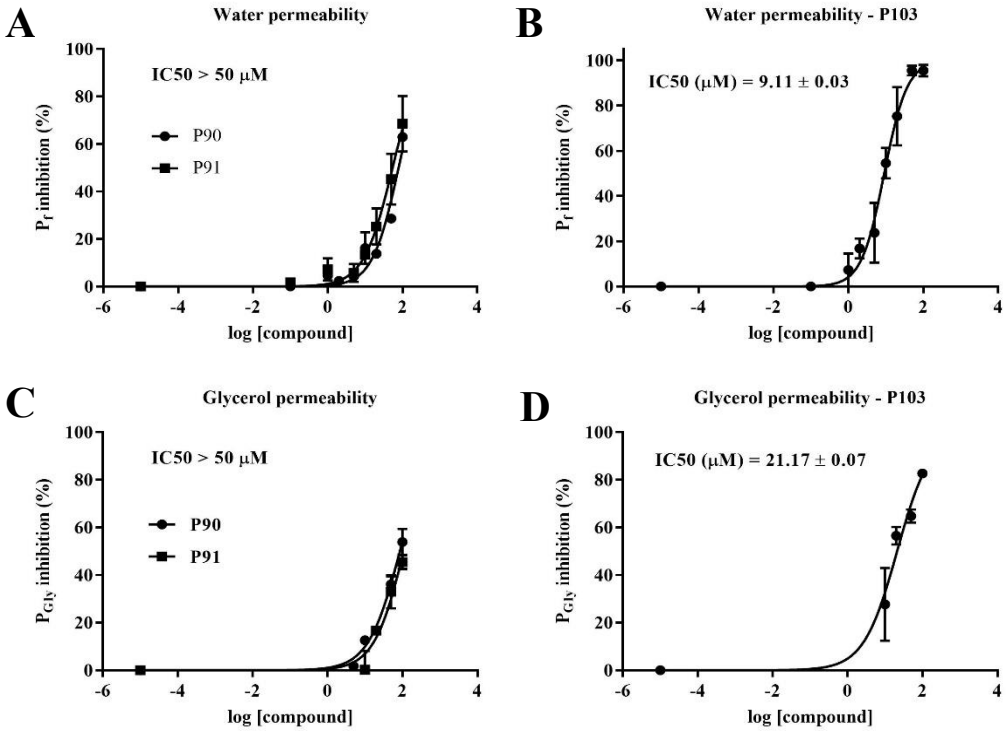

Figure 4.11: Inhibitory effect of vanadium compounds (P90, P91 and P103) in RBCs permeability. **A** - Concentration dependent inhibition of water permeability in RBCs by P90 and P91 for concentrations between 0.1-100 μM (incubated for 30 minutes at RT) with an IC_{50} > 50 μM (n=2 for P90 and n=3 for P91). **B** – Concentration dependent inhibition of water permeability in RBCs by P103 for concentrations between 0.1-100 μM (incubated for 30 minutes at RT) with an IC_{50} value of (9.11 ± 0.03) μM (n=2). **C** - Concentration dependent inhibition of glycerol permeability in RBCs by P90 and P91 for concentrations between 0.1-100 μM (incubated for 30 minutes at RT) with an IC_{50} > 50 μM (n=2 for P90 and n=1 for P91). **D** - Concentration dependent inhibition of glycerol permeability in RBCs by P103 for concentrations between 0.1-100 μM (incubated for 30 minutes at RT) with an IC_{50} value of (21.17 ± 0.07) μM (n=1).

By **Figures 4.11A** and **4.11C**, it was noticeable that both P90 and P91 slightly inhibited the glycerol and water transport by AQP3 and AQP1 respectively, considering their high IC_{50} values. Therefore, these two vanadium compounds did not show potential to be inhibitors of glycerol and water permeability. Concerning P103, this metallodrug greatly inhibited the water permeability, exhibiting an IC_{50} value of (9.11 ± 0.03) μM. This result is very promising considering that until now, there is no known potent AQP1 inhibitors. Therefore, with an IC_{50} value in the micromolar range, P103 has reveal its potential to be an AQP1 inhibitor. However, it

is important to highlight that at concentrations above 20 µM, the presence of the compound in the cells leads to a decrease in cell volume, so this compound should not be use above this concentration. For the determination of the IC_{50} value, the water permeability values for concentrations above 20 µM were included to get a better dose-response curve. Moreover, the inhibition of the water transport by P103 is also confirmed by the following graph (**Figure 4.12**).

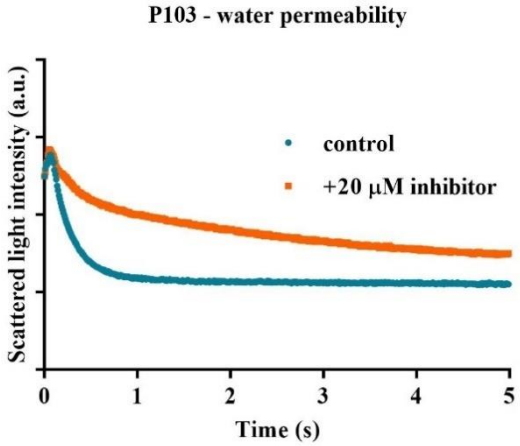

Figure 4.12: Stopped-flow signal for water transport after imposing a hyperosmotic sucrose solution on the cells, for control RBCs and in the presence of 20 µM of P103.

These stopped-flow traces support the high inhibition of water permeability by P103 since it represents the cell behaviour in the presence of this compound. After being exposed to a hyperosmotic sucrose solution, the cells shrink due to the water efflux caused by the osmotic shocks. Considering that AQP1 is inhibited and cannot facilitate the water transport, the water takes more time to exit the cell since it can only pass through the lipid bilayer. About the glycerol permeability, P103 presented a high IC_{50} value of (21.17 ± 0.07) µM, thus it weakly inhibited the glycerol transport. Therefore, it did not show potential to be an AQP3 inhibitor as Auphen or POT-A that presented much lower IC_{50} values.

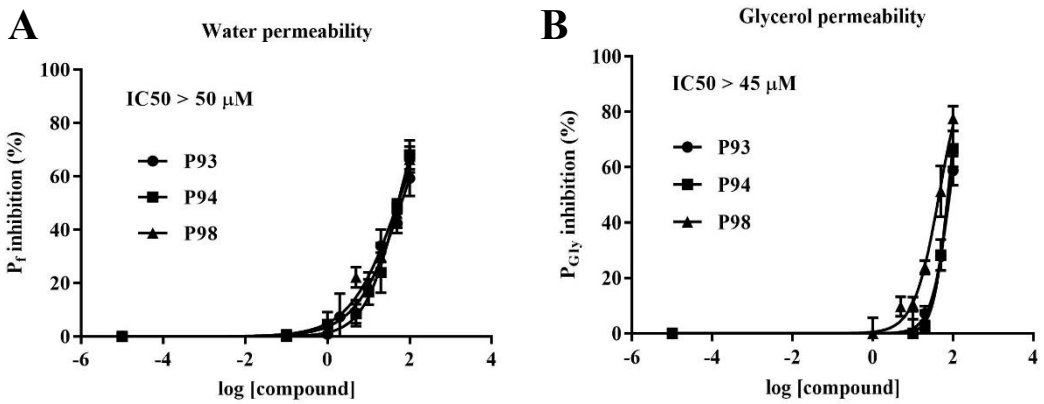

Figure 4.13: Inhibitory effect of copper compounds (P93, P94 and P98) in RBCs permeability. **A** - Concentration dependent inhibition of water permeability in RBCs by copper compounds for concentrations between 0.1-100 μM (incubated for 30 minutes at RT) with an IC_{50} > 50 μM (n=1 for all compounds). **B** – Concentration dependent inhibition of glycerol permeability in RBCs by copper compounds for concentrations between 0.1-100 μM (incubated for 30 minutes at RT) with an IC_{50} > 45 μM (n=1 for all compounds).

In **Figure 4.13**, it was observed that copper compounds weakly inhibited water and glycerol permeability, presenting high IC_{50} values above 45 μM. Therefore, these metallodrugs did not exhibit strong efficacy in inhibiting any of the two aquaporins expressed in RBCs. Furthermore, it is known by the literature that Cuphen inhibits the glycerol permeability with an IC_{50} value of (81.9 ± 4.1) μM which agrees with the results obtained for P93, P94 and P98, especially for P93 which scaffold corresponds to two molecules of Phen [92].

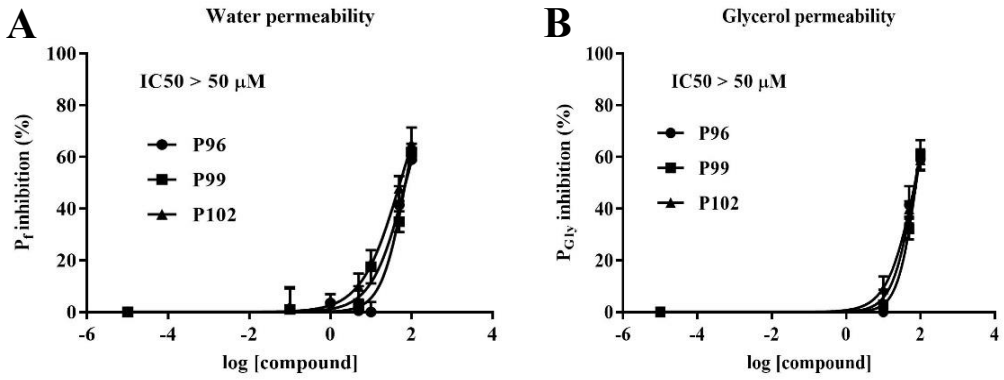

Figure 4.14: Inhibitory effect of zinc compounds (P96, P99 and P102) in RBCs permeability. **A** - Concentration dependent inhibition of water permeability in RBCs by zinc compounds for concentrations between 0.1-100 μM (incubated for 30 minutes at RT) with an IC_{50} > 50 μM (n=1 for all compounds). **B** – Concentration dependent inhibition of glycerol permeability in RBCs by zinc compounds for concentrations between 0.1-100 μM (incubated for 30 minutes at RT) with an IC_{50} > 50 μM (n=1 for all compounds).

The three zinc compounds slightly inhibited glycerol and water permeability, displaying high IC_{50} values above 50 µM. Thus, zinc did not exhibit high efficacy in inhibiting AQP1 and AQP3 and so, these metallodrugs are not potential inhibitors of water or glycerol transport.

For the scaffolds Phen, Amphen and Me_2phen, the IC_{50} values were not determined. However, it seems that for most of the compounds, their inhibitory effect is due to the presence of the scaffolds, since they show similar values of percent of inhibition for water and glycerol permeability. By the literature, it is known that Phen does not inhibit the glycerol permeability which is not confirmed by the results obtained for the scaffolds with a 100 µM concentration. Considering this is a high concentration that could possibly disturb the membrane lipids instead of actually inhibit the aquaporins, these compounds were also tested at 10 µM to confirm the literature results for Phen (that was tested at 10 µM concentration in the literature) and to ensure that the observed decrease in permeability is due to the inhibitory effect of the compounds [96]. The results from testing the compounds at 10 µM are shown in the next bar graph (**Figure 4.15**)

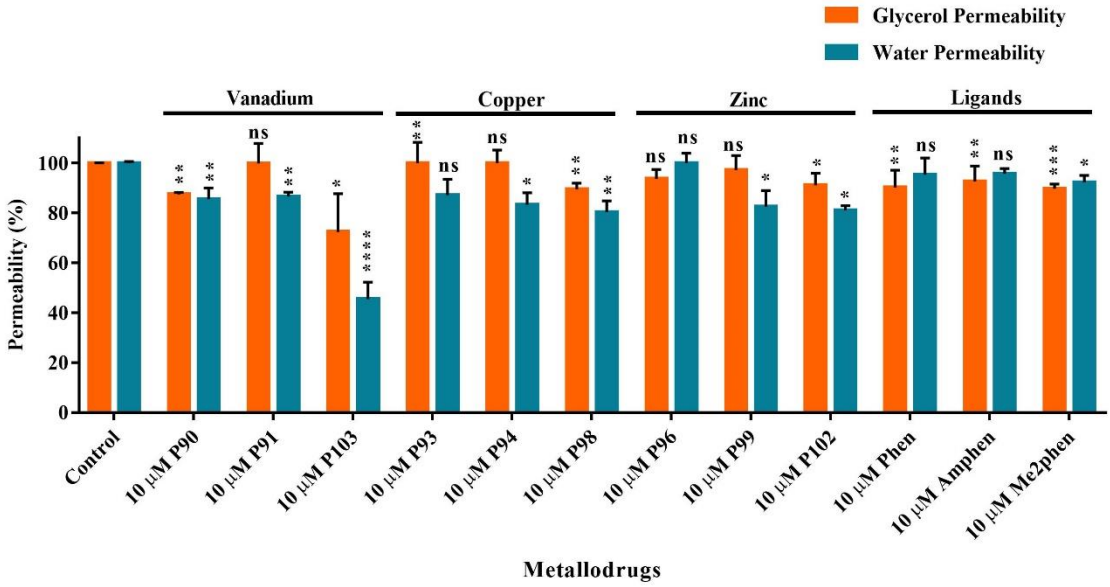

Figure 4.15: Inhibition of water and glycerol transport in RBCs by metallodrugs at a concentration of 10 µM after 30 minutes incubation at RT. Data are shown as media ± SEM from one to three experiments. Significance levels: **** P < 0.0001, *** P < 0.001, ** P < 0.01, * P < 0.05, ns – nonsignificant, compared to the control by student t-test.

From **Figure 4.15**, it can be observed that most of the compounds and their scaffolds, presented similar values of percent of inhibition of both water and glycerol permeability, as observed for 100 µM. This corroborates the hypothesis that the inhibitory effect of most compounds was due to being composed by one of the three scaffolds under study. However, at this concentration, the water and glycerol permeability inhibition were very weak for nearly all the metallodrugs tested with a maximum inhibition of approximately 15%, which also corroborates the results from the literature about the non-inhibitory effect of Phen in glycerol

permeability. Moreover, the only compound exhibiting a strong inhibition of water transport was P103, being the most promising compound in inhibiting AQP1. This suggest that the effect of the compound on AQP1 was not only due to the effect of the scaffold but also to the effect of the vanadium metal, since P103 showed a higher percent of inhibition than the scaffolds, with a difference of almost 50% between them. Furthermore, P103 slightly inhibits the glycerol permeability showing a high SEM, suggesting that more studies are needed to draw conclusions about P103 selectivity towards AQP1.

Overall, P103 revealed to be the most promising AQP1 inhibitor of this set of compounds, with an IC_{50} value of (9.11 ± 0.03) μM. Hence, this compound exhibited great potency and efficacy to AQP1 inhibition, suggesting that both the vanadium metal and the two molecules of Amphen contributed to the water transport inhibition. Further studies are needed to validate these results by testing P103 in yeast cells transformed with plasmid encoding AQP1 and yeast cells transformed with plasmid encoding AQP3. In addition, it is also necessary to study its reversibility, establish structure/activity relationships and then, test it in cancer cell lines (on-going work), to understand if P103 is a suitable AQP1 inhibitor that could be used in cancer therapy.

4.1.3. Inhibition studies of water and glycerol permeability in aquaporins by gold compounds

4.1.3.1. Inhibitory effect of gold compounds in RBCs permeability

Three gold compounds from Cardiff University were screened in RBCs: RBA31, STAM013 and RBA29. The interest in investigating new gold compounds as potential AQP3 inhibitors started when it was discovered a potent and selective inhibitor of glycerol permeability – Auphen – that is a water-soluble gold (III) coordination compound [92], [96]. Remarkably, Auphen strongly inhibited glycerol permeability in RBCs, with an IC_{50} value of (0.80 ± 0.08) μM and exhibited a slight inhibition on water permeability mediated by AQP1. Considering these promising results, RBA31 and STAM013 were synthetized considering the Auphen structure to try to optimize its efficiency, potency and selectivity towards AQP3. On the other hand, RBA29 was also synthetized based on the Auphen structure in order to obtain a compound capable of inhibiting AQP9, that is an aquaglyceroporin that as still no known potent inhibitors. Considering that AQP9 has a positively charged extracellular surface [112], this will attract anions and for that reason, RBA29 was synthetized to become an anion by deprotonation of the hydroxyl group from the carboxylic acid, capable of interacting with hAQP9 (**Figure 4.16**).

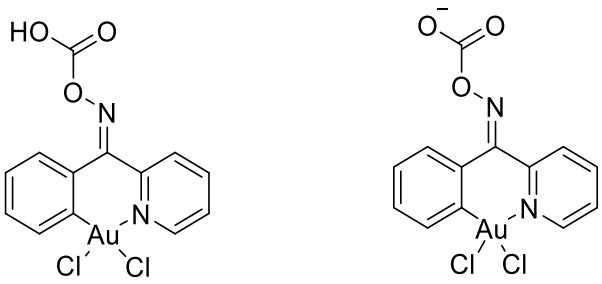

Figure 4.16: Protonated and deprotonated state of the gold compound RBA29 provided by Cardiff University

The inhibitory effect of the gold compounds on water and glycerol permeability in RBCs is displayed in the following bar graph, expressed as the percent of permeability relative to the control (%) (**Figure 4.17**).

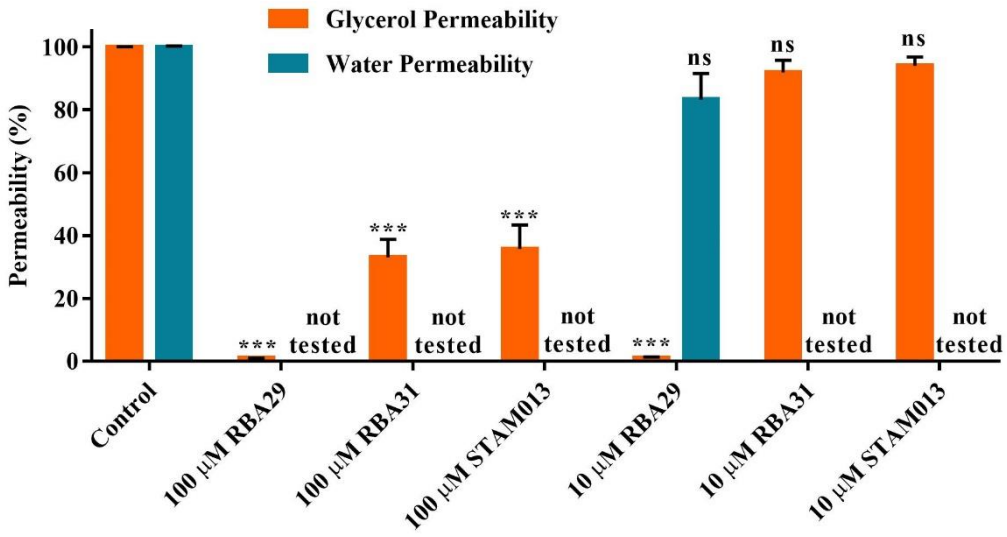

Figure 4.17: Inhibition of water and glycerol permeability in RBCs by gold compounds at a concentration of 100 and 10 µM after 30 minutes incubation at RT. Data are shown as media ± SEM for one or three experiments. Significance levels: *** $P < 0.001$, ns – nonsignificant, compared to the control by student t-test.

In **Figure 4.17**, besides the percent of inhibition for the maximum concentration tested (100 µM), it is also shown the inhibition observed for testing 10 µM of each compound to facilitate the comparison with Auphen that exhibits its maximum inhibition of glycerol permeability at 10 µM. At both concentrations, RBA29 exhibited a strong inhibition of glycerol permeability, while RBA31 and STAM013 at 100 µM decreased the glycerol permeability to 35%, showing less potency than RBA29. At 10 µM, these two compounds were unable to inhibit the glycerol transport, suggesting that the structural differences from Auphen were determinant to cause the lack of potency of these compounds to AQP3. By analysing the structures, the

difference between the two compounds and Auphen is that the gold compound is bound to three nitrogen atoms from the scaffold and is not bound to two chloride atoms as Auphen. (**Figure 4.18**).

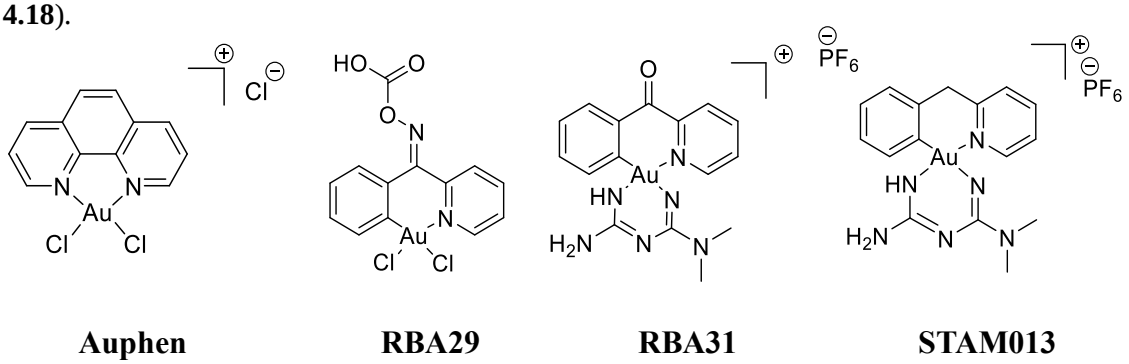

Auphen **RBA29** **RBA31** **STAM013**

Figure 4.18: Structures of Auphen,RBA29, RBA31 and STAM013 provided by Cardiff University.

This direct bond to the nitrogen atoms and the absence of the two chloride atoms may explain why RBA31 and STAM013 cannot bind to the AQP3, since it suggests that the gold metal is restrained and cannot bind to the accessible cysteine residues of AQP3, unlike Auphen that is bound to two chloride atoms. On RBA29 structure, the gold metal is bound to two atoms of chloride as Auphen, suggesting that the metal is accessible to bind the AQP3 cysteine residues. This may explain the strong inhibition of glycerol transport exhibited for RBA29. About water permeability, RBA29 showed no inhibition of AQP1 and the effect of the other two compounds were not evaluated for water transport at that time but since it is an on-going work, water permeability in the presence of RBA31 and STAM013 will be assessed later on.

To study the inhibitory effect of these gold-based compounds on glycerol permeability, the IC_{50} value was calculated. The following graphs display the results obtained for the inhibition of glycerol permeability by RBA31, STAM013 and RBA29 and respective IC_{50} values (**Figure 4.19 and 4.20**).

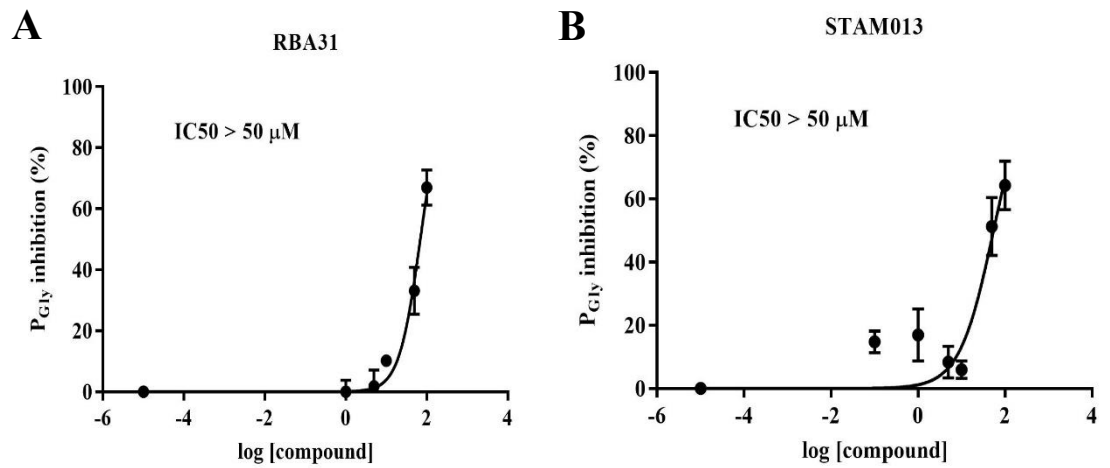

Figure 4.19: Inhibitory effect of RBA31 and STAM013 in RBCs glycerol permeability. **A** - Concentration dependent inhibition of glycerol permeability in RBCs by RBA31 for concentrations between 0.1-100 µM (incubated for 30 minutes at RT) with an IC_{50} > 50 µM (n=1). **B** – Concentration dependent inhibition of glycerol permeability in RBCs by STAM013 for concentrations between 0.1-100 µM (incubated for 30 minutes at RT) with an IC_{50} > 50 µM (n=1).

As shown by **Figure 4.19**, both RBA31 and STAM013 slightly inhibited AQP3 glycerol permeability, presenting an IC_{50} value higher than 50 µM. Thus, these two gold-based compounds exhibit lack of potency in inhibiting AQP3 activity and so, they do not demonstrate potential to be AQP3 inhibitors.

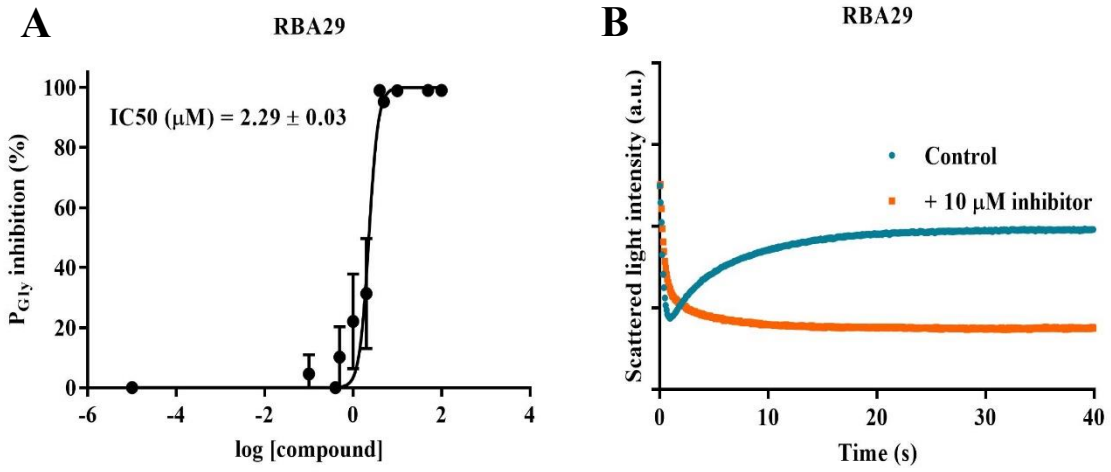

Figure 4.20: Inhibitory effect of RBA29 on RBCs glycerol permeability. **A** – Concentration dependent inhibition of glycerol permeability in RBCs by RBA29 for concentrations between 0.1-10 µM (incubated for 30 minutes at RT) with an IC_{50} value of (2.29 ± 0.03) µM (n=1). B – Stopped-flow signal for glycerol transport after imposing a hyperosmotic glycerol solution on the cells, for control RBCs and in the presence of 10 µM of RBA29 (concentration at which the compound already shows maximum inhibition).

RBA29 showed a very low IC_{50} value of (2.29 ± 0.03) µM, demonstrating that this gold compound strongly inhibited AQP3 glycerol transport. This is supported by the cell behaviour illustrated in **Figure 4.20B**, in which it is observed the drastically inhibition of AQP3 by RBA29

that could not facilitate the glycerol transport into the cells, preventing cell reswelling. Even though the gold metal from RBA29 was accessible to reach the AQP3 cysteine residues as much as Auphen, the IC_{50} values obtained were not the same since Auphen has a value of 0.8 µM that is lower than the one for RBA29 (2.29 µM).

Overall, RBA29 was the most promising of this set of gold compounds as a potential AQP3 inhibitor, with a low IC_{50} value (2.29 ± 0.03) µM and does not show potential to be an AQP1 inhibitor considering its lack of effect on water transport. Therefore, this compound exhibits great potency in inhibiting the glycerol transport in RBCs.

4.1.3.2. Inhibitory effect of gold compounds in aquaporin-expressing yeast cells permeability

In order to assess the effect of RBA29, RBA31 and STAM013 in AQP9, they were tested in yeast cells transformed with plasmid encoding hAQP9. The results for their effect on glycerol permeability are shown in the next bar graph (**Figure 4.21**).

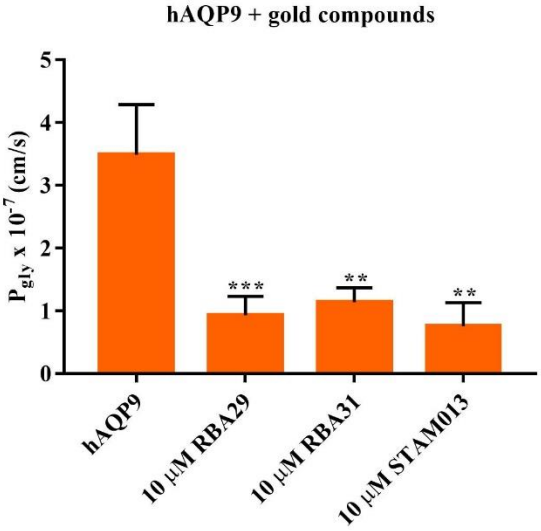

Figure 4.21: Inhibitory effect of RBA29, STAM013 and RBA31 on glycerol permeability in hAQP9 at a concentration of 10 µM (incubation for 30 minutes at RT). Data are shown as media ± SEM for one experiment. Significance levels: *** P < 0.001, ** P < 0.01, compared to the control by student t-test.

In **Figure 4.21**, it was observed that the three gold compounds under study, strongly inhibited hAQP9 glycerol permeability, with a percent of inhibition between 65% and 80%. RBA29 showed that it can strongly inhibit both AQP9-expressing yeast cells and AQP3 in RBCs, revealing its potency and non-selectivity. On one hand, this compound has a structure composed by an accessible gold metal to bind to AQP3 cysteine residues as the potent glycerol permeability inhibitor Auphen. On the other hand, it has a hydroxyl group from the carboxylic acid that when deprotonated, can interact with the positively charged extracellular surface of AQP9. Regarding RBA31 and STAM013, they strongly inhibited AQP9, suggesting a potential selectivity to this

aquaporin, considering their lack of potency in inhibiting AQP3 in RBCs. Overall, it is important to study the structure/activity relationships for these three gold compounds to understand their binding sites.

Moreover, to study the inhibitory effect of RBA29 on hAQP9 glycerol permeability in yeast cells, it was calculated the IC_{50} value. The determination of the IC_{50} values for RBA31 and STAM013 was not yet possible since it is still an on-going work and the last experiments failed to obtain appropriate dose-response curves to their determination. The results for the AQP9 glycerol permeability inhibition by RBA29 are displayed on the next graphs (**Figure 4.22**).

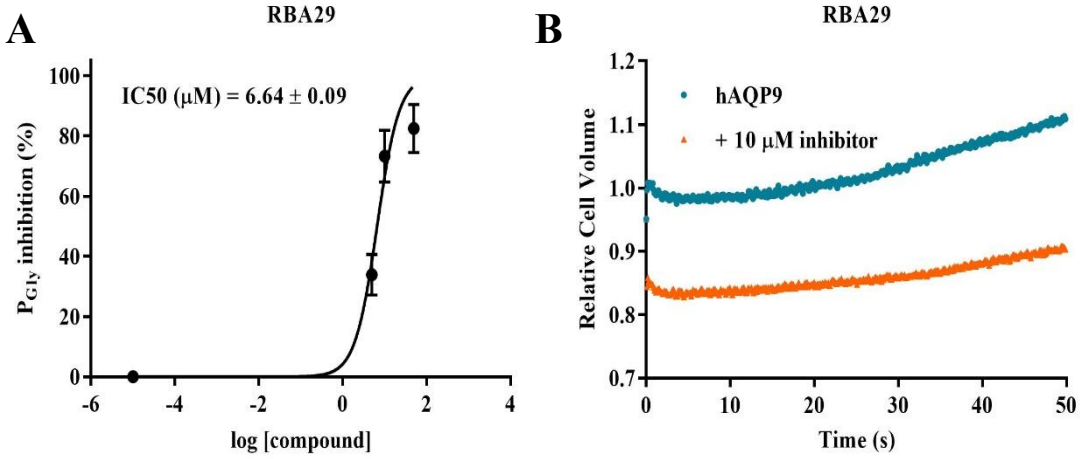

Figure 4.22: Inhibitory effect of RBA29 on hAQP9 glycerol permeability. **A** - Concentration dependent inhibition of hAQP9 glycerol permeability by RBA29 for concentrations between 0.1-50 µM (incubated for 30 minutes at RT) with an IC_{50} value of (6.64 ± 0.09) µM (n=1). **B** – Time course of the relative cell volume changes after being exposed to a hyperosmotic glycerol solution, for cells transformed with plasmid encoding hAQP9 in the absence of compound and in the presence of 10 µM of RBA29.

RBA29 showed a low IC_{50} value in the micromolar range of (6.64 ± 0.09) µM, confirming its potency in inhibiting the glycerol transport mediated by AQP9. Moreover, this is also supported by **Figure 4.22B** where the cells in the presence of RBA29, are unable to facilitate the glycerol transport because of AQP9 blockage, preventing the cell reswelling.

Overall, these are promising results since there are no known potent and selective inhibitors of AQP9. Therefore, these new golds compounds must be validated in yeast transformed with plasmid encoding human AQP3 and repeat the assays with human AQP9 to then be tested in cancer cell lines in order to discover their anticancer properties.

4.2. Functional assays of hAQP5 and important residues for permeability[1]

AQP5 was found to be aberrantly expressed in a variety of human tumors and has been considered a potential therapeutic target and biomarker with prognostic value [78]. Thus, aiming to contribute for the design of new inhibitors able to modulate AQP5 in tumors, we expressed hAQP5 in yeasts and evaluated the important residues that are crucial for channel permeability.

4.2.1. hAQP5 localization and function in the yeast plasma membrane

To evaluate the hAQP5 function, yeast cells (aqy-null cells) were transformed with either the empty vector pUG35 or the plasmid encoding hAQP5. First, the expression and localization of AQP5 at the yeast plasma membrane were evaluated by fluorescence microscopy using GFP-tagging (**Figure 4.23A**).

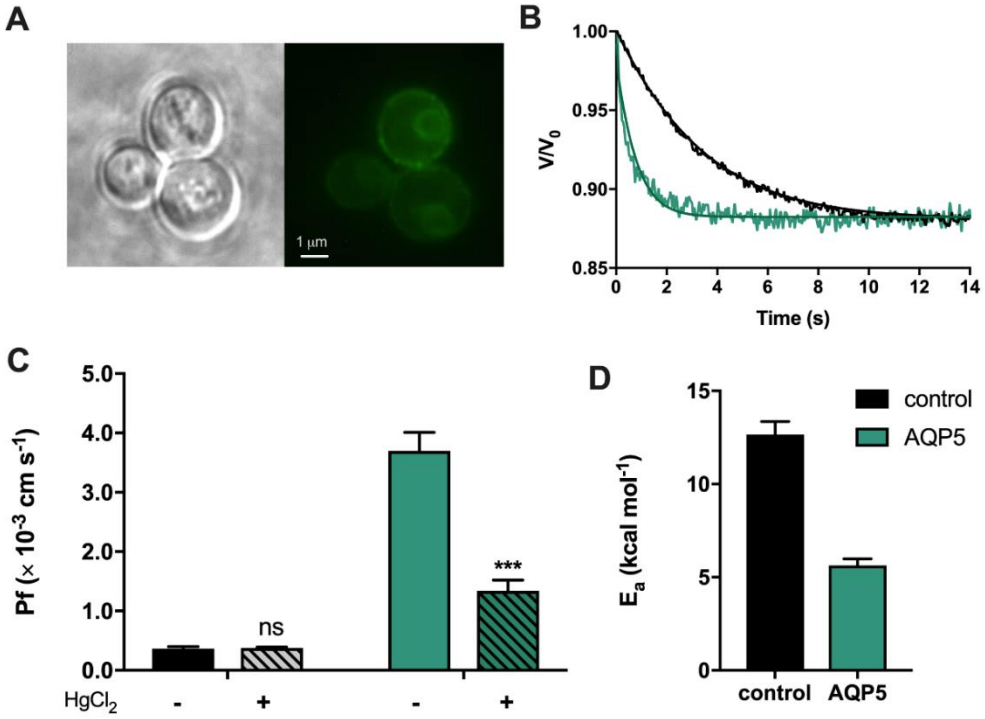

Figure 4.23: Localization, expression and function of hAQP5-expressing yeast cells. **A** – Phase contrast (left) and epifluorescence (right) microscopy images of yeast aqy-null cells transformed with plasmid encoding GFP-tagged human AQP5 (100× objective). **B** – Representative time course of relative cell volume (V/V_0) changes after exposure to a hyperosmotic shock. **C** – Water permeability coefficients of control and hAQP5-expressing yeast cells before and after incubation with $HgCl_2$ for 5 minutes at RT at pH 5.1. Data are shown as mean ± SEM of ten measurements. **D** – Activation energy for water permeability of control and hAQP5 cells. Data are shown as mean ± SEM of three independent experiments. Significance levels: *** $P < 0.001$, ns – nonsignificant, compared to the control by student t-test.

[1] Adapted from C. Rodrigues**, C. Pimpão** *et al.*, "Human Aquaporin-5 Facilitates Hydrogen Peroxide Permeation and Cancer Cell Migration," *Cancers (Basel).*, vol. 11, 2019.

As observed by **Figure 4.23A**, AQP5 is located in the membrane. Subsequently, the hAQP5 function was assessed by stopped-flow fluorescence where cells incubated with the volume sensitive dye CFDA, balanced in an isotonic solution, were mixed with a 2.1 M hyperosmotic sorbitol solution to evaluate water permeability. The experiments were performed at 23ºC for pH 5.1 and 5 signals were acquired. To obtain accurate permeability values, the software Berkeley Madonna was used to obtain P_f, using customized mathematical models as previously described. Moreover, the fluorescence signals were converted to relative cell volume to enable the direct visualization of the cell volume changes in response to an osmotic shock as shown in **Figure 4.23B**. When exposed to a hyperosmotic sorbitol solution, cells expressing hAQP5 reach the new osmotic equilibrium faster than control cells, indicating that hAQP5 facilitates the water transport. Furthermore, the absolute values of water and glycerol permeability are useful to predict if the water and glycerol transport are being mediated by aquaporin channels or if these molecules are crossing the hydrophobic bilayer [6]. By **Figure 4.23C**, it is observed that the P_f value is 10-fold higher for AQP5-expressing yeast cells $(3.70 \pm 0.31) \times 10^{-3}$ cm/s than the P_f value for control cells $(0.37 \pm 0.03) \times 10^{-3}$ cm/s. When incubated with 0.5 mM $HgCl_2$, that is a known potent and toxic inhibitor of aquaporins, there is a strong reduction on water permeability of the AQP5-expressing yeast cells, demonstrating that AQP5 is sensitive to mercury effect. Furthermore, the activation energies (E_a) was estimated from Arrhenius plot for a range of temperatures from 9ºC to 34ºC. It is known that water may cross cell membranes by two pathways: diffusion of water molecules across the hydrophobic bilayer (with high activation energy) and diffusion of water molecules through the channels (with low activation energy). Considering the flux of water across the membrane is the sum of the fluxes through these two pathways [5], [6], the activation energy needs to be measured to understand which pathway is dominant in the cell system. Therefore, if the activation energy is high, it means that water is crossing the hydrophobic bilayer and if it is low, then the water transport is being mediated by aquaporin. In **Figure 4.23D**, the activation energy was lower for AQP5-expressing cells (5.63 ± 0.36) kcal.mol^{-1} than for the control cells (12.66 ± 0.69) kcal.mol^{-1}. These results corroborate that the observed increase in water permeability is due to the expression of AQP5 that is functional and capable of water permeation.

4.2.2. Role of hAQP5 residues in gating

Recent evidences have revealed that human aquaporins can be gated by different mechanisms as pH or post-translational modifications as phosphorylation [103], [113]. Aquaporins' regulation has been investigated to understand the gating mechanisms and which residues are involved in this regulation process. About AQP5, regulation was proposed to involve phosphorylation at Ser156 in cytoplasmatic loop D since its phosphomimetic mutation – S156E - led to increase of the relative membrane expression of AQP5 [82] in HEK293 cells, thereby

enhancing cancer cell proliferation. However, this mutation did not cause a significant structural change, suggesting that it is needed more than one phosphorylation site to generate a conformational change. Ser156 is a consensus PKA site in AQP5 that is often phosphorylated in certain tumors, such as in colon cancer cells, indicating that phosphorylation of AQP5 in Ser156 mediate cell proliferation via Ras/ERK/Rb signalling pathway [114].

Moreover, *in silico* studies have suggested another gating mechanism where the human AQP5 monomer experience conformational changes from open to close state and from wide to narrow state [115]. These studies proposed that AQP5 can change from open to closed state through a tap-like gating mechanism at the cytoplasmic end, by changing the orientation of His67 ringed sidechain, being the key residue to completely block the water passage through the channel. Also, AQP5 can exhibit two different conformations: narrow state, where the residues His173 and Ser183 can restrict the water passage by being very close to each other (< 5.5 Å) and wide state that allows the passage of water molecules being the distance between the two residues higher than 7 Å and lower than 10 Å. Moreover, the authors found that the two states (wide/narrow) are determined by H173 side chain orientation wherein His173 ring flips into its mirror orientation in the wide state, and to switch to the narrow state, His173 sidechain returns to its normal orientation. In addition, a recent study from our lab with rAQP5 indicated that channel widening results from deprotonation when the protein is in the phosphorylated state [79]. Therefore, using the same yeast system, we investigated the gating mechanism for hAQP5 by phosphorylation and pH. The location of the residues previously mentioned are show in hAQP5 monomer structure (**Figure 4.24**).

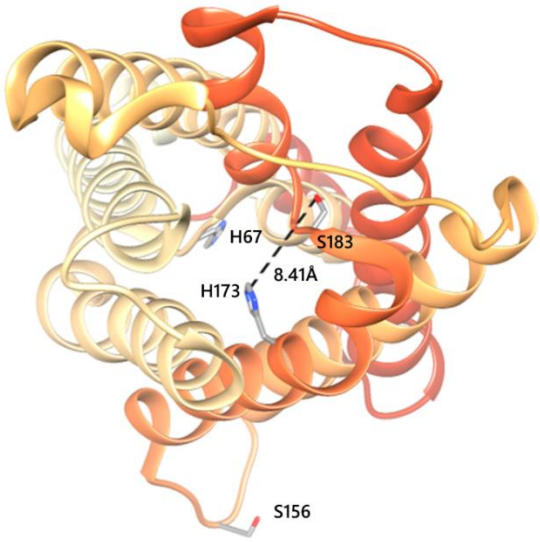

Figure 4.24: Top view of human AQP5 monomer structure with phosphorylation consensus sites Ser156 localized in intracellular loop D and Ser183 and His173 both localized in the selectivity filter. As proposed, when His67 side chain switches its orientation, it opens the channel, allowing the water passage. In such cases, if the proximity of His173 to Ser183 is higher than 7 Å and lower than 10 Å, the hAQP5 monomer

shows a wide conformation. Structures were generated with Chimera (http://www.cgl.ucsf.edu/chimera) and are based on the AQP5 X-ray structure (PDB databank code 3D9S).

It was generated point mutations in AQP5 selectivity filter and in intracellular loop D as shown in **Figure 4.24**, to investigate hAQP5 gating mechanisms. Mutations to change wide and narrow state were attained by substitution of histidine 173 (H173) with alanine (A) and with tryptophan (W), respectively, Furthermore, mutations to prevent the phosphorylation of S156 and S183 were obtained by substitution of serine (S) with alanine (A). Also, mutations to mimic the phosphorylation of hAQP5 in the previously mentioned serine residues, serine (S) was substituted with glutamic acid (E).

Water permeability of yeast cells transformed with plasmid encoding wild-type AQP5 (AQP5 WT) or AQP5 mutants was determined at 23ºC at pH 5.1 and pH 7.4 (**Figure 4.25A**). In addition, expression and localization of all AQP5 mutants were confirmed at pH 5.1 and pH 7.4 by fluorescence microscopy using GFP-tagging. All mutants exhibited similar GFP-fluorescence intensity at the plasma membrane. By **Figure 4.25B**, it was observed that all of them showed similar relative membrane expression, showing that differences in permeability cannot be assigned to impairment of AQP5 trafficking due to mutations.

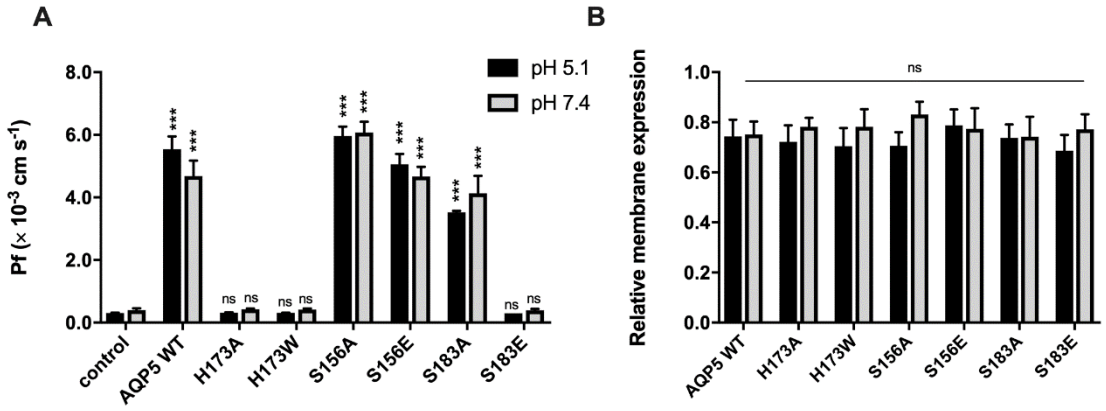

Figure 4.25: Residues involved in water permeability through hAQP5. **A** – Water permeability values for control cells and for yeast transformed with plasmid encoding AQP5 WT and mutants, at 23ºC at pH 5.1 and pH 7.4. Data are shown as mean ± SEM of 10 measurements. **B** – Relative membrane expression of AQP5 WT and mutants for pH 5.1 and pH 7.4, calculated from fluorescence intensity profiles (10 cells in each experimental condition, 4 profiles for each cell, from at least 3 independent experiments). Significance levels: *** $P < 0.001$, ns – nonsignificant, compared to the control by student t-test.

Permeability experiments with control cells, AQP5 WT and mutants performed at two pHs (pH 5.1 and pH 7.4), showed that alteration of external pH did not affect water permeability, and that this is not dependent on aquaporin phosphorylation. As already mentioned, a recent study proposed that phosphomimetic mutation S156E increased the AQP5 relative membrane expression in HEK293 cells [82]. In this present work, preventing or mimicking S156 phosphorylation did not alter AQP5 membrane expression (**Figure 4.25B**), nor did it modify

AQP5 water permeability at any pH tested, which may be in part explained by a different signalling pathway for AQP5 trafficking used by yeasts. In the case of histidine, water permeability was impaired when it was mutated (H173A and H173W). It is known that histidine is a highly conserved residue in the selective filter of orthodox aquaporins, being essential to their selectivity and water transport [116], [117]. Thus, the histidine importance for the selectivity filter was validated by the completely blockage of water transport when H173 was mutated. About S183 residue, **Figure 4.24A** showed that the prevention of phosphorylation by S183A mutation did not affected water permeability, indicating that AQP5 channel remains in the wide state and that the distance between S183 and H173 side chain is higher than 7 Å and lower than 10 Å. Concerning the phosphomimetic mutation S183E, water permeability was totally blocked, suggesting that the proximity of S183 to H173 side chain is lower than 5.5 Å, probably due to the negatively charged group that leads to the narrow state.

Overall, these mutagenesis studies demonstrated that phosphorylation of S156 does not affect water permeability at the cytoplasmatic end, that H173 is a highly conserved residue in the selectivity filter and its interaction with phosphorylated S183 possibly results in pore constriction. In particular, the phosphorylation of S183 at the selectivity filter represents a new AQP5 gating mechanism that has never been reported, unveiling the important residues for water permeation, further contributing to the design of new drugs.

4.3. Functional assays of aquaporins from diverse organisms

The aim of this part of the work was to investigate aquaporins from diverse organisms for University of Copenhagen and Aquaporin A/S company. This company takes advantage of aquaporins strictly selective to water, to develop water filtering devices to be employed in the industry and in household for water filtration and purification [118]. For this purpose, they developed a biomimetic membrane for the selective transport of water since biological membranes exhibit mechanical and chemical stability to a wide range of various external stress factors unlike the traditional polymeric separation membranes. This biomimetic membrane is composed by lipids, artificial components mimicking block-copolymers and the aquaporin protein to generate an artificial water filtration membrane. Nowadays, this technology is available for both forward osmosis (FO) and reverse osmosis (RO) applications. FO consists in two aqueous solution, one with low solute concentration and one with high solute concentration, which concentration differences leads to solute or water transport to equalize the system. By adding a semi-permeable membrane that does not permit solute transport, the only way for the system to equilibrate is by water transport from one side to the other. This allows to induce a water flux that will result in bringing the water to one side and concentrating the solute in the other side. Therefore, the products available for forward osmosis are mostly applied to high rejection of

contaminants and/or retaining valuable compounds. Whereas FO happens naturally without energy required, in reverse osmosis it is needed to apply energy to the highest solute concentrated solution [119]. For RO, it is also used a semi-permeable membrane that allows the passage to water molecules but not most salts, bacteria, among others. Nevertheless, it is needed to apply a pressure higher than the natural osmotic pressure to obtain pure water with most of the solutes retained. Thus, the products available for reverse osmosis are mostly applied to produce high-quality water and for seawater desalination.

The production of biomimetic membranes with aquaporin inside, led to the need of discovering aquaporins with higher selectivity, high water permeability, more stable and resistant to external factors. Accordingly, in University of Copenhagen, yeast cells were transformed with plasmid encoding eight aquaporins in the pUG35 vector (aqy-null cells) from different species:

- Three plant aquaporins: eucalyptus (*Eucalyptus globulus*), rice (*Oryza sativa*) and potato (*Solanum tuberosum*);
- One tardigrade (*Hypsibius dujardini*) aquaporin;
- Four bacterial aquaporins: *Methanocella conradii*, K*yrpidia tusciae, Methanothermobacter thermautotrophicus* and *Novibacillus thermophilus.*

Concerning plant aquaporins, there are evidences that eucalyptus, rice and potato are associated with drought tolerance [120]–[122] and also with salt resistance in the case of rice. About the tardigrades [123], these are small invertebrate that are known for their capacity of surviving complete dessecation by undergoing anhydrobiosis (survive the loss of all water). In this anhydrobiotic condition, they enter in a dormancy state wherein metabolism and aging stops. Besides this great capacity, tardigrades can survive to all kind of environments since they are resistant to extreme temperatures and pressures, starvation and radiation. Regarding the four bacterial aquaporins, they are all known thermophiles with resistance to extreme high temperatures.

Overall, the goal of this work section is to discover an aquaporin selective to water with high water permeability, resistant to stress factors and stable. Therefore, yeast cells were transformed with either the empty vector or with the plasmid encoding the aquaporins under study. The assessment of the aquaporins function was assessed by stopped-flow fluorescence where cells incubated with the volume sensitive dye CFDA, balanced in an isotonic solution, were mixed with a 2.1 M hyperosmotic sorbitol solution to evaluate water permeability or with a 2.1 M hyperosmotic glycerol solution to evaluate glycerol permeability. The experiments were performed at 23ºC for pH 5.0 and pH 7.4 and 5 signals were acquired for each organism. To obtain accurate permeability values, the software Berkeley Madonna was used to obtain P_f and P_{gly}, using customized mathematical models as previously described. The glycerol permeability at pH 5.0 could not be calculated as it was not possible to exponentially fit the obtained signals for both

control cells and for each aquaporin tested. The results for the glycerol and water permeability values for the control cells and for each aquaporin tested at pH 5.0 and pH 7.4, are shown in the next bar graph (**Figure 4.26**).

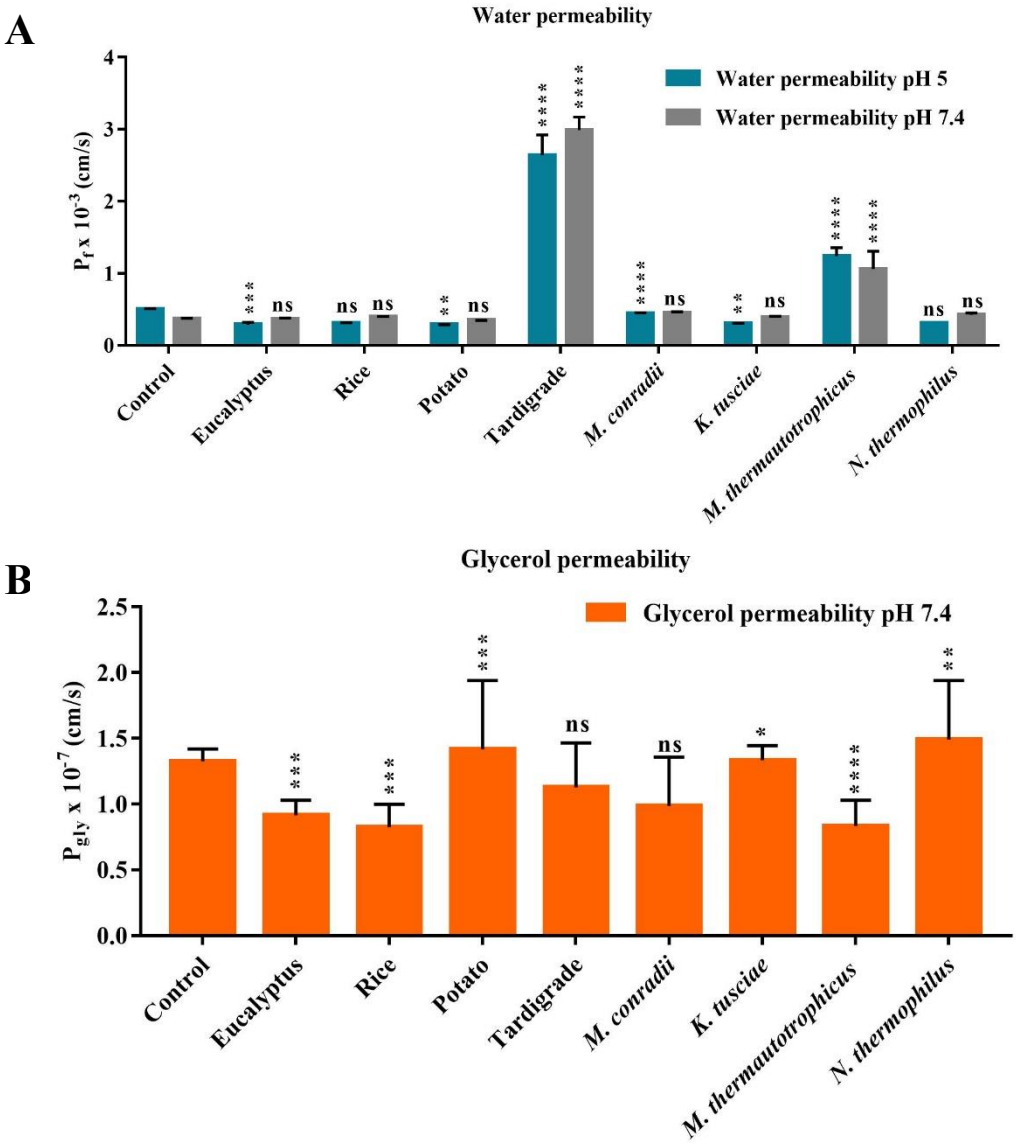

Figure 4.26: Water and glycerol permeability coefficients for pH 5.0 and pH 7.4 for the eight aquaporins under study. **A** – Water permeability values for control cells and yeast transformed with plasmid encoding the aquaporins of interest, at 23ºC for pH 5.0 and pH 7.4. **B** – Glycerol permeability values for control cells and yeast transformed with plasmid encoding aquaporins of interest, at 23ºC for pH 7.4. Data are shown as media ± SEM for two measurements. Significance levels: **** P < 0.0001, *** P < 0.001, ** P < 0.01, * P < 0.05, ns – nonsignificant, compared to the control by student t-test.

Water permeability coefficients for pH 5.0 and pH 7.4 were very similar, showing that the alteration of the external pH does not affect water permeability in any of the aquaporins. For pH 5.0, all the aquaporins that exhibit low water permeability showed statistical significance, however the water transport mediated by these aquaporins is not biologically relevant since their permeability values were similar or even lower than the value for control cells water permeability.

Also, for glycerol permeability values, almost all aquaporins-expressing yeast cells showed statistical significance relative to the control cells, but biologically they are not relevant since the permeability values are lower or very similar to the glycerol permeability value for control cells. By **Figure 4.26A**, it is observed that tardigrade and *M. thermautotrophicus* aquaporins exhibited the highest water permeabilities from all the compounds: $(2.64 \pm 0.28) \times 10^{-3}$ cm/s and $(1.24 \pm 012) \times 10^{-3}$ cm/s, respectively. Moreover, P_f value for the tardigrade aquaporin is 2-fold higher than P_f value for *M. thermautotrophicus* aquaporin and 5-fold higher that the permeability value for control cells ($(0.50 \pm 0.01) \times 10^{-3}$ cm/s). These high permeability values associated with the fact that these two aquaporins do not transport glycerol, reveal that tardigrade and *M. thermautotrophicus* aquaporins are the most functional water channels with high permeability and selectivity for these molecules, to be then applied in biomimetic membranes for water filtration. Moreover, to confirm these high permeabilities for water and that these molecules are actually being transported by the aquaporins and not crossing the hydrophobic bilayer, E_a were estimated from Arrhenius plot for a range of temperatures from 9ºC to 34ºC for pH 5.0 and pH 7.4. (**Figure 4.27**)

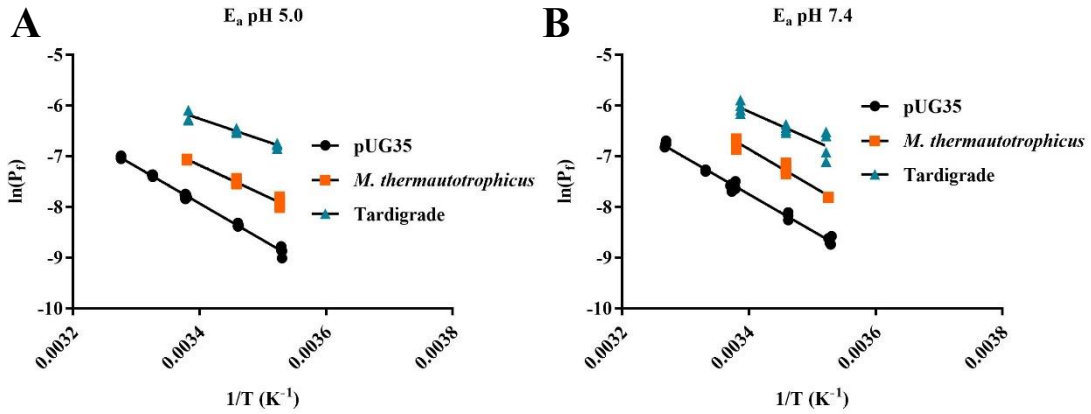

Figure 4.27: Arrenhius plot for water permeability assays at pH 5.0 and pH 7.4 for control cells and *M. thermautotrophicus* and tardigrades aquaporins-expressing yeast cells. **A** – Arrhenius plot for water permeability assays at pH 5.0 for yeast transformed with the empty vector and transformed with plasmid encoding *M. thermautotrophicus* and tardigrade aquaporins, for a range of temperatures from 9ºC to 34ºC. **B** - Arrhenius plot for water permeability assays at pH 7.4 for yeast transformed with the empty vector and transformed with plasmid encoding *M. thermautotrophicus* and tardigrade aquaporins, for a range of temperatures from 9ºC to 34ºC

Table 4.1: Activation energy values calculated from the slope determined from the experimental points using simple linear regression.

	E_a (kcal.mol^{-1})	
	pH 5.0	**pH 7.4**
pUG35 (empty vector)	14.38 ± 0.22	14.32 ± 0.34
***M. thermautotrophicus* Aquaporin**	11.52 ± 0.68	14.58 ± 1.02
Tardigrade Aquaporin	8.40 ± 0.70	11.05 ± 1.75

E_a measures the energy barrier to water movement across a membrane. When the water transport is across the lipid membrane, the E_a is generally high (>8-10 kcal.mol^{-1}) since the water molecules are interacting with the lipid molecules. When the water transport is mediated by an aquaporin channel, E_a is generally lower (3-6 kcal.mol^{-1}) [6]. From **Figure 4.27** and **Table 4.1**, it is observed differences for activation energy values by alteration of the external pH from pH 5.0 to pH 7.4, indicating that at pH 5.0, aquaporins exhibit higher permeability probably due to higher aquaporin expression, which agrees with the fact that this pH is optimal for yeast growth. At pH 5.0, *M. thermautotrophicus* and tardigrade aquaporins exhibited E_a values of (11.52 ± 0.68) kcal.mol^{-1} and (8.40 ± 0.70) kcal.mol^{-1}, respectively that are lower than E_a value for empty vector: (14.38 ± 0.22) kcal.mol^{-1}. Even though the literature considers 8 kcal.mol^{-1} in the threshold for the absence of aquaporin water channels, the tardigrade aquaporin reveals to be functional and capable of mediating water transport with high water permeability, when compared to E_a value for the control cells. However, the difference from the activation energy for *M. thermautotrophicus* and the E_a value for control cells suggests that this aquaporin is not functional, which is confirmed when comparing to the literature values. At pH 7.0, tardigrade aquaporin presents an E_a value of (11.05 ± 1.75) kcal.mol^{-1}, being the lowest energy activation comparing with the similar E_a values for *M. thermautotrophicus* aquaporin and control cells: (14.58 ± 1.02) kcal.mol^{-1} and (14.32 ± 0.34) kcal.mol^{-1}, respectively. Comparing with the literature, the tardigrade aquaporin at this pH does not appear to be functional. Therefore, yeast transformed with plasmid encoding tardigrade AQP at pH 5.0, has revealed to be the most promising aquaporins in water transport from all the ones tested, exhibiting water selectivity, with high water permeability values. These features combined with the remarkable resistance to stress environments and survival when exposed to multiple external factors as extreme temperature and pressure, dessecation and starvation, unveil the great potential of this aquaporin to be employed in biomimetic membranes capable of water filtration associated with possible industrial and household applications.

5. Conclusions

This thesis was focused on the assessment of aquaporins function and in the discover of potential inhibitors that could target aquaporins overexpressed in cancer and prevent cell processes responsible for tumor development as cell proliferation and migration.

In the first part of the thesis, eleven polyoxometalates were screened in RBCs and validated in aquaporin-expressing yeast cells to evaluate their inhibitory effect on aquaporins permeability. By RBCs assays, POT-A was identified as the most promising inhibitor of AQP3, exhibiting a low IC_{50} value of (0.71 ± 0.04) µM which shows the great potency of this compound in inhibiting the glycerol permeability. Moreover, this compound slightly inhibited the water permeability, probably due to the inhibitory effect on AQP3, that also transports water besides glycerol. Through yeast assays, the potency of this compound was confirmed by the near 100% inhibition on AQP3-expressing yeast. In addition, POT-A did not inhibit AQP7 and AQP9, suggesting the selectivity towards AQP3. Considering that Auphen has a similar IC_{50} value to POT-A and that it inhibits both AQP3 and AQP7, POT-A appears to be a suitable drug candidate for targeting AQP3 in cancer, where AQP3 is overexpressed. POT-A is being tested in cancer cell lines, in particular pancreatic cancer (on-going studies in our lab), to investigate its anticancer properties. Further studies are needed to establish structure/activity relationships and understand the effect of POT-A in AQP10 that was still not tested.

On the second part of the thesis work, vanadium, copper and zinc compounds were tested in RBCs in the same conditions as for polyoxometalates. P103, a compound with a vanadium metal and two molecules of Amphen, revealed to be the most promising compound in inhibiting AQP1 with an IC_{50} value of (9.11 ± 0.03) µM. This is an important discovery considering there are no known AQP1 inhibitors until now that show great potency in AQP1 inhibition as P103. In the future, it is essential to study its reversibility in binding AQP1, establish structure/activity relationships and to validate these results by testing P103 in aquaporin-expressing yeast cells and cancer cell lines to comprehend if it has potential to be used in AQP1-overexpressing cancers treatment.

In the third study performed during this thesis, gold compounds were tested in RBCs and validated in yeast transformed with plasmid encoding aquaporins. In RBCs assays, RBA29, that was studied for its potential for AQP9 inhibition, was the most promising from the set of gold-based compounds as a potential AQP3 inhibitor, exhibiting an IC_{50} value of (2.29 ± 0.03) µM and lack of effect on water transport mediated by AQP1. By yeast assays, RBA29, RBA31 and STAM013 showed AQP9 inhibition, being the IC_{50} value for RBA29 of (6.64 ± 0.09) µM. These

are very promising results considering there are no known AQP9 inhibitors until now with such potency. Therefore, the validation of these results in AQP3-expressing yeast cells, AQP9-expressing yeast cells and in cancer cell lines is of utmost importance.

In the fourth part of this work, the important residues for AQP5 permeability were investigated, Moreover, mutagenesis studies demonstrated that while phosphorylation of S156 at the cytoplasmic end does not affect AQP5 permeability, His173 located in the selectivity filter revealed to be crucial for water permeability and possibly interacts with phosphorylated S183 for permeability regulation, resulting in the blockage of the pore. This reported gating mechanism has never been described before, unveiling the important residues for water permeation, contributing to the design of novel selective and potent inhibitors with potential for cancer therapeutics.

In the final section of this thesis, the function of aquaporins from diverse organisms was assessed with the goal of understanding their features as selective water channels with potential application in biomimetic membranes for water filtration. The aquaporin from tardigrade revealed as the most promising in terms of water selectivity, high water permeability in addition with the remarkable advantage of possessing high resistance to numerous external factors as extreme temperature and pressure, dessecation, starvation and radiation. Therefore, this aquaporin has great potential to be employed in biomimetic membranes, capable of water filtration.

Overall, POT-A, P103 and gold-based compounds tested revealed as suitable drug candidates to be applied in cancer treatment where AQP1, AQP3 and AQP9 are overexpressed. In fact, few aquaporin inhibitors have been described until now, which demonstrates the great outcome from these AQP-modulators studies performed during this work. Moreover, the disclosure of a new gating mechanism for AQP5 and of the important residues for water permeation may be used for the design of selective modulators. Altogether, these results contribute to new aspects of aquaporin research that may be used in benefit of pharmaceutics (drug discovery and drug design) and industry (in terms of water filtering systems).

6. References

[1] G. Soveral, S. Nielsen, and A. Casini, *Aquaporins in health and disease: New molecular targets for drug discovery*. CRC Press, 2015.

[2] A. Madeira, T. F. Moura, and G. Soveral, "Detecting aquaporin function and regulation," *Front. Chem.*, vol. 4, pp. 1–8, 2016.

[3] P. Agre, "The Aquaporin Water Channels," *Proc. Am. Thorac. Soc.*, vol. 3, pp. 5–13, 2006.

[4] C. V. Paganelli; A.K. Solomon, "THE RATE OF EXCHANGE OF TRITIATED WATER ACROSS THE HUMAN RED CELL MEMBRANE," vol. 41, no. 2, pp. 259–277, 1957.

[5] G. Soveral, A. Veiga, M. C. Loureiro-Dias, A. Tanghe, P. Van Dijck, and T. F. Moura, "Water channels are important for osmotic adjustments of yeast cells at low temperature," vol. 152, pp. 1515–1521, 2006.

[6] A. S. Verkman, "Water permeability measurement in living cells and complex tissues," *J. Membr. Biol.*, vol. 173, no. 2, pp. 73–87, 2000.

[7] G. M. Preston, T. P. Carroll, W. B. Guggino, and P. Agre, "Appearance of Water Channels in Xenopus Oocytes Expressing Red Cell CHIP28 Protein," *Science (80-.).*, vol. 256, pp. 385–387, 1992.

[8] F. Abascal, I. Irisarri, and R. Zardoya, "Diversity and evolution of membrane intrinsic proteins," *Biochim. Biophys. Acta - Gen. Subj.*, vol. 1840, no. 5, pp. 1468–1481, 2014.

[9] E. Kruse, N. Uehlein, and R. Kaldenhoff, "The aquaporins," *Genome Biol.*, vol. 7, no. 2, 2006.

[10] D. Kozono *et al.*, "Functional expression and characterization of an archaeal aquaporin. AqpM from Methanothermobacter marburgensis," *J. Biol. Chem.*, vol. 278, no. 12, pp. 10649–10656, 2003.

[11] G. Calamita, W. R. Bishai, G. M. Preston, W. B. Guggino, and P. Agre, "Molecular cloning and characterization of AqpZ, a water channel from Escherichia coli," *J. Biol. Chem.*, vol. 270, no. 49, pp. 29063–29066, 1995.

[12] C. Maurel, J. Reizer, J. I. Schroeder, M. J. Chrispeels, and M. H. Saier, "Functional characterization of the Escherichia coli glycerol facilitator, GlpF, in Xenopus oocytes," *J. Biol. Chem.*, vol. 269, no. 16, pp. 11869–11872, 1994.

[13] G. Soveral, C. Prista, T. F. Moura, and M. C. Loureiro-Dias, "Yeast water channels: an overview of orthodox aquaporins," *Biol. Cell*, vol. 103, no. 1, pp. 35–54, 2011.

[14] C. Maurel, L. Verdoucq, D.-T. Luu, and V. Santoni, "Plant Aquaporins: Membrane Channels with Multiple Integrated Functions," *Annu. Rev. Plant Biol.*, vol. 59, pp. 595–624, 2008.

[15] K. Ishibashi, S. Hara, and S. Kondo, "Aquaporin water channels in mammals," *Clin. Exp. Nephrol.*, vol. 13, no. 2, pp. 107–117, 2009.

[16] K. Ishibashi, Y. Tanaka, and Y. Morishita, "The role of mammalian superaquaporins inside the cell," *Biochim. Biophys. Acta - Gen. Subj.*, vol. 1840, no. 5, pp. 1507–1512, 2014.

[17] A. Madeira *et al.*, "Human Aquaporin-11 is a water and glycerol channel and localizes in the vicinity of lipid droplets in human adipocytes," *Obes. Biol. Integr. Physiol.*, vol. 22, no. 9, pp. 2010–2017, 2014.

[18] H. Sui, B. G. Han, J. K. Lee, P. Walian, and B. K. Jap, "Structural basis of water-specific transport through the AQP1 water channel," *Nature*, vol. 414, no. 6866, pp. 872–878, 2001.

[19] A. S. Verkman, M. O. Anderson, and M. C. Papadopoulos, "Aquaporins : important but elusive drug targets," *Nat. Publ. Gr.*, vol. 13, no. 4, pp. 259–277, 2014.

[20] Y. Wang and E. Tajkhorshid, "Molecular Mechanisms of Conduction and Selectivity in Aquaporin Water Channels," *J. Nutr.*, vol. 137, no. 6, pp. 1509S-1515S, 2007.

[21] A. J. Yool and A. M. Weinstein, “New roles for old holes: Ion channel function in aquaporin-1,” *News Physiol. Sci.*, vol. 17, pp. 68–72, 2002.
[22] T. Gonen and T. Walz, “The structure of aquaporins,” *Q. Rev. Biophys.*, vol. 39, no. 4, pp. 361–396, 2006.
[23] K. Murata *et al.*, “Structural determinants of water permeation through aquaporin-1,” *Nature*, vol. 407, no. 6804, pp. 599–605, 2000.
[24] D. Fu and M. Lu, “The structural basis of water permeation and proton exclusion in aquaporins (Review),” *Mol. Membr. Biol.*, vol. 24, no. 5–6, pp. 366–374, 2007.
[25] A. De Almeida, G. Soveral, and A. Casini, “Gold compounds as aquaporin inhibitors: New opportunities for therapy and imaging,” *Medchemcomm*, vol. 5, no. 10, pp. 1444–1453, 2014.
[26] D. F. Savage, P. F. Egea, Y. Robles-Colmenares, J. D. O’Connell III, and R. M. Stroud, “Architecture and selectivity in aquaporins: 2.5 Å X-ray structure of aquaporin Z,” *PLoS Biol.*, vol. 1, no. 3, pp. 334–340, 2003.
[27] A. S. Verkman, “Aquaporins in clinical medicine,” *Annu. Rev. Med.*, vol. 63, pp. 303–316, 2012.
[28] T. Ma, B. Yang, A. Gillespie, E. J. Carlson, C. J. Epstein, and A. S. Verkman, “Severely impaired urinary concentrating ability in transgenic mice lacking aquaporin-1 water channels,” *J. Biol. Chem.*, vol. 273, no. 8, pp. 4296–4299, 1998.
[29] C. L. Chou *et al.*, “Reduced water permeability and altered ultrastructure in thin descending limb of Henle in aquaporin-1 null mice,” *J. Clin. Invest.*, vol. 103, no. 4, pp. 491–496, 1999.
[30] A. S. Verkman, “More than just water channels: Unexpected cellular roles of aquaporins,” *J. Cell Sci.*, vol. 118, no. 15, pp. 3225–3232, 2005.
[31] B. M. Christensen *et al.*, “Acute effects of vasopressin V2-receptor antagonist on kidney AQP2 expression and subcellular distribution,” *Am. J. Physiol. - Ren. Physiol.*, vol. 275, no. 2, pp. 285–297, 1998.
[32] S. Sasaki, “Aquaporin 2: From its discovery to molecular structure and medical implications,” *Mol. Aspects Med.*, vol. 33, no. 5–6, pp. 535–546, 2012.
[33] B. Yang, D. Zhao, and A. S. Verkman, “Hsp90 inhibitor partially corrects nephrogenic diabetes insipidus in a conditional knock-in mouse model of aquaporin-2 mutation,” *FASEB J.*, vol. 23, no. 2, pp. 503–512, 2009.
[34] Y. Song and A. S. Verkman, “Aquaporin-5 Dependent Fluid Secretion in Airway Submucosal Glands,” *J. Biol. Chem.*, vol. 276, no. 44, pp. 41288–41292, 2001.
[35] K. Oshio, H. Watanabe, Y. Song, A. S. Verkman, and G. T. Manley, “Reduced cerebrospinal fluid production and intracranial pressure in mice lacking choroid plexus water channel Aquaporin-1,” *FASEB J.*, vol. 19, no. 1, pp. 76–78, 2004.
[36] D. Zhang, L. Vetrivel, and A. S. Verkman, “Aquaporin deletion in mice reduces intraocular pressure and aqueous fluid production,” *J. Gen. Physiol.*, vol. 119, no. 6, pp. 561–569, 2002.
[37] S. Mader and L. Brimberg, “Aquaporin-4 Water Channel in the Brain and Its Implication for Health and Disease,” *Cells*, vol. 8, no. 2, p. E90, 2019.
[38] E. A. Nagelhus and O. P. Ottersen, “Physiological roles of Aquaporin-4 in brain,” *Physiol. Rev.*, vol. 93, no. 4, pp. 1543–1562, 2013.
[39] N. N. Haj-Yasein *et al.*, “Glial-conditional deletion of aquaporin-4 (Aqp4) reduces blood-brain water uptake and confers barrier function on perivascular astrocyte endfeet,” *Proc. Natl. Acad. Sci. U. S. A.*, vol. 108, no. 43, pp. 17815–17820, 2011.
[40] G. T. Manley *et al.*, “Aquaporin-4 deletion in mice reduces brain edema after acute water intoxication and ischemic stroke,” *Nat. Med.*, vol. 6, no. 2, pp. 159–163, 2000.
[41] M. C. Papadopoulos, G. T. Manley, S. Krishna, and A. S. Verkman, “Aquaporin-4 facilitates reabsorption of excess fluid in vasogenic brain edema,” *FASEB J.*, vol. 18, no. 11, pp. 1291–1293, 2004.
[42] O. Bloch, K. I. Auguste, G. T. Manley, and A. S. Verkman, “Accelerated progression of kaolin-induced hydrocephalus in aquaporin-4-deficient mice,” *J. Cereb. Blood Flow Metab.*, vol. 26, no. 12, pp. 1527–1537, 2006.

[43] D. K. Binder, E. A. Nagelhus, and O. P. Ottersen, “Aquaporin-4 and epilepsy,” *Glia*, vol. 60, no. 8, pp. 1203–1214, 2012.
[44] M. Papadopoulos and A. S. Verkman, “Aquaporin 4 and neuromyelitis optica,” *Lancet Neurol.*, vol. 11, no. 6, pp. 535–544, 2012.
[45] V. A. Lennon *et al.*, “A serum autoantibody marker of neuromyelitis optica: distinction from multiple sclerosis,” *Lancet*, vol. 364, no. 9451, pp. 2106–2112, 2004.
[46] A. S. Verkman, P.-W. Phuan, N. Asavapanumas, and L. Tradtrantip, “Biology of AQP4 and anti-AQP4 antibody: therapeutic implications,” *Brain Pathol.*, vol. 23, no. 6, pp. 684–695, 2013.
[47] “Cancers,” 2019. [Online]. Available: https://www.who.int/health-topics/cancer#tab=overview. [Accessed: 07-Sep-2019].
[48] Y. Tomita *et al.*, “Role of aquaporin 1 signalling in cancer development and progression,” *Int. J. Mol. Sci.*, vol. 18, no. 2, p. E299, 2017.
[49] M. Endo, R. K. Jain, B. Witwer, and D. Brown, “Water channel (aquaporin 1) expression and distribution in mammary carcinomas and glioblastomas,” *Microvasc. Res.*, vol. 58, no. 2, pp. 89–98, 1999.
[50] B. Aikman, A. De Almeida, S. M. Meier-Menches, and A. Casini, “Aquaporins in cancer development: Opportunities for bioinorganic chemistry to contribute novel chemical probes and therapeutic agents,” *Metallomics*, vol. 10, no. 5, pp. 696–712, 2018.
[51] S. Saadoun, M. C. Papadopoulos, M. Hara-Chikuma, and A. S. Verkman, “Impairment of angiogenesis and cell migration by targeted aquaporin-1 gene disruption,” *Nature*, vol. 434, no. 7034, pp. 786–792, 2005.
[52] J. Hu and A. S. Verkman, “Increased migration and metastatic potential of tumor cells expressing aquaporin water channels,” *FASEB J.*, vol. 20, no. 11, pp. 1892–1894, 2006.
[53] M. C. Papadopoulos, S. Saadoun, and A. S. Verkman, “Aquaporins and cell migration,” *Pflugers Arch. Eur. J. Physiol.*, vol. 456, no. 4, pp. 693–700, 2008.
[54] Y. H. Huang, X. Y. Zhou, H. M. Wang, H. Xu, J. Chen, and N. H. Lv, “Aquaporin 5 promotes the proliferation and migration of human gastric carcinoma cells,” *Tumor Biol.*, vol. 34, no. 3, pp. 1743–1751, 2013.
[55] Z. Zhang, Z. Chen, Y. Song, P. Zhang, J. Hu, and C. Bai, “Expression of aquaporin 5 increases proliferation and metastasis potential of lung cancer,” *J. Pathol.*, vol. 221, no. 2, pp. 210–220, 2010.
[56] T. Song *et al.*, “Expression of aquaporin 5 in primary carcinoma and lymph node metastatic carcinoma of non-small cell lung cancer,” *Oncol. Lett.*, vol. 9, no. 6, pp. 2799–2804, 2015.
[57] H. J. Jung, J. Y. Park, H. S. Jeon, and T. H. Kwon, “Aquaporin-5: A marker protein for proliferation and migration of human breast cancer cells,” *PLoS One*, vol. 6, no. 12, p. e28492, 2011.
[58] A. S. Verkman, M. Hara-Chikuma, and M. C. Papadopoulos, “Aquaporins - New players in cancer biology,” *J. Mol. Med.*, vol. 86, no. 5, pp. 523–529, 2008.
[59] M. Hara-Chikuma and A. S. Verkman, “Prevention of Skin Tumorigenesis and Impairment of Epidermal Cell Proliferation by Targeted Aquaporin-3 Gene Disruption,” *Mol. Cell. Biol.*, vol. 28, no. 1, pp. 326–332, 2008.
[60] J. H. Yang, C. X. Yan, X. J. Chen, and Y. S. Zhu, “Expression of aquaglyceroporins in epithelial ovarian tumours and their clinical significance,” *J. Int. Med. Res.*, vol. 39, no. 3, pp. 702–711, 2011.
[61] A. Warth, M. Mittelbronn, P. Hülper, B. Erdlenbruch, and H. Wolburg, “Expression of the water channel protein aquaporin-9 in malignant brain tumors,” *Appl. Immunohistochem. Mol. Morphol.*, vol. 15, no. 2, pp. 193–198, 2007.
[62] W. Zhang *et al.*, “Aquaporin 9 is down-regulated in hepatocellular carcinoma and its over-expression suppresses hepatoma cell invasion through inhibiting epithelial-to-mesenchymal transition,” *Cancer Lett.*, vol. 378, no. 2, pp. 111–119, 2016.
[63] J. Wang *et al.*, “Aquaporins as diagnostic and therapeutic targets in cancer: How far we are?,” *J. Transl. Med.*, vol. 13, 2015.
[64] T. Ma, M. Hara, R. Sougrat, J. M. Verbavatz, and A. S. Verkman, “Impaired stratum

corneum hydration in mice lacking epidermal water channel aquaporin-3," *J. Biol. Chem.*, vol. 277, no. 19, pp. 17147–17153, 2002.
[65] M. Hara and A. S. Verkman, "Glycerol replacement corrects defective skin hydration, elasticity, and barrier function in aquaporin-3-deficient mice," *Proc. Natl. Acad. Sci. U. S. A.*, vol. 100, no. 12, pp. 7360–7365, 2003.
[66] M. Hara-Chikuma and A. S. Verkman, "Aquaporin-3 facilitates epidermal cell migration and proliferation during wound healing," *J. Mol. Med.*, vol. 86, no. 2, pp. 221–231, 2008.
[67] J. R. Thiagarajah, D. Zhao, and A. S. Verkman, "Impaired enterocyte proliferation in aquaporin-3 deficiency in mouse models of colitis," *Gut*, vol. 56, no. 11, pp. 1529–1535, 2007.
[68] N. Zhu *et al.*, "Defective macrophage function in aquaporin-3 deficiency," *FASEB J.*, vol. 25, no. 12, pp. 4233–4239, 2011.
[69] M. Hara-Chikuma *et al.*, "Progressive adipocyte hypertrophy in aquaporin-7-deficient mice: Adipocyte glycerol permeability as a novel regulator of fat accumulation," *J. Biol. Chem.*, vol. 280, no. 16, pp. 15493–15496, 2005.
[70] M. P. Marrades, F. I. Milagro, J. A. Martínez, and M. J. Moreno-Aliaga, "Differential expression of aquaporin 7 in adipose tissue of lean and obese high fat consumers," *Biochem. Biophys. Res. Commun.*, vol. 339, no. 3, pp. 785–789, 2006.
[71] A. M. Rojek *et al.*, "Defective glycerol metabolism in aquaporin 9 (AQP9) knockout mice," *Proc. Natl. Acad. Sci. U. S. A.*, vol. 104, no. 9, pp. 3609–3614, 2007.
[72] H. Sies, "Hydrogen peroxide as a central redox signaling molecule in physiological oxidative stress: Oxidative eustress," *Redox Biol.*, vol. 11, pp. 613–619, 2017.
[73] C. Prata, S. Hrelia, and D. Fiorentini, "Peroxiporins in cancer," *Int. J. Mol. Sci.*, vol. 20, no. 6, p. E1371, 2019.
[74] A. Acharya, I. Das, D. Chandhok, and T. Saha, "Redox regulation in cancer: A double-edged sword with therapeutic potential," *Oxid. Med. Cell. Longev.*, vol. 3, no. 1, pp. 23–34, 2010.
[75] M. Schieber and N. S. Chandel, "ROS function in redox signaling and oxidative stress," *Curr. Biol.*, vol. 24, no. 10, pp. R453–R462, 2014.
[76] H. Kawagishi and T. Finkel, "ROS and disease: Finding the right balance," *Nat. Med.*, vol. 20, no. 7, pp. 711–713, 2014.
[77] F. Vieceli Dalla Sega *et al.*, "Specific aquaporins facilitate Nox-produced hydrogen peroxide transport through plasma membrane in leukaemia cells," *Biochim. Biophys. Acta - Mol. Cell Res.*, vol. 1843, no. 4, pp. 806–814, 2014.
[78] I. Direito, A. Madeira, M. A. Brito, and G. Soveral, "Aquaporin-5: From structure to function and dysfunction in cancer," *Cell. Mol. Life Sci.*, vol. 73, no. 8, pp. 1623–1640, 2016.
[79] C. Rodrigues *et al.*, "Rat aquaporin-5 is pH-gated induced by phosphorylation and is implicated in oxidative stress," *Int. J. Mol. Sci.*, vol. 17, no. 12, p. E2090, 2016.
[80] V. Sidhaye, J. D. Hoffert, and L. S. King, "cAMP has distinct acute and chronic effects on aquaporin-5 in lung epithelial cells," *J. Biol. Chem.*, vol. 280, no. 5, pp. 3590–3596, 2005.
[81] J. Woo, J. Lee, M. S. Kim, S. J. Jang, D. Sidransky, and C. Moon, "The effect of aquaporin 5 overexpression on the Ras signaling pathway," *Biochem. Biophys. Res. Commun.*, vol. 367, no. 2, pp. 291–298, 2008.
[82] P. Kitchen *et al.*, "Plasma membrane abundance of human aquaporin 5 is dynamically regulated by multiple pathways," *PLoS One*, vol. 10, no. 11, p. e0143027, 2015.
[83] M. Zelenina, S. Tritto, A. A. Bondar, S. Zelenin, and A. Aperia, "Copper inhibits the water and glycerol permeability of aquaporin-3," *J. Biol. Chem.*, vol. 279, no. 50, pp. 51939–51943, 2004.
[84] M. Abir-Awan, P. Kitchen, M. M. Salman, M. T. Conner, A. C. Conner, and R. M. Bill, "Inhibitors of mammalian aquaporin water channels," *Int. J. Mol. Sci.*, vol. 20, no. 7, p. E1589, 2019.
[85] C. M. Niemietz and S. D. Tyerman, "New potent inhibitors of aquaporins: silver and gold compounds inhibit aquaporins of plant and human origin," *FEBS Lett.*, vol. 531, no. 3, pp. 443–447, 2002.

[86] A. Bijelic, M. Aureliano, and A. Rompel, “Polyoxometalates as Potential Next-Generation Metallodrugs in the Combat Against Cancer,” *Angew. Chemie Int. Ed.*, vol. 58, no. 10, pp. 2980–2999, 2019.
[87] N. Gumerova *et al.*, “The P-type ATPase inhibiting potential of polyoxotungstates,” *Metallomics*, vol. 10, no. 2, pp. 287–295, 2018.
[88] D. Marques-da-Silva, G. Fraqueza, R. Lagoa, A. A. Vannathan, S. S. Mal, and M. Aureliano, “Polyoxovanadate inhibition of Escherichia coli growth shows a reverse correlation with Ca 2+ -ATPase inhibition,” *New J. Chem.*, 2013.
[89] G. Fraqueza *et al.*, “Inhibition of Na + /K + - and Ca 2+ -ATPase activities by phosphotetradecavanadate,” *J. Inorg. Biochem.*, vol. 197, p. 110700, 2019.
[90] E. Kioseoglou, S. Petanidis, C. Gabriel, and A. Salifoglou, “The chemistry and biology of vanadium compounds in cancer therapeutics,” *Coord. Chem. Rev.*, vol. 301–302, pp. 87–105, 2015.
[91] L. Ruiz-Azuara and M. E. Bravo-Gomez, “Copper Compounds in Cancer Chemotherapy,” *Curr. Med. Chem.*, vol. 17, no. 31, pp. 3606–3615, 2010.
[92] A. P. Martins *et al.*, “Aquaporin Inhibition by Gold (III) Compounds : New Insights,” *ChemMedChem*, vol. 8, no. 7, pp. 1086–1092, 2013.
[93] Y. Yukutake, Y. Hirano, M. Suematsu, and M. Yasui, “Rapid and reversible inhibition of aquaporin-4 by zinc,” *Biochemistry*, vol. 48, no. 51, pp. 12059–12061, 2009.
[94] L. C. Costello and R. B. Franklin, “Cytotoxic/tumor suppressor role of zinc for the treatment of cancer: An enigma and an opportunity,” *Expert Rev. Anticancer Ther.*, vol. 12, no. 1, pp. 121–128, 2012.
[95] G. Soveral and A. Casini, “Aquaporin modulators: a patent review (2010–2015),” *Expert Opin. Ther. Pat.*, vol. 27, no. 1, pp. 49–62, 2016.
[96] A. P. Martins *et al.*, “Targeting Aquaporin Function : Potent Inhibition of Aquaglyceroporin-3 by a Gold-Based Compound,” *PLoS One*, vol. 7, no. 5, p. e37435, 2012.
[97] A. Serna *et al.*, “Functional Inhibition of Aquaporin-3 With a Gold-Based Compound Induces Blockage of Cell Proliferation,” *J. Cell. Physiol.*, vol. 229, no. 11, pp. 1787–1801, 2014.
[98] A. Madeira *et al.*, “A gold coordination compound as a chemical probe to unravel aquaporin-7 function,” *ChemBioChem*, vol. 15, no. 10, pp. 1487–1494, 2014.
[99] B. Yang, J. K. Kim, and A. S. Verkman, “Comparative efficacy of HgCl2 with candidate aquaporin-1 inhibitors DMSO, gold, TEA+ and acetazolamide,” *FEBS Lett.*, vol. 580, no. 28–29, pp. 6679–6684, 2006.
[100] C. Esteva-Font, B.-J. Jin, S. Lee, P.-W. Phuan, M. O. Anderson, and A. S. Verkman, “Experimental evaluation of proposed small-molecule inhibitors of water channel aquaporin-1,” *Mol. Pharmacol.*, vol. 89, no. 6, pp. 686–693, 2016.
[101] Y. Sonntag *et al.*, “Identification and characterization of potent and selective aquaporin-3 and aquaporin-7 inhibitors,” *J. Biol. Chem.*, vol. 294, no. 18, pp. 7377–7387, 2019.
[102] G. Soveral, A. Madeira, M. C. Loureiro-Dias, and T. F. Moura, “Water transport in intact yeast cells as assessed by fluorescence self-quenching,” *Appl. Environ. Microbiol.*, vol. 73, no. 7, pp. 2341–2343, 2007.
[103] A. F. Mósca *et al.*, “Molecular Basis of Aquaporin-7 Permeability Regulation by pH,” *Cells*, vol. 7, no. 11, p. E207, 2018.
[104] X. Zheng, C. Bi, Z. Li, M. Podariu, and D. S. Hage, “Analytical methods for kinetic studies of biological interactions: A review,” *J. Pharm. Biomed. Anal.*, vol. 113, pp. 163–180, 2015.
[105] S. R. Martin and M. J. Schilstra, “Rapid Mixing Kinetic Techniques,” vol. 1008, pp. 119–138, 2013.
[106] D. Pérez-Bendito, A. Gómez-Hens, and M. Silva, “Advances in drug analysis by kinetic methods,” *J. Pharm. Biomed. Anal.*, vol. 14, no. 8–10, pp. 917–930, 1996.
[107] E. Campos, T. F. Moura, A. Oliva, P. Leandro, and G. Soveral, “Lack of Aquaporin 3 in bovine erythrocyte membranes correlates with low glycerol permeation,” *Biochem. Biophys. Res. Commun.*, vol. 408, no. 3, pp. 477–481, 2011.

[108] A. Maggio, R. L. Bernardino, P. Gena, M. G. Alves, P. F. Oliveira, and G. Calamita, “A stopped-flow light scattering methodology for assessing the osmotic water permeability of whole sertoli cells,” *Methods Mol. Biol.*, vol. 1748, pp. 279–286, 2018.
[109] S. Hamann, J. F. Kiilgaard, T. Litman, F. J. Alvarez-Leefmans, B. R. Winther, and T. Zeuthen, “Measurement of Cell Volume Changes by Fluorescence Self-Quenching,” *J. Fluoresc.*, vol. 12, no. 2, pp. 139–145, 2002.
[110] M. R. Curry, F. W. Kleinhans, and P. F. Watson, “Measurement of the water permeability of the membranes of boar, ram, and rabbit spermatozoa using concentration-dependent self-quenching of an entrapped fluorophore,” *Cryobiology*, vol. 41, no. 2, pp. 167–173, 2000.
[111] A. Madeira, M. Camps, A. Zorzano, T. F. Moura, and G. Soveral, “Biophysical assessment of human aquaporin-7 as a water and glycerol channel in 3T3-L1 adipocytes,” *PLoS One*, vol. 8, no. 12, p. e83442, 2013.
[112] M. Rothert, D. Rönfeldt, and E. Beitz, “Electrostatic attraction of weak monoacid anions increases probability for protonation and passage through aquaporins,” *J. Biol. Chem.*, vol. 292, no. 22, pp. 9358–9364, 2017.
[113] S. Törnroth-Horsefield, K. Hedfalk, G. Fischer, K. Lindkvist-Petersson, and R. Neutze, “Structural insights into eukaryotic aquaporin regulation,” *FEBS Lett.*, vol. 584, no. 12, pp. 2580–2588, 2010.
[114] K. K. Sung *et al.*, “Role of human aquaporin 5 in colorectal carcinogenesis,” *Am. J. Pathol.*, vol. 173, no. 2, pp. 518–525, 2008.
[115] L. Janosi and M. Ceccarelli, “The Gating Mechanism of the Human Aquaporin 5 Revealed by Molecular Dynamics Simulations,” *PLoS One*, vol. 8, no. 4, p. e59897, 2013.
[116] J. S. Hub and B. L. De Groot, “Mechanism of selectivity in aquaporins and aquaglyceroporins,” *Proc. Natl. Acad. Sci. U. S. A.*, vol. 105, no. 4, pp. 1198–1203, 2008.
[117] G. Hu, L. Y. Chen, and J. Wang, “Insights into the mechanisms of the selectivity filter of Escherichia coli aquaporin Z,” *J. Mol. Model.*, vol. 18, no. 8, pp. 3731–3741, 2012.
[118] A. | J. the revolution now-. (2019)., “No Title.” [Online]. Available: https://aquaporin.com/. [Accessed: 20-Aug-2019].
[119] “Puretec Industrial Water | What is Reverse Osmosis?” [Online]. Available: https://puretecwater.com/reverse-osmosis/what-is-reverse-osmosis#understanding-reverse-osmosis. [Accessed: 20-Aug-2019].
[120] F. C. e Silva, A. Shvaleva, J. P. Maroco, M. H. Almeida, M. M. Chaves, and J. S. Pereira, “Responses to water stress in two Eucalyptus globulus clones differing in drought tolerance,” *Tree Physiol.*, vol. 24, no. 10, pp. 1165–1172, 2004.
[121] C. Liu *et al.*, “Aquaporin OsPIP1;1 promotes rice salt resistance and seed germination,” *Plant Physiol. Biochem.*, vol. 63, pp. 151–158, 2013.
[122] L. Wang, Y. Liu, S. Feng, J. Yang, D. Li, and J. Zhang, “Roles of plasmalemma aquaporin gene StPIP1 in enhancing drought tolerance in potato,” *Front. Plant Sci.*, vol. 8, pp. 1–14, 2017.
[123] M. A. Grohme, B. Mali, W. Wełnicz, S. Michel, R. O. Schill, and M. Frohme, “The Aquaporin Channel Repertoire of the Tardigrade Milnesium tardigradum,” *Bioinform. Biol. Insights*, vol. 7, pp. 153–165, 2013.